

PRESSURE-DROP CHARACTERISTICS OF
PULSATING FLUIDIZED BEDS

BY

THEUNIS C. ERASMUS

SUBMITTED IN PARTIAL FULFILMENT OF THE
REQUIREMENTS FOR THE DEGREE OF
M.Sc. (ENG.)

IN THE FACULTY OF ENGINEERING

UNIVERSITY OF PRETORIA
APRIL 1965

CONTENTS

	<u>Page</u>
1. Summary	1
2. Symbols and Terms	5
3. Introduction	9
4. Literature Review	10
5. Development of a Theory for the Pulsating Fluidized Bed	17
5.1 Qualitative Description	17
5.2 Theory	20
6. Utilization of Equations	23
7. Experimental Apparatus	27
7.1 Rotary valve and drive mechanism	27
7.2 Bed container	28
7.3 Pressure-drop transducer	29
7.4 Bed-height transducer	30
7.5 Transducer circuit	31
7.6 Manometers	32
8. Experimental Procedure	33
8.1 The fixed bed	33
8.2 The pulsating fluidized bed	34
8.3 The instantaneous functions	35
9. Experimental Results	38
9.1 Fixed bed	39
9.2 Pulsating fluidized bed	40
9.21 Effect of particle size	40
9.22 Effect of bed depth	42

CONTENTS
(continued)

	<u>Page</u>
9.23 Effect of bed diameter	44
9.24 Reproducibility of results ...	45
9.25 Instantaneous functions	46
10. Discussion of Results	48
10.1 Properties of the pulsating bed	48
10.11 Bubble suppression	48
10.12 Bed oscillation	48
10.2 Fixed bed	49
10.3 Pulsating fluidized bed	49
10.31 Pressure-drop-velocity relation	49
10.32 Effect of pulse frequency on pressure drop	50
10.33 Factors limiting the bed depth	50
10.34 Void fraction within the pulsating fluidized bed	51
10.35 Effect of various factors on the voidage of the pulsating fluidized bed	52
10.36 Modified Reynolds number and modified friction factor	53
10.37 Velocity range	53
10.38 Instantaneous functions	54
11. Final Conclusions	56
12. Appendices:	
Appendix 1: Fixed-Bed Experiments	58
Appendix 2: Pulsating fluidized bed results	63

Appendix 3/...

CONTENTS
(continued)

	<u>Page</u>
Appendix 3: Mean pressure-drop-velocity values, for the pulsating fluidized bed, employed in the calculations	76
Appendix 4: Overall mean void fractions existing in the pulsating fluidized bed	81
Appendix 5: Modified Reynolds number and modified friction factor	88
Appendix 6: Instantaneous pressure-drop-velocity functions in the pulsating fluidized bed	95
Appendix 7: Theory	103
Appendix 8: Evaluation of the form factor ..	115
Appendix 9: Specimen calculations	117
13. References	125

oooOooo

1. SUMMARY

An original mathematical treatment was developed, giving the pressure drop for a fluid traversing a bed of solid particles. The energy equation for a fluid in motion, together with the assumption that the particle bed is equivalent to a group of parallel and equal-sized channels, formed the basis of the mathematical treatment.

Pressure-drop equations were developed for uniform fluid-flow through fixed beds and for pulsating fluid-flow through fluidized beds. In both cases the final pressure-drop equation contained two terms, viz. a frictional loss term and a kinetic energy loss term. The latter term differs somewhat from that introduced, by other investigators, for uniform fluid-flow through fixed and fluidized beds.

The pressure-drop equation for pulsating fluid-flow through fluidized beds may be reduced to:

$$\overline{\Delta P_m} = a \left[\frac{\epsilon_m}{\overline{\epsilon_m}} \right]^3 \left[\frac{1-\overline{\epsilon_m}}{1-\epsilon_m} \right] \overline{U_m} + bF \left[\frac{\epsilon_m}{\overline{\epsilon_m}} \right]^2 \left[\frac{1-\overline{\epsilon_m}}{1-\epsilon_m} \right] \overline{U_m}^2$$

This equation may be solved for the overall mean void-fraction, $\overline{\epsilon_m}$, provided the following are known:

- (a) The mean superficial velocity, $\overline{U_m}$, and the corresponding pressure drop, $\overline{\Delta P_m}$.
- (b) The constants a and b.
- (c) The fixed-bed voidage, ϵ_m .
- (d) The form factor, F.

The constants a and b are obtained from the fixed bed. The pressure-drop equation for uniform

fluid-flow/...

fluid-flow through a fixed bed may be reduced to:

$$\Delta P_{fm} = a U_m + b U_m^2$$

This equation may be solved for a and b.

The experimental procedure entails treating the particle bed as a fixed bed by passing the fluid downwards through the bed. Superficial fluid velocities and the corresponding pressure drops obtained are employed to yield the constants a and b. The fixed-bed voidage results from the bed volume and the particle density. The particle bed is then fluidized by passing a pulsating fluid upwards through the bed. The mean superficial velocities and the corresponding pressure drops obtained, together with the constants a and b, are employed to evaluate the voidage in the fluidized bed.

From such experiments the following was found general to all pulsating fluidized beds: As the fluid velocity is increased the pressure drop initially increases parabolically, similar to uniform flow through fixed beds. When the minimum fluidization velocity is exceeded the pressure drop still increases, but is less than the parabolic value. The deviation is due to voidage increase. Above the maximum fluidization velocity the pressure drop becomes independent of velocity due to bubble formation. When the bed is fluidized the pressure drop, in addition, increases with pulse frequency. Thus a family of pressure-drop curves is obtained.

The pressure-drop equation for pulsating flow through fluidized beds contains a form factor, F, in

the/...

the kinetic energy term. From theoretical considerations, F was found to equal 1.2. This may be substantiated from the plot of the modified Reynolds number versus the modified friction factor, $\bar{\phi}$. The product of the dimensionless groups may be reduced to:

$$\overline{Re} \times \bar{\phi} = \frac{5}{F^2}$$

Correlation of the experimental data by the above equation indicates $F = 1.2$ to be reasonable.

The effect of factors such as particle size, pulse frequency and bed depth and diameter on the pulsating fluidized bed, may be studied from the voidage behaviour. For this purpose, an empirical method of void-fraction representation is introduced.

It was found that the overall mean void-fraction for any solid material may be correlated for all pulse frequencies by a single straight line. The voidage increases with increase in fluid velocity and decreases with increase in pulse frequency. The slope of the correlation line increases with increase in bed depth. It follows that the voidage of the pulsating bed is a function of bed depth and decreases, at constant velocity, with increase in depth. Increasing the particle size at constant bed depth causes the slope of the correlation line to decrease. Thus, the velocity increment required to effect a given voidage increase, increases with particle size. The correlation line is unaffected by increase of bed diameter. Thus, the voidage of the pulsating bed is unaffected by bed diameter.

The/...

The theory also enables the instantaneous velocity curve to be constructed from the instantaneous pressure-drop curve. For this purpose, a pressure-drop transducer was constructed to reproduce the instantaneous pressure-drop on an oscilloscope. Graphical integration of the resulting instantaneous velocity curve yields the computed mean superficial velocity. Good agreement between the computed and observed mean superficial velocities appeared to substantiate the proposed theory.

Large particles, 1 - 2 mm in diameter, are fluidized as readily as small particles. For larger particles the pressure drop at increased bed depths becomes unstable. This is due to an additional oscillation of the bed proper, quite apart from that due to fluid pulsations.

All experiments were performed with air, at relatively low temperatures and pressures, as the fluidizing medium. Particles ranging from 0.1 - 2.0 mm in diameter were used in beds ranging from 9 - 58 cm in depth. Pulse frequencies ranged from 500 - 1200 pulses/minute.

2. SYMBOLS AND TERMS EMPLOYED

2.1 Symbols

<u>Symbol</u>	<u>Description</u>	<u>Unit</u>
a	= constant	gm sec/cm ⁵
A	= cross sectional area of container	cm ²
b	= slope of straight line	gm sec ² /cm ⁴
d_c	= inside diameter of channel	cm
D	= diameter of container	cm
F'	= frictional energy	cm ² /sec ²
F	= form factor	-
g	= Newton's conversion factor	cm/sec ²
K	= constant	cm
L	= length of channel	cm
L_o	= unit bed length	cm
M	= mass of solids	gm
n	= number of observations	-
N	= total number of channels	-
dP	= pressure drop increment	gm/cm ²
ΔP_{ifm}	= instantaneous pressure drop in fixed bed	gm/cm ²
ΔP_{im}	= instantaneous pressure drop in fluidized bed	gm/cm ²
ΔP_{fm}	= total pressure drop across fixed bed	gm/cm ²
$\overline{\Delta P_{fm}}$	= mean total pressure drop across fixed bed	gm/cm ²
$\overline{\Delta P_m}$	= mean total pressure drop across fluidized bed	gm/cm ²
Q	= volumetric flow	cm ³
S	= specific surface of solids	cm ² /cm ³

t/...

<u>Symbol</u>	<u>Description</u>	<u>Unit</u>
t	= time	secs
T	= period	secs
U	= superficial velocity based on empty container	cm/sec
U*	= fluid velocity in channel	cm/sec
U _d	= deviation velocity	cm/sec
U _m	= superficial velocity at mean bed conditions	cm/sec
U _{im}	= instantaneous superficial velocity	cm/sec
U _{ipm}	= instantaneous particle velocity	cm/sec
U _{irm}	= instantaneous relative velocity	cm/sec
\overline{U}_m	= mean superficial velocity	cm/sec
v	= specific volume	cm ³ /gm
W	= work done by system	cm ² /sec ²
ρ	= fluid density	gm/cm ³
ρ _c	= fluid density in channel	gm/cm ³
ρ _s	= density of solids	gm/cm ³
α, β	= statistical correction constants	
μ	= viscosity	gm/cm sec
Re	= Reynolds number	-
\overline{Re}	= modified Reynolds number	-
φ	= friction factor	-
$\overline{\phi}$	= modified friction factor	-
ε	= void fraction	-
ε _m	= mean void fraction	-
$\overline{\epsilon}$	= overall mean void fraction.	-

2.2/...

2.2 Definition of Terms

For the simplification of the text, the following terms are defined:

(a) Mean bed conditions

The mean bed conditions are the pressure and temperature conditions existing at the geometric centre of the bed of solid particles.

(b) Mean superficial velocity

The mean superficial velocity is the ratio of the total fluid volume, at mean bed conditions, passed through the bed per unit time to the cross-sectional area of the bed container.

(c) Minimum fluidization velocity

The minimum fluidization velocity is the mean superficial velocity at which the particles in the lowest layers just commence vibrating.

(d) Maximum fluidization velocity

The maximum fluidization velocity is the mean superficial velocity at which bubble formation commences.

(e) Pulse frequency

The pulse frequency is the time rate of distinct fluid admissions. The duration of each cycle may be denoted by T seconds.

(f) The mean void fraction

The mean void fraction is the ratio of the interstitial volume to the total volume occupied by the particle bed.

(g)/...

(g) Overall mean void fraction

The overall mean void fraction is the effective void fraction existing in the pulsating bed and may be defined by the equation:

$$\overline{\epsilon_m} = \frac{1}{T} \int_0^T \epsilon_m dt$$

where T is defined in (e) above.

3./...

3. INTRODUCTION

Although a number of the most important industrial processes depends upon the efficient contact between a bed of broken solid particles and a stream of ascending gas or vapour, at the time this investigation was instituted little work had been done on the laws that govern the pulsating flow of fluids through such beds.

The original object of the study was to treat solid particles with gases under fluidized-bed conditions, with the ultimate application of these results to the design of a reactor to produce a low-volatile-content char from South African coal.

The difficulties encountered when attempting to fluidize relatively coarse materials, and especially particles of a fairly close size-range, led to the idea of using a pulsating flow of gas to overcome channelling and bubble formation.

As far as could be established in the available literature, this idea had only been utilized in a British Patent Specification (Patent No. 806,677), where the pulsating-flow technique was used for the plastic coating of objects. However, this pamphlet gave very little detail about the procedure employed and of the effect of the different variables. Therefore, a more detailed study of the fundamental principles involved was undertaken.

4./...

4. LITERATURE REVIEW

As far as could be established from the available literature, no work had been published on the pulsating flow of fluids through fluidized beds. A basis for the mathematical development presented in the text was thus required. The object of the literature review presented is to define a basis for the subsequent mathematical treatment, as well as to gain an insight into the properties of the fluidized bed and the difficulties that may be encountered, e.g. the formation of bubbles and their stability.

The classical expression for fluid flow through porous media is based on the investigations of D'Arcy¹⁾ on the flow of water through various types of soil, and is usually written as:

$$U = K \Delta P / L$$

where U = velocity, K = coefficient of permeability,

ΔP = pressure drop, L = length.

This equation is almost identical with Poiseuille's relation for viscous flow through capillaries, which is theoretically derivable from Newton's shear-stress definition of viscosity, and is usually given in the form known as the Hagen-Poiseuille equation²⁾:

$$U = (d^2 g / 32 \mu) \Delta P / L$$

where d = tube diameter, μ = viscosity.

The similarity of these two equations was responsible for the extensive attempts to analyse the flow of fluids through packed and fluidized beds on the

assumption/...

assumption that the bed is analogous to a group of capillaries parallel to the direction of flow. The problem, however, was to define the nature and size of the equivalent capillaries in such a manner as to establish their equivalence rigorously.

Due to these difficulties, several empirical relationships were put forward. One such relationship was suggested by C.C. Furnas³⁾ for cases of "tortuous" fluid flow, under isothermal conditions, in a fixed bed of broken solids, and may be expressed as:

$$\Delta P = KU^N$$

where K, N = constants.

Dupuit⁴⁾, realizing that the fluid velocity through the interstices of the fixed bed must be greater than the superficial velocity, extended the simple D'Arcy Law to include the bed voidage. Assuming the bed voidage to be uniformly distributed through the bed, the interstitial velocity becomes U/ϵ and the D'Arcy Law takes the form:

$$U = K\epsilon(\Delta P/L)$$

where ϵ = void fraction.

Blake⁵⁾ was the first to apply the methods of dimensional analysis to describe the flow of fluids through a packed bed, and also the first to describe the particles in terms of surface area instead of particle diameter. Essentially, Blake applied the results of Stanton and Pannell⁶⁾, who had demonstrated that for the flow of fluids through circular ducts a unique plot is obtained if the dimensionless groups $R/\rho U^2$ and $DU\rho/\mu$ are plotted against each other. The application of

Dupuit's/...

Dupuit's and his own assumptions resulted in the dimensionless groups $Re^2/\rho J^2$ and $Up/\mu S$.

The first pamphlet to appear which dealt with the mechanics of fluidization as it is known today, was that of Daniels⁷⁾, who discussed the mechanics of flow in a fluid catalytic cracking unit. This was followed by a paper reporting the extensive work of Parent⁸⁾ et al. Based on a balance of forces, Parent gave the bed pressure drop as the weight of the bed in the fluid stream per unit area, or:

$$\Delta P = (U/A)(1 - \epsilon)(\rho_S - \rho_F)$$

where A = area, ρ_S = density of solid, ρ_F = density of fluid.

At this point in the development of the theory a serious drawback was realized, in that neither of the assumptions of equivalent capillaries and/or equivalent rods takes cognizance of the continuously varying flow cross-sections presented by the bed. The average voidage at any cross-section of the bed may be assumed to be equal to the average voidage at any other cross-section. However, the size, shape, number, and location of the voids differ at any cross-section. The voids are all interconnected, either laterally or axially. Thus, a form of veering braided flow results when a fluid passes through a bed. This is conducive to the production of eddies and turbulence, and in turbulent flow the rapidly changing shape and area of the flow cross-sections introduce uncertainties in formulating the flow conditions. From the mathematical point of view, it is no longer possible

to/...

to neglect the inertia terms in the basic hydrodynamical equation.

Ergun⁹⁾ was the first to recognise the fact that the pressure loss experienced by a fluid flowing through a bed is caused by simultaneous kinetic and viscous losses and he proposed the following equation:

$$\frac{\Delta P_g}{L} = 150 \frac{(1-\epsilon)^2}{\epsilon^3} \frac{\mu U}{d^2} + 1.75 \frac{(1-\epsilon)}{\epsilon^3} \frac{GU}{d}$$

where d = diameter of particle, μ = viscosity of fluid,
 U = superficial velocity.

The derivation of the above equation was subject to the following assumptions:

- (1) The granular bed is equivalent to a group of parallel and equal-sized channels, so that the total internal surface and the internal free volume are equal to the total packing surface and void volume, respectively, of the packed bed..
- (2) The pressure drop across a channel is given by the Poiseuille equation, to which a term representing kinetic energy losses, analogous to that introduced by Brillouin¹⁰⁾ for capillary flow, was added.

Richardson and Meikle¹¹⁾, in their investigation of sedimentation and fluidization, represented their results by plotting a modified Reynolds number against a modified friction factor. In the Reynolds number the average velocity of the fluid relative to the particles was used, whilst the characteristic linear dimension was

taken/...

taken as the reciprocal of the surface area per unit volume of solid material, which resulted in the expression:

$$Re'_m = \frac{U\rho}{S_\mu(1-\epsilon)}$$

The friction factor was obtained by considering the forces acting on an individual sedimenting particle, and resulted in the expression:

$$\phi'_m = \frac{\epsilon^3 g (\rho_S - \rho_F)}{S \rho_F U^2}$$

where U = relative velocity, S = specific surface.

The relation between the modified Reynolds number and the modified friction factor was found to be:

For fluidization and sedimentation

$$\phi'_m = 3.36/Re'_m$$

For flow through fixed beds

$$\phi'_m = 5.0/Re'_m$$

The lower coefficient in the relationship for fluidization reflects the fact that the particles in the fluidized bed system are free to arrange themselves in such a way as to offer the minimum resistance to fluid flow.

Rowe and Henwood¹²⁾, in order to explain the characteristics of a fluidized system, performed experiments to illustrate the drag experienced by a sphere in a fluid stream and how this drag varied in the presence of neighbouring spheres. As a result, the following conclusions were drawn:

- (1) Spheres in line shield one another so that the drag of each is reduced. This is quite a long-range effect.

(2)/...

- (2) In a close assembly the drag on a sphere is increased.
- (3) Adjacent spheres repel one another.
- (4) Upstream-facing surfaces strongly attract particles to any defect.
- (5) Downstream-facing surfaces strongly expel particles, but this is a force that falls off rapidly with distance.
- (6) A sphere in a downstream-facing surface is subjected to a higher drag than any other in a uniformly packed array.
- (7) The drag on a sphere in an array varies with packing arrangement.

The liquid-like properties of a fluidized bed can be explained in general terms by these conclusions. Lateral repulsive forces will cause the bed to spread and fill its container, whilst the greatly reduced drag experienced by a particle which leaves the top will cause it to fall back and so maintain a stable and definite upper limit. When the fluid velocity is just sufficient to support a particle in the interior of the bed, one on the surface will tend to be expelled since the drag there is higher than elsewhere. If expelled, the particle will soon fall back as the drag falls off rapidly with distance from the surface, but its departure will reduce the drag on those remaining, which will then tend to close the vacated site. Thus, there is activity on the surface of a bed,

with/...

with numerous particles leaping free for a few diameters and falling back again. The surface has very great stability and a property somewhat analogous to surface tension. The repulsive forces will keep the particles separated and physical contacts between them will be limited, so that the bulk of the bed has liquid-like properties. Before the minimum fluidization velocity is reached, the topmost layer of particles, being subjected to the greatest drag, will begin to lift. Under conditions of uniform flow, fluidization will start at the top and develop downwards as each layer lifts and allows the one below it to follow suit

The foregoing also assists in the understanding of the stability of voids and bubbles, once formed. It has been shown that the forces associated with a surface lead to a form of surface tension and so maintain the stability of a downstream-facing surface. An upstream-facing surface is similarly stable, for the drag forces increase enormously as a particle approaches it.

The relationships and arguments set out above constitute the basis for the mathematical expressions related to, and the physical characteristics of, pulsating fluidized beds, both of which will be developed and extended upon in the following chapters.

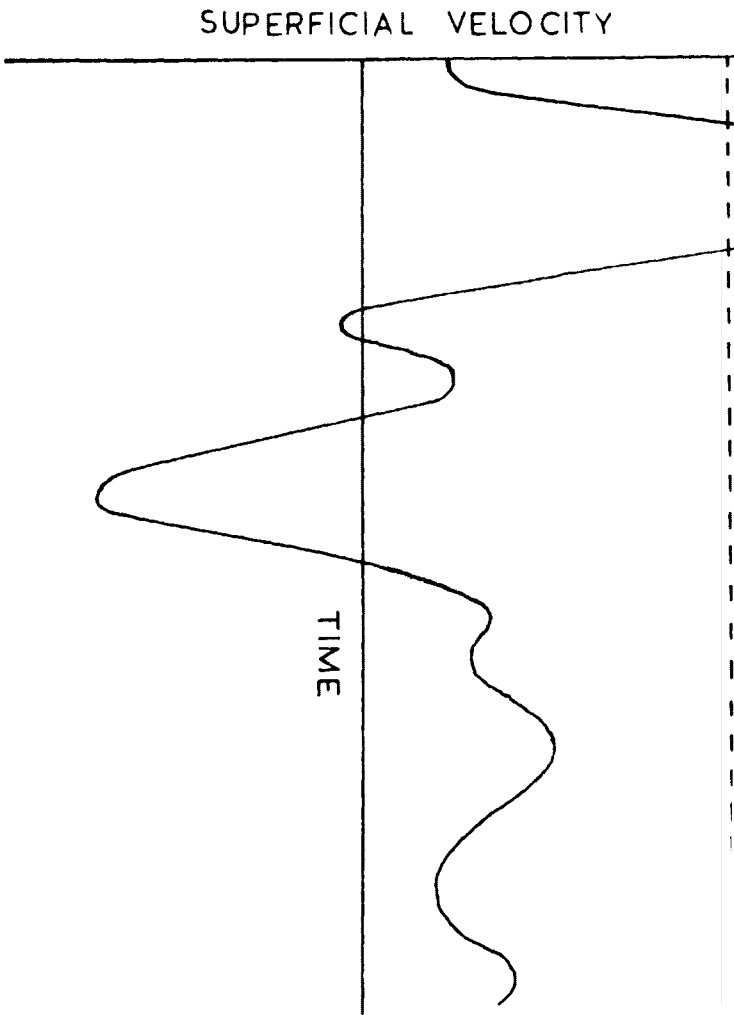
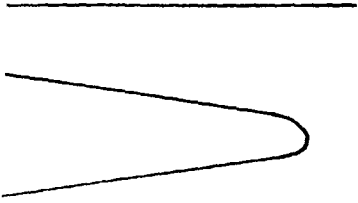


FIGURE 1 – TYPICAL TRANSIENT VELOCITY CURVE



BUOYANCY VELOCITY

5. DEVELOPMENT OF A THEORY FOR THE PULSATING FLUIDIZED BED

5.1 Qualitative Description

If the fluid flow-rate through a bed of solid particles is slowly increased, the pressure drop will increase correspondingly and eventually a point will be reached where the upward drag exerted on the particles by the fluid just equals the weight of the particles. Increasing the fluid velocity still further will cause the pressure drop, and hence the upward drag on the particles, to increase further, thereby exceeding the gravitational force on the particles. The ascending fluid will, therefore, lift the particles, increasing the bed voidage and decreasing the interstitial velocity until the forces acting on the particles are again in equilibrium. Further increase in fluid velocity will cause further bed expansion.

In the case of the pulsating fluidized system, the ascending fluid is admitted to the bed in periodically repeated pulses. A typical transient velocity curve is shown in Figure 1. The transient fluid velocity curve is comprised of two sections, viz. a prominent peak and a damped cyclic decaying section. The maximum amplitude in the latter portion of the curve is generally about one-fourth that of the peak amplitude for the type of valve utilized in these investigations. As the volumetric fluid flow-rate is increased, the peak amplitude will increase until a point is reached where the peak fluid-velocity is

such/...

such that the drag exerted on the particles is just sufficient to buoy the topmost layer of particles. Any further increase in the volumetric fluid flow-rate will cause the peak velocity to exceed the buoyancy fluid flow value, and the particles in the topmost layers will be lifted. When the fluid velocity decreases to a value below the buoyancy velocity, gravity will cause the particles to fall back to their original positions. As the drag experienced by the particles in the topmost layer is greater than that experienced by particles in the interior of the bed, bed expansion will be initiated at the solid-gas interface and develop downward. A further increase in the volumetric fluid flow-rate will cause a gradual downward development of particle vibration until the point is reached when all particles in the bed vibrate. At this point fluidization is fully developed.

For the first part of the cycle the particles will be lifted and accelerated in an upward direction. During the latter part of the cycle, when the drag on the particles is less than the gravitational force, the resultant downward force will decelerate the particles and eventually impart to them a downward velocity. If the expansion of the bed is such that it exceeds the contraction, the bed will undergo a nett expansion. At this increased volumetric flow-rate, each particle will vibrate in a vertical plane about a mean position elevated relative to its previous position at a lower volumetric flow-rate. Further

increase/...

increase of volumetric flow-rate in the pulsating fluidized bed will result in a further increase in effective bed-voidage.

Another factor influencing the effective bed-voidage in the pulsating fluidized bed is the pulse frequency. If the volumetric fluid flow-rate is maintained at a constant value and the pulse frequency is increased, the period of particle acceleration will be decreased. The amplitude of vibration of the solid particles will thus be decreased, resulting in a relative decrease in bed voidage during each cycle. Due to the inertia of the solid particles, which is a function of particle density, there exists an upper limit of pulse frequency beyond which a point will be reached where the particles cease to vibrate. This upper limit will also be affected by particle shape. A lower limit generally exists where pressure-drop determinations become inaccurate.

The progressive increase in volumetric flow-rate will eventually result in bubble formation, followed by pneumatic transport of the solid particles. The pulsating fluidized bed is thus a relatively stable condition of fluid-solid contacting, which is intermediate to a packed column, on the one hand, and a normal fluidized bed on the other hand. A stable fluid bed can be maintained, with a distinct bed surface and little loss of particles through escape from the bed.

5.2 Theory

An original pressure-drop equation was developed for uniform fluid-flow through fixed beds. The final equation differs somewhat from other similar equations¹⁶⁾, the difference being in the kinetic energy term. This pressure-drop equation was modified to apply to pulsating fluid-flow through fluidized beds.

The pressure-drop equation for uniform fluid-flow through fixed beds.

A general pressure-drop equation may be developed, based on the assumption that the particle bed is equivalent to a group of parallel and equal-sized channels. The energy equation for a fluid in motion indicates that the total pressure-drop is composed of frictional and kinetic energy losses. The pressure drop across a channel is thus given by the Poiseville equation, to which a term representing kinetic energy losses is added.

The velocity in the channel and the channel dimensions may be eliminated in favour of the superficial fluid-velocity and the specific surface of the solids, respectively. This is effected by the use of the Kozeny¹⁷⁾ assumption, which states: The total internal surface and the free internal volume of the channels are equivalent to the total packing surface and the void volume, respectively, of the granular bed. The final pressure-drop equation is given by:

g/\dots

$$g\Delta P_{fm} = 2K \alpha \mu S^2 \left(\frac{1-\epsilon_m}{\epsilon_m^3} \right) U_m + \frac{\beta \rho K U_m^2}{L_0 \epsilon_m^2 (1-\epsilon_m)} \dots \dots \dots (10)*$$

The pressure-drop equation for pulsating fluid-flow through fluidized beds.

In the case of pulsating fluid-flow through fluidized beds the pressure drop, velocity and voidage vary with time. At any instant, however, an equation such as Equation (10) above will be applicable, provided appropriate corrections are made. Since the particle velocity is not negligible, the velocity relative to the particles must be introduced. The instantaneous pressure-drop equation is thus given by:

$$g\Delta P_{im} = 2 \alpha K \mu S^2 \frac{(1-\epsilon_m)}{\epsilon_m^3} (U_{im} - U_{ipm}) + \frac{\beta K \rho (U_{im} - U_{ipm})^2}{L_0 \epsilon_m^2 (1 - \epsilon_m)}$$

In order to obtain mean values for a pulse cycle, the above equation must be integrated with respect to time and divided by the period. Integration is possible if the instantaneous voidage is replaced by the overall mean void-fraction, which, by definition, is independent of time. The final equation is given by:

g/...

* The equations are numbered in accordance with Appendix 7.

$$\overline{g \Delta P_m} = 2 \alpha K \mu S^2 \frac{(1 - \overline{\epsilon_m})}{\overline{\epsilon_m^3}} \overline{U_m} + \frac{\beta K \rho F \overline{U_m^2}}{L_o \overline{\epsilon_m^2} (1 - \overline{\epsilon_m})} \dots\dots\dots (15)$$

Integration of the square of the relative velocity introduces an additional term, the form factor F, in the kinetic energy term. From theoretical considerations, F was found to equal 1.2. (See Appendix 8.)

Modified Reynolds Number and Modified Friction Factor.

The theoretical value assigned to the form factor may be tested by a plot of a Reynolds number versus a friction factor. For this purpose a modified Reynolds number and a modified friction factor, applicable to pulsating fluid flow, were developed along the lines suggested by Richardson and Meikle¹¹). Mean values of the dimensionless groups are obtained by integrating with respect to time. The final result is divided by the period. The characteristic dimension, in both cases, is taken as the specific surface of the solids.

The resulting equation for the modified Reynolds number is given by:

$$\overline{Re} = \frac{\rho \overline{U_m}}{\mu S (1 - \overline{\epsilon_m})} \dots\dots\dots (18)$$

The equation for the modified friction factor is given by:

$$\overline{\phi} = \frac{\overline{\epsilon_m^3} \overline{g \Delta P_m}}{SF^2 K \rho \overline{U_m^2}} \dots\dots\dots (20)$$

6. UTILIZATION OF EQUATIONS

The pressure-drop equation for uniform fluid-flow through fixed beds,

$$g \Delta P_{fm} = 2K \alpha \mu S^2 \frac{(1-\epsilon_m)}{\epsilon_m^3} U_m + \frac{\beta \rho K U_m^2}{L_o \epsilon_m^2 (1-\epsilon_m)}$$

may be rewritten as:

$$\Delta P_{fm} = a U_m + b U_m^2$$

where

$$a = 2\alpha K \mu S^2 (1-\epsilon_m)/g \epsilon_m^3 \dots\dots\dots (24)$$

$$b = \beta \rho K/g L_o \epsilon_m^2 (1-\epsilon_m) \dots\dots\dots (25)$$

In the pressure-drop equation for pulsating fluid-flow through fluidized beds:

$$\overline{\Delta P_m} = \frac{2K \alpha \mu S^2}{g} \times \frac{(1-\overline{\epsilon_m})}{\overline{\epsilon_m^3}} \overline{U_m} + \frac{\beta K \rho F \overline{U_m^2}}{g L_o \overline{\epsilon_m^2} (1-\overline{\epsilon_m})}$$

the constants $2K \alpha \mu S^2/g$ and $\beta K \rho/L_o g$ may be eliminated in favour of a and b, respectively.*

The resulting equation is given by:

$$\overline{\Delta P_m} = a \left[\frac{\overline{\epsilon_m}}{\epsilon_m} \right]^3 \left[\frac{1-\overline{\epsilon_m}}{1-\epsilon_m} \right] \overline{U_m} + b F \left[\frac{\overline{\epsilon_m}}{\epsilon_m} \right]^2 \left[\frac{1-\overline{\epsilon_m}}{1-\epsilon_m} \right] \overline{U_m^2} \dots\dots\dots (26)$$

From the above equation the overall mean void-fraction, $\overline{\epsilon_m}$, existing in the pulsating fluidized bed,/...

* The constants α , β , S and L_o will differ from fixed to fluidized beds. For the velocity ranges considered, the variation will be small. The elimination procedure is thus justifiable.

bed, may be evaluated if the following are known:

- (i) The pressure-drop-velocity relation.
- (ii) The fixed-bed voidage, ϵ_m .
- (iii) The constants a and b.
- (iv) The form factor F.

The fixed-bed voidage follows from the volume of the fixed bed and the particle density.

The constants a and b, defined by the equation

$$\Delta P_{fm} = a U_m + b U_m^2,$$

may be evaluated from the fixed-bed pressure-drop-velocity relation. Use is made of the following statistical equations¹⁵⁾:

$$\overline{\Delta P_{fm}/U_m} = a \bar{n} + b \overline{U_m} \dots\dots\dots (27)$$

$$\overline{\Delta P_{fm}} = a \overline{U_m} + b \overline{U_m^2} \dots\dots\dots (28)$$

The value of F was found, from theoretical considerations, to equal 1.2. This value may be verified from a plot of the modified Reynolds number versus the inverse modified friction factor. The product of the dimensionless groups, with the subsequent elimination of the specific surface, can be reduced to:

$$\overline{Re} \times \overline{\phi} = \frac{5}{F^2}$$

Correlation of the experimental data by such an equation will indicate whether the adopted theoretical value is valid.

Representation/...

Representation of the Void Fractions existing in
the pulsating fluidized bed.

The effect of factors such as particle size, bed depth and bed diameter on the pulsating fluidized bed may be studied from the voidage behaviour. To this effect an empirical method of voidage representation is introduced.

For the conventionally fluidized bed the voidage is usually plotted against the superficial velocity. For the pulsating fluidized bed the void fraction is plotted against the mean superficial velocity in excess of the deviation velocity. The deviation velocity is defined as that velocity at which the pressure drop across the pulsating fluidized bed deviates from the fixed-bed pressure-drop-velocity relation.

The deviation velocity is generally difficult to ascertain. This may be overcome by computing the pressure-drop-velocity relation for the fixed bed at a slightly increased voidage. This ensures a clear intercept of the pressure-drop curves of the fixed and fluidized beds.

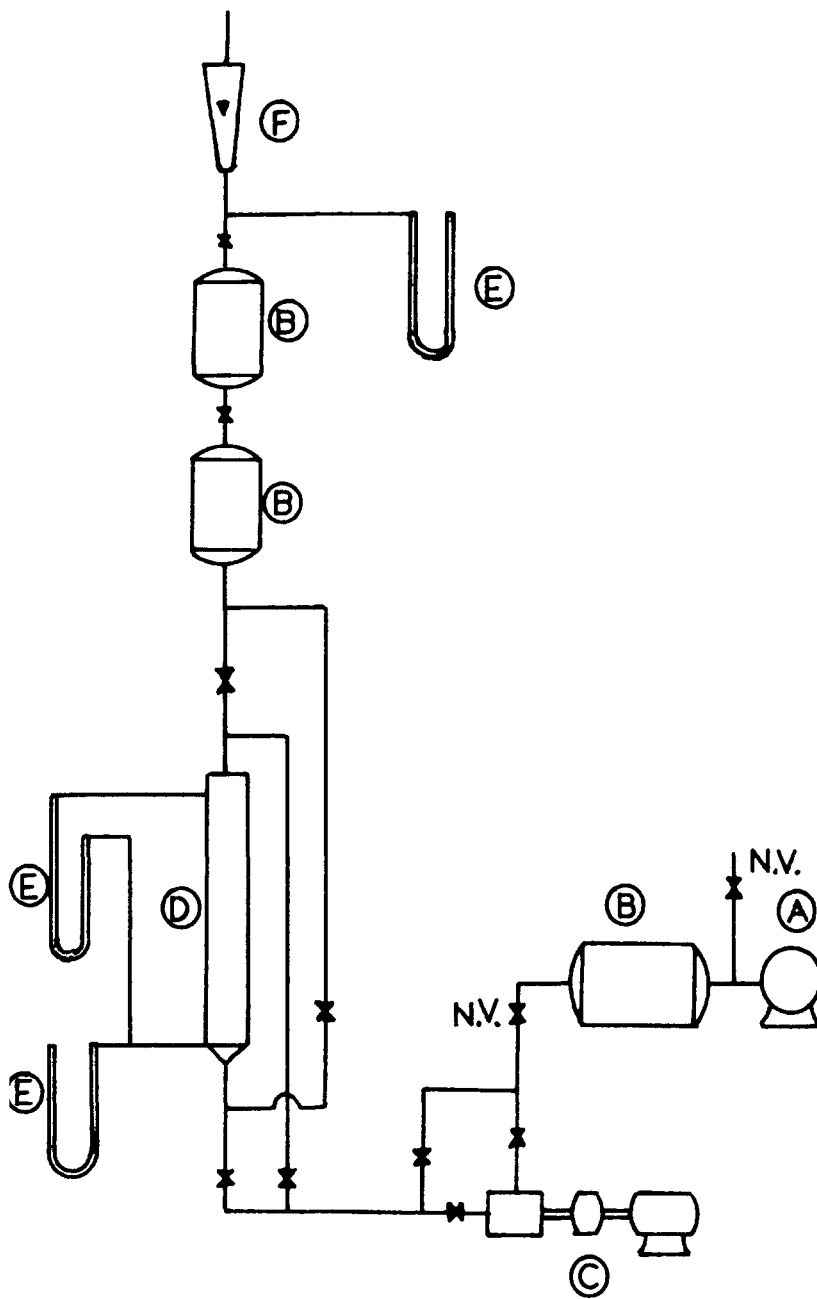
Instantaneous Functions.

The instantaneous pressure-drop-velocity relation for the pulsating fluidized bed is given by equation (14) in Appendix 7. Rearrangement and substitution of equations (24) and (25), Section 6, yield:

$$\Delta P_{im}/\dots$$

$$\Delta P_{im} = a \left[\frac{\epsilon_m}{\epsilon_m} \right]^3 \left[\frac{1-\epsilon_m}{1-\epsilon_m} \right] \left[U_{im} - U_{ipm} \right] + b \left[\frac{\epsilon_m}{\epsilon_m} \right]^2 \left[\frac{1-\epsilon_m}{1-\epsilon_m} \right] \left[U_{im} - U_{ipm} \right]^2$$

The instantaneous relative velocity curve may be constructed from the instantaneous pressure-drop curve by means of the above equation. Graphical integration of the instantaneous relative velocity curve yields the calculated mean superficial velocity. If the agreement between the calculated and observed mean superficial velocities is good, it may be concluded that the proposed theory is acceptable.



- A - COMPRESSOR E - MANOMETER
B - TANKS F - ROTAMETER
C - VALVE & DRIVE N.V. - NEEDLE VALVE
D - CONTAINER

**FIGURE 2 - DIAGRAMMATIC LAYOUT
OF APPARATUS**

7. EXPERIMENTAL APPARATUS

The following experimental apparatus had to be designed and constructed:

- (a) Rotary valve and drive mechanism.
- (b) Bed container.
- (c) Pressure-drop transducer.
- (d) Bed-height transducer.
- (e) The transducer circuit.

The diagrammatic layout of the apparatus employed is shown in Figure 2. Air from the compressor (A) flows to a tank (B), where the flow is smoothed. The coarse adjustment of the flow rate is effected by means of a needle valve by-passing air from the compressor to the atmosphere. From tank (B) the air flows through a second needle valve, facilitating fine adjustment of the flow rate, to the rotary valve (C), where pulses are imparted to the flow, and then to the bed container (D). A by-pass system was incorporated across the rotary valve to produce either a uniform or a pulsed flow. A fluid flow-direction cross-over system was incorporated across the bed container, facilitating the conversion of the fixed bed into a pulsating fluidized bed. From the bed container (D) the air flows through two tanks (E) in series, rendering the air flow smooth, and then through a rotameter (F) before being discharged into the atmosphere.

7.1 Rotary Valve and Drive Mechanism

For the mechanical details of construction of the rotary valve and the pictorial view of the

complete/...

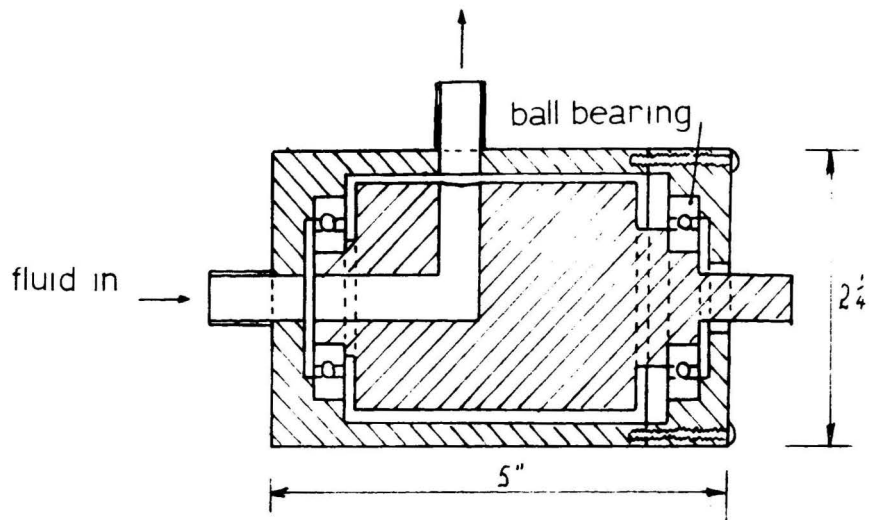


FIGURE 3 SECTIONAL VIEW OF ROTARY VALVE

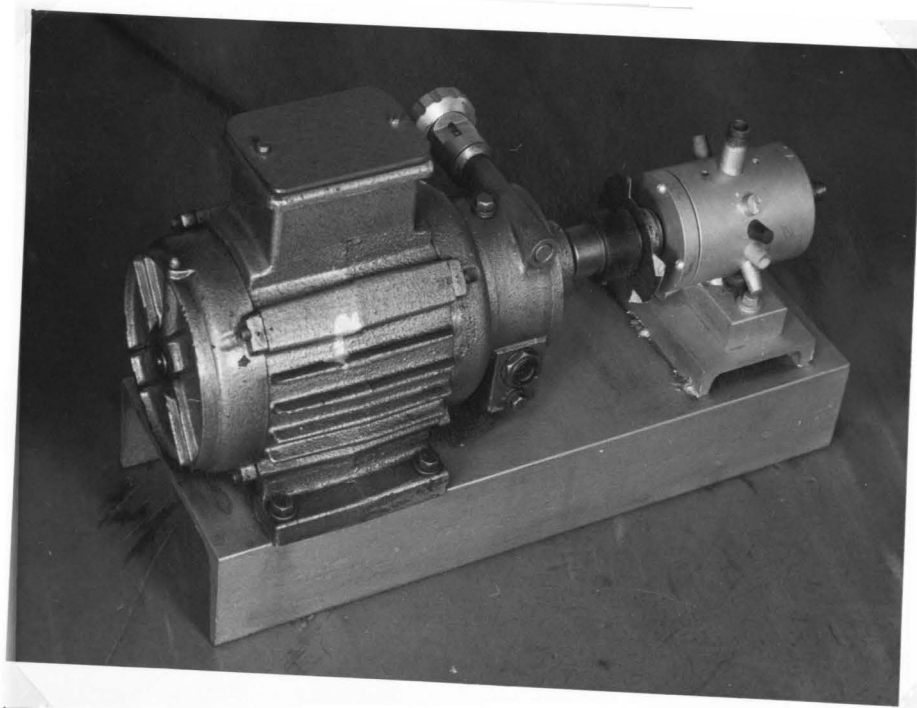


FIGURE 4 VIEW OF ROTARY VALVE AND DRIVE MECHANISM

complete unit, see Figures 3 and 4 respectively. The valve consists essentially of a piston, positioned and secured by means of two ball bearings, rotating in a cylinder. The clearance between the piston and cylinder was such that virtually no air leakage occurred when the flow was interrupted. The valve was so constructed that passage occurred once with each revolution. The valve was coupled via a variable speed drive to a synchronous motor. A slotted disc was attached to the valve driving-shaft to determine the pulse frequency by means of a stroboscope. The volumetric flow-rate through the rotary valve was regulated by means of a needle valve.

7.2 Bed Container

The fluidized bed unit employed, see Figure 5, consisted essentially of two sections, viz. a conical section at the bottom serving to distribute the entering air, and a cylindrical perspex column, 3 feet long by 5.7 inches in diameter, serving as the bed container. These two sections, bolted together and sealed with a rubber gasket, rigidly fixed the bed support between the flanges. The bed support consisted of a perforated plate, affording rigidity, covered by a 200-mesh wire screen. The fluidized bed unit was fitted with a lower pressure probe, protruding into the fluidized solids directly above the bed support. The pressure probe was constructed of $\frac{1}{8}$ " i.d. copper tubing, slotted on each side and with the slots covered with 200-mesh

screen/...

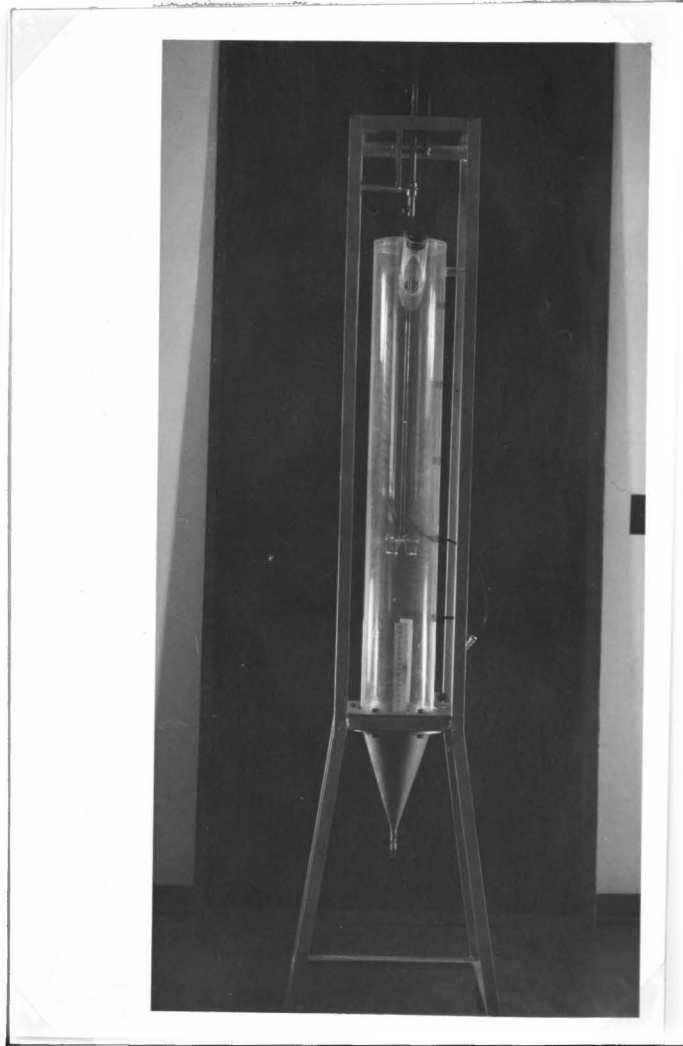


FIGURE 5 A VIEW OF THE
FLUIDIZED BED UNIT

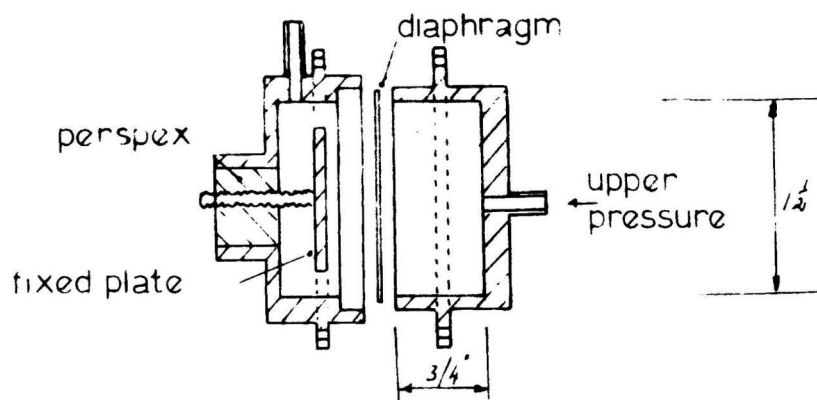


FIGURE 6 SECTIONAL VIEW OF THE
PRESSURE-DROP TRANSDUCER

screen wire. The pressure probe, covering the entire diameter of the container, was positioned so that the slots were perpendicular to the direction of fluid flow. Pressure ports, introduced at 6" intervals, facilitated the positioning of an upper pressure-probe directly above the solid-gas interface. The pressure drop across the bed was obtained either from a manometer or a pressure-drop transducer, or both in parallel, connected across the upper and lower pressure-probes. The lower pressure-probe, in addition, facilitated the determination of the pressure relative to atmospheric pressure. The bed temperature was obtained from a thermometer placed above the lower pressure-probe.

The bed-height transducer was supported above the solid-gas interface by means of a metal rod passing through a rubber seal in the "blanked-off" end of the container and fitted with a micrometer screw attachment. The micrometer screw attachment allowed for the accurate positioning and calibration of the bed height transducer. A 2" i.d. perspex tube, at an angle of 45° at the top of the container, facilitated admission of the solids.

7.3 Pressure-Drop Transducer (See Figure 6)

The principle of operation of the pressure-drop transducer is essentially that of a variable condenser. The transducer, consisting of a fixed plate and a diaphragm, converts pressure variations

into/...

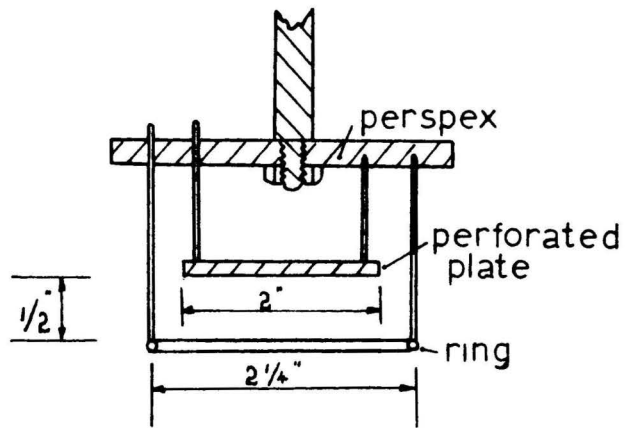


FIGURE 7 SECTIONAL VIEW OF
BED-HEIGHT TRANSDUCER .

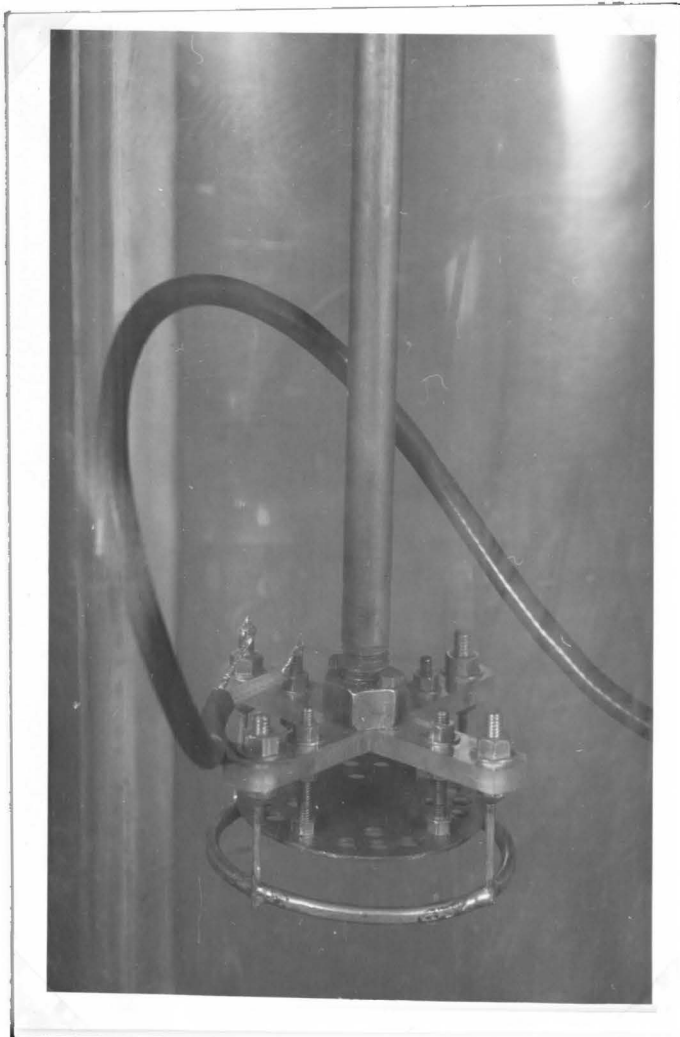


FIGURE 8 A VIEW OF THE
BED-HEIGHT TRANSDUCER

into capacitive variations by deflection of the diaphragm. The diaphragm was designed so that the natural frequency of the diaphragm, being a function of dimensions and material of construction, exceeds the maximum pulse frequency to be encountered by a factor of at least 10.

The fixed plate, constructed from $\frac{1}{8}$ " thick brass plate to ensure rigidity, was positioned and electrically insulated from the transducer body by means of a set screw mounted in perspex. Capacity adjustment, i.e. adjustment of the distance between the fixed plate and the diaphragm, was effected by rotation of the set screw. The volume of the pressure chambers was designed to be as small as possible and the chambers were lined with acoustic-absorbing foam plastic. A water jacket was provided to ensure constant operating temperatures.

The transducer, connected across the bed so that an increase in pressure difference across the diaphragm increased the capacity, registered any change in pressure drop as a D.C. potential.

7.4 Bed-Height Transducer (See Figures 7 & 8)

The principle of operation of the bed-height transducer is essentially the same as that of the pressure-drop transducer. In the case of the bed-height transducer, however, capacitive changes are produced by variation of the dielectric value.

The bed-height transducer consisted of a

perforated/...

perforated circular fixed plate and a metal ring electrically insulated from each other. Both the ring and perforated plate were rigid constructions, preventing any capacitive changes due to vibrations, and were fixed relative to each other. The transducer may be raised or lowered into the fluidized bed by means of a micrometer screw attachment. The micrometer screw attachment, externally situated to the bed, was attached to the transducer by means of a connecting rod.

The transducer was lowered into the fluidized bed so that the solid-gas interface was between the ring and the perforated plate. The motion of the solid-gas interface, changing the dielectric value, was registered as a D.C. potential.

7.5 Transducer Circuit

The transducer forms part of a tuned circuit¹⁸⁾ which is kept in oscillation by a type 6J6 valve. The oscillation is fed to a type 6BN6 gated-beam discriminator valve, the anode current of which depends on the deviation of the oscillation frequency from the resonant frequency of a parallel resonant circuit. The variation of the anode current was registered as a D.C. potential on the oscilloscope. The registered D.C. potential is proportional to transducer capacity, which in turn is proportional to the measured variable.

7.6/...

7.6 Manometers

All manometers were filled with a sufficient quantity of distilled water to ensure sufficient damping. Pressure connections to the manometers were kept as short as possible, thus ensuring the elimination of reflected pressure waves.

8./...

8. EXPERIMENTAL PROCEDURE

8.1 The Fixed Bed

The fixed bed is characterized by the fact that the solid particles have no degree of freedom or, in other words, that the void fraction is independent of fluid velocity. In practice, the fixed bed may be obtained by passing the fluid through the bed from the top downwards. The particles experiencing a downward drag, and being supported by the bed support, have no degree of freedom. The bed may thus be regarded as a fixed bed. In order to attach any significance to the results obtained from the experiments performed on the fixed bed, it is necessary to obtain a randomly-packed fixed bed which will be representative of conditions to be expected in the fluidized bed. Experimentally, the above requirement was obtained as follows:

The container was filled with suitable solid particles and the fluid, in this case air, was admitted through the bed from the bottom at a pulse frequency of 800 pulses per minute. The bed was fluidized for a sufficient period so that the bed could attain equilibrium. The fluid velocity, during fluidization, was adjusted to be within the minimum and maximum fluidization velocities. The fluid velocity was then slowly decreased to zero.

The experiments performed on the fixed bed prepared in this manner were to establish the

pressure/...

pressure-drop-velocity relationship. The fluid, under uniform flow conditions, was admitted from the top. The fluid velocity was increased from zero in suitable increments, and with each increment the following observations were made:

- (1) Pressure drop across the bed.
- (2) Pressure above atmospheric pressure at the lower pressure probe.
- (3) Temperature in the bed.
- (4) Rotameter reading.
- (5) Temperature of fluid entering rotameter.
- (6) Atmospheric pressure.

Sufficient velocity increments were taken to ensure that the statistical methods of analysing the results obtained were valid.

8.2 Fluidized Bed

The fluidized bed is characterized by the fact that the solid particles attain a degree of freedom or that the void fraction is dependent upon the fluid velocity. In practice, the fluidized bed may be obtained by admitting the fluid at the bottom of the bed. The experiments performed on the fluidized bed were to determine the pressure-drop-velocity relationship. The fluid was intermittently admitted to the bed at a fixed, predetermined pulse frequency and adjusted to maximum fluidization velocity. The fluid velocity was then decreased, in

suitable/...

suitable decrements, to the minimum fluidization velocity. The process was reversed, increasing the fluid velocity incrementally back to the maximum value. After each incremental change, the following observations were made:

- (1) Pressure drop across the bed.
- (2) Pressure above atmospheric pressure at the lower pressure probe.
- (3) Temperature in the bed.
- (4) Rotameter reading.
- (5) Temperature of fluid entering the rotameter.
- (6) Atmospheric pressure.

The procedure was repeated, employing different pulse frequencies.

8.3 Instantaneous Pressure Drop and Particle Velocity

These experiments were performed to establish the instantaneous pressure-drop-velocity relationship and the behaviour of the solid-gas interface during a single pulse-cycle.

The pressure-drop transducer, in parallel with a manometer, was connected across the bed. All pressure connections were kept as short as possible, ensuring the elimination of reflected pressure waves. If any reflected pressure waves do arise in the short pressure leads, their frequency will be such that, on superimposition

on/...

on the pressure complex existing across the bed, they will appear as high frequency, low amplitude superimpositions.

The bed was fluidized, and the bed-height transducer positioned and allowed to attain temperature equilibrium. The fluid velocity was incrementally increased from the minimum to the maximum fluidization velocity, and with each increment the following observations and determinations were made:

- (1) Pressure drop across the bed (from manometer).
- (2) Pressure above atmospheric pressure (at the lower pressure probe).
- (3) Temperature in the bed.
- (4) Rotameter reading.
- (5) Temperature of fluid entering rotameter.
- (6) Atmospheric pressure.
- (7) Photographic images of the instantaneous pressure drop and interface traces.

With a double-beam oscilloscope, the one beam serving as the base line for both pressure drop and bed height at static conditions, photo images of the following traces were obtained by utilization of the second beam:

- (1) A trace of the instantaneous pressure-drop transient response relative to the zero pressure-drop base line.

(2)/...

- (2) A trace of the interface transient response relative to the minimum bed-height base line.
- (3) The trace of the interface transient response relative to the pressure-drop transient response curve, utilizing both the bed-height transducer and the pressure-drop transducer.

Superimposition of the three photo images yielded a composite trace of the pressure-drop transient response curve and the interface transient response curve relative to the base line.

The pressure-drop transducer was calibrated against a water manometer. Calibration of the bed-height transducer was effected by the lowering of the transducer into the fixed bed.

9. EXPERIMENTAL RESULTS

In essence, each experiment consisted of of treating a bed of solid particles, first as a fixed bed and then as a pulsating fluidized bed. From the fixed-bed pressure-drop-velocity observations the constants a and b , defined by:

$$\Delta P_{fm} = a U_m + b U_m^2 \quad \dots\dots\dots (10a)$$

may be evaluated. The constants a and b are subsequently employed in the evaluation of the overall mean void-fraction existing in the pulsating fluidized bed.

The constants α , β , K , μ , ρ , S and L_0 are eliminated from equation (15), in favour of a and b , resulting in:

$$\overline{\Delta P_m} = a \left[\frac{\overline{\epsilon_m}}{\overline{\epsilon_m}} \right]^3 \left[\frac{1-\overline{\epsilon_m}}{1-\overline{\epsilon_m}} \right] \overline{U}_m + b \left[\frac{\overline{\epsilon_m}}{\overline{\epsilon_m}} \right]^2 \left[\frac{1-\overline{\epsilon_m}}{1-\overline{\epsilon_m}} \right] \overline{U}_m^2 \quad \dots\dots\dots (26)$$

From the pressure-drop-velocity observations for the pulsating fluidized bed, the overall mean void-fraction, $\overline{\epsilon_m}$, may be evaluated.

For each experiment performed, the overall mean void-fraction existing in the pulsating fluidized bed was evaluated in velocity ranges and pulse-frequency ranges determined by the solid particles employed.

Apart from the effect of pulse frequency upon the overall mean void-fraction, the effect of the following additional variables was studied:

(1)/...

- (1) particle size,
- (2) bed depth,
- (3) bed diameter,
- (4) the reproducibility of results.

In addition, the pressure drop per cycle was obtained, from which the instantaneous relative velocity curves were constructed by means of equation (30).

9.1 Fixed-Bed Results:

The results of experiments performed on the various fixed beds are tabulated in Table A below.

TABLE A

Experiment Number	Material Employed	Fixed-Bed Depth cm	Size Range mm	Constants	
				a	b x 10 ⁻³
A1	Zeolite	9.7	0.1-0.7	0.793	4.35
B1	Clover Seed	10.1	0.9-1.1	0.663	4.34
C1	Rape Seed	9.0	1.2-1.9	0.130	2.40
D1	Zeolite	15.7	0.1-0.7	1.520	6.10
E1	Zeolite	25.0	0.7-1.0	0.899	5.90
F1	Rape Seed	58.0	1.2-1.9	0.870	13.70
G1	Clover Seed	11.0	0.9-1.1	0.646	3.50

9.2/...

9.2 Pulsating Fluidized Bed Results

9.21 The effect of particle size

The effect of particle size on the overall mean void-fraction existing in the pulsating fluidized bed was studied by employing particles ranging from 150 mesh to 1.9 mm in diameter. Bed depths varying from 9 to 10 cm were employed. The bed cross-sectional area was 6.6 cm² and air was used as the fluidizing medium. The physical characteristics of the solid materials and the experimental conditions employed are summarized below.

Experiments A2 - A5

Material used: Zeolite.

Size range: 0.1 to 0.7 mm in diameter.

Specific surface: 106.4 cm²/cm³

Fixed-bed depth: 9.7 cm.

Fixed-bed void-fraction: 0.365.

Experiment No.	Velocity Range cm/sec	Pulse Frequency pulses/min
A2	6.4 - 10.4	800
A3	7.0 - 10.4	900
A4	7.7 - 10.4	1000
A5	7.7 - 10.4	1100

Experiments/...

Experiments B2 - B3

Material used: Clover seeds.

Size range: 0.9 to 1.1 mm in diameter.

Specific surface: $80.3 \text{ cm}^2/\text{cm}^3$.

Fixed-bed depth: 10.1 cm.

Fixed-bed void-fraction: 0.335.

Experiment No.	Velocity Range	Pulse Frequency
	cm/sec	pulses/min
B2	6.0 - 12.2	800
B3	6.3 - 12.0	900

Experiments C2 - C3

Material used: Rape seed.

Size range: 1.2 to 1.9 mm in diameter.

Specific surface: $53.3 \text{ cm}^2/\text{cm}^3$.

Fixed-bed depth: 9.0 cm.

Fixed-bed voidage: 0.365.

Experiment No.	Velocity Range	Pulse Frequency
	cm/sec	pulses/min
C2	23.0-36.7	800
C3	22.2-36.9	900

The pressure-drop-velocity observations for experiments A, B and C are represented graphically in figures 9, 10 and 11.

The overall mean void-fractions existing in the pulsating fluidized beds are represented graphically for the experimental series A, B and C in figures 12, 13 and 14.

Individual readings and computed results are given in the appendices.

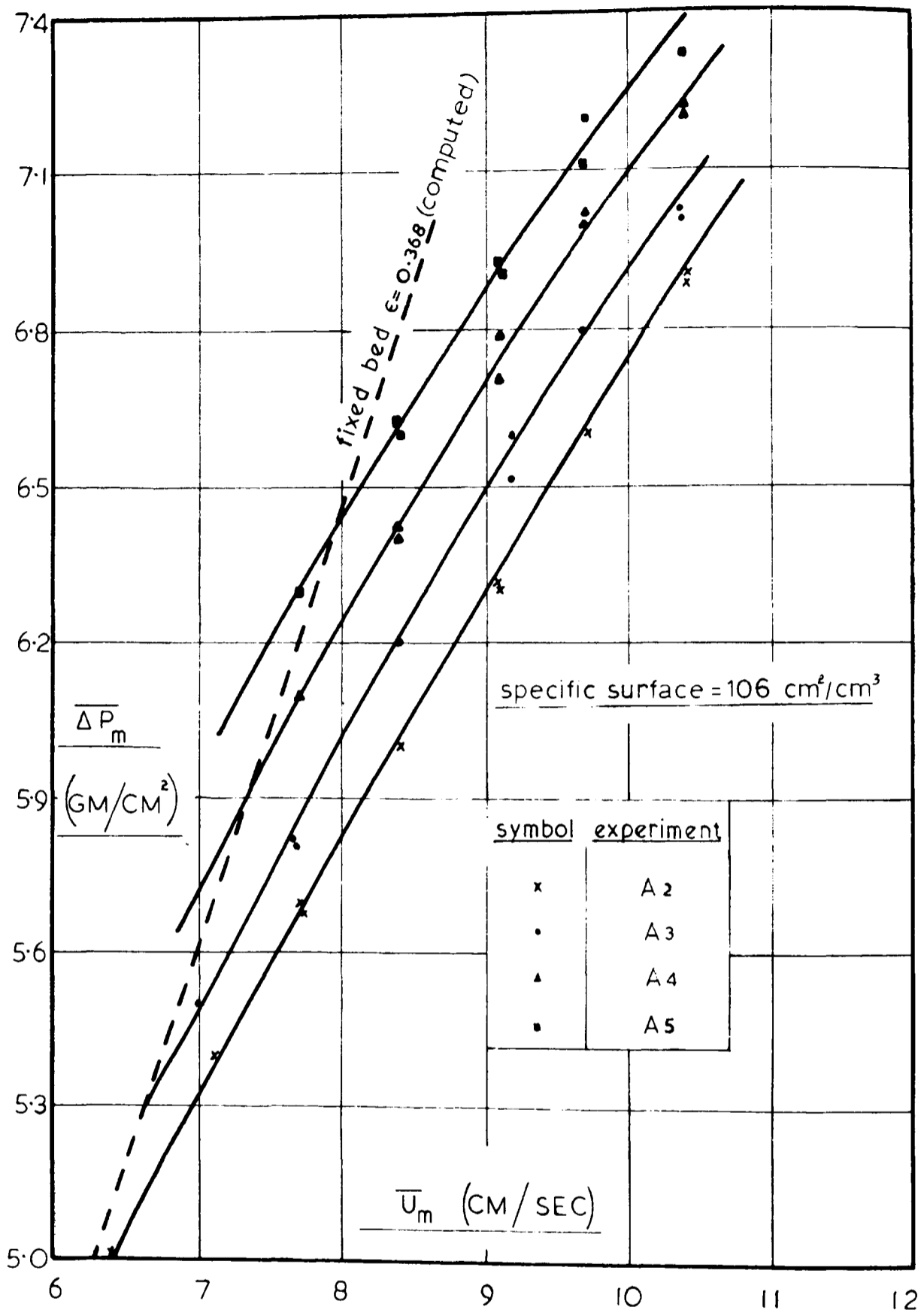


Figure 9

The mean total pressure-drop ($\overline{\Delta P_m}$) across the fluidized bed as a function of the mean superficial velocity ($\overline{U_m}$).

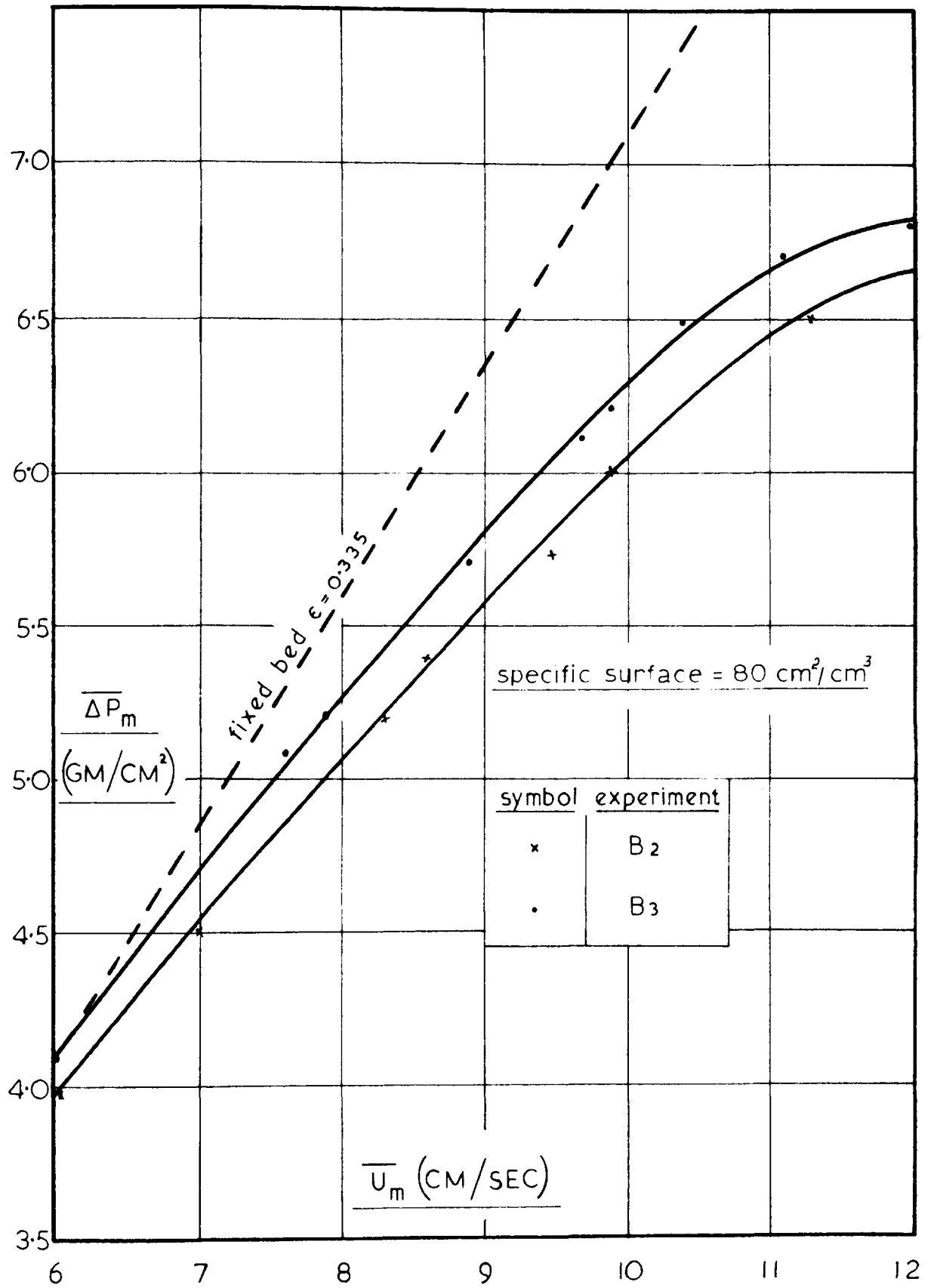


Figure 10

The mean total pressure-drop ($\overline{\Delta P_m}$) across the fluidized bed as a function of the mean superficial velocity ($\overline{U_m}$).

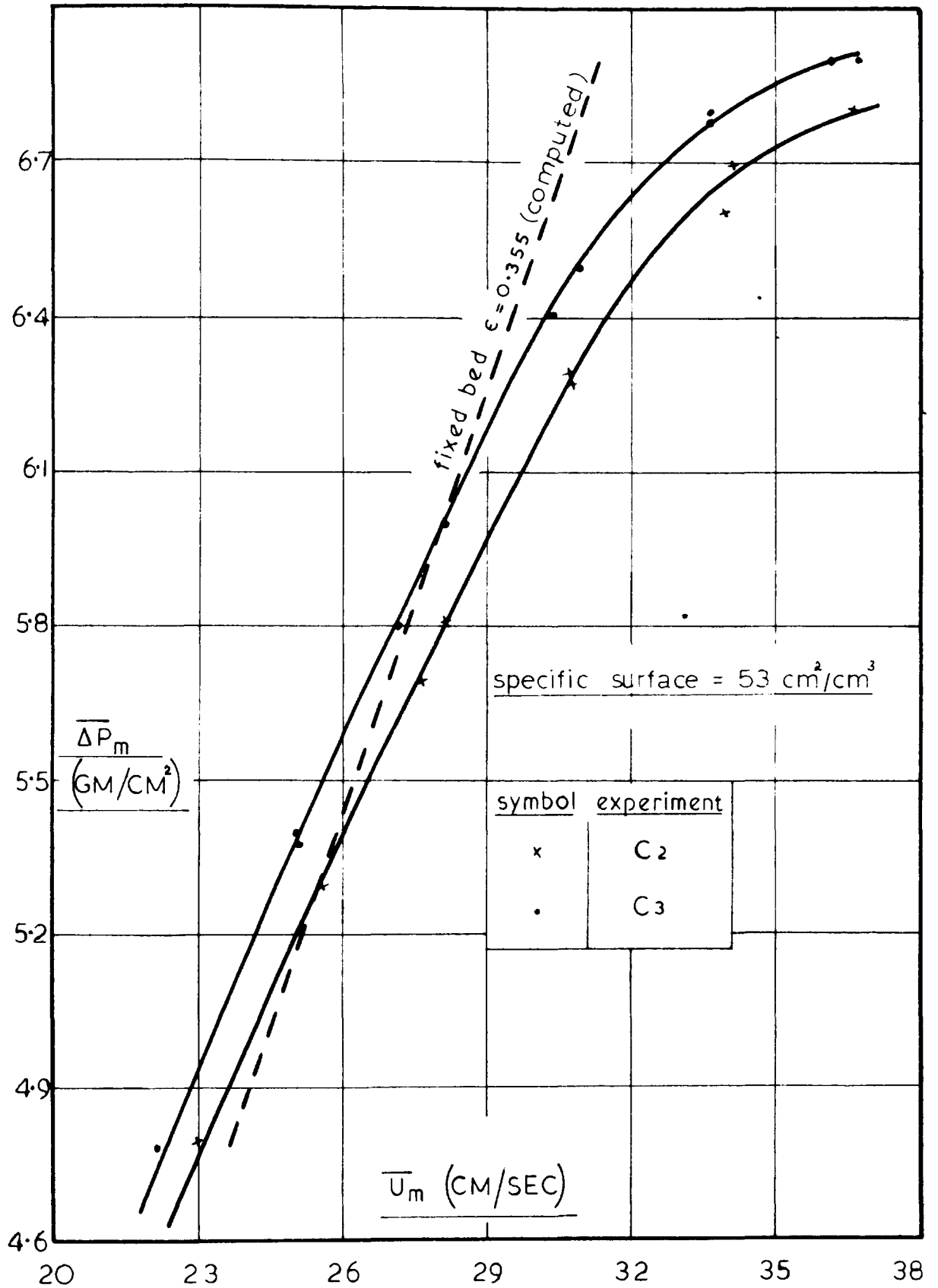


Figure 11

The mean total pressure-drop ($\overline{\Delta P_m}$) across the fluidized bed as a function of the mean superficial velocity ($\overline{U_m}$).

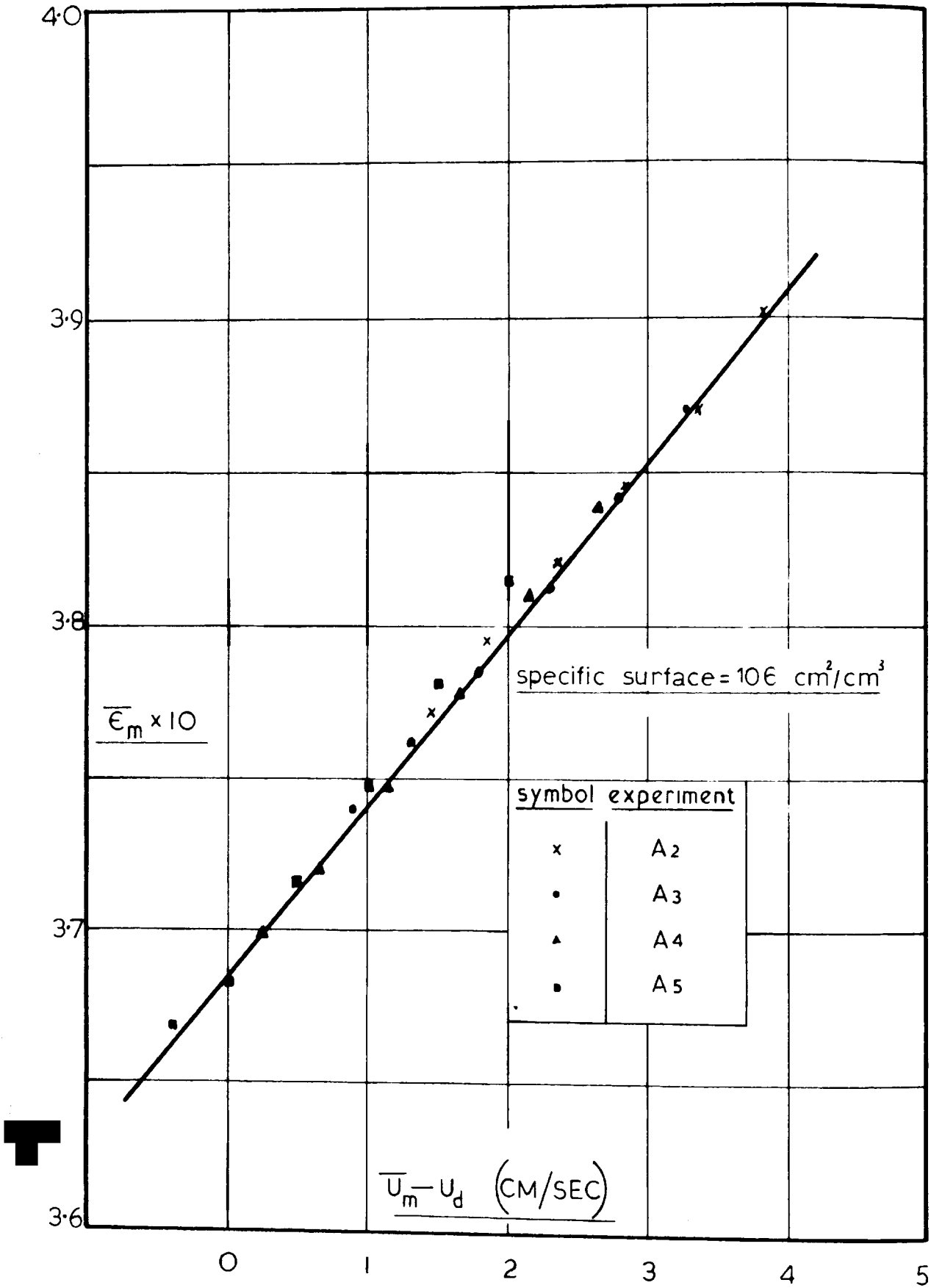


Figure 12

The overall mean void fraction ($\overline{\epsilon}_m$) in the fluidized bed versus the mean superficial velocity in excess of the deviation velocity ($\overline{U}_m - U_d$).

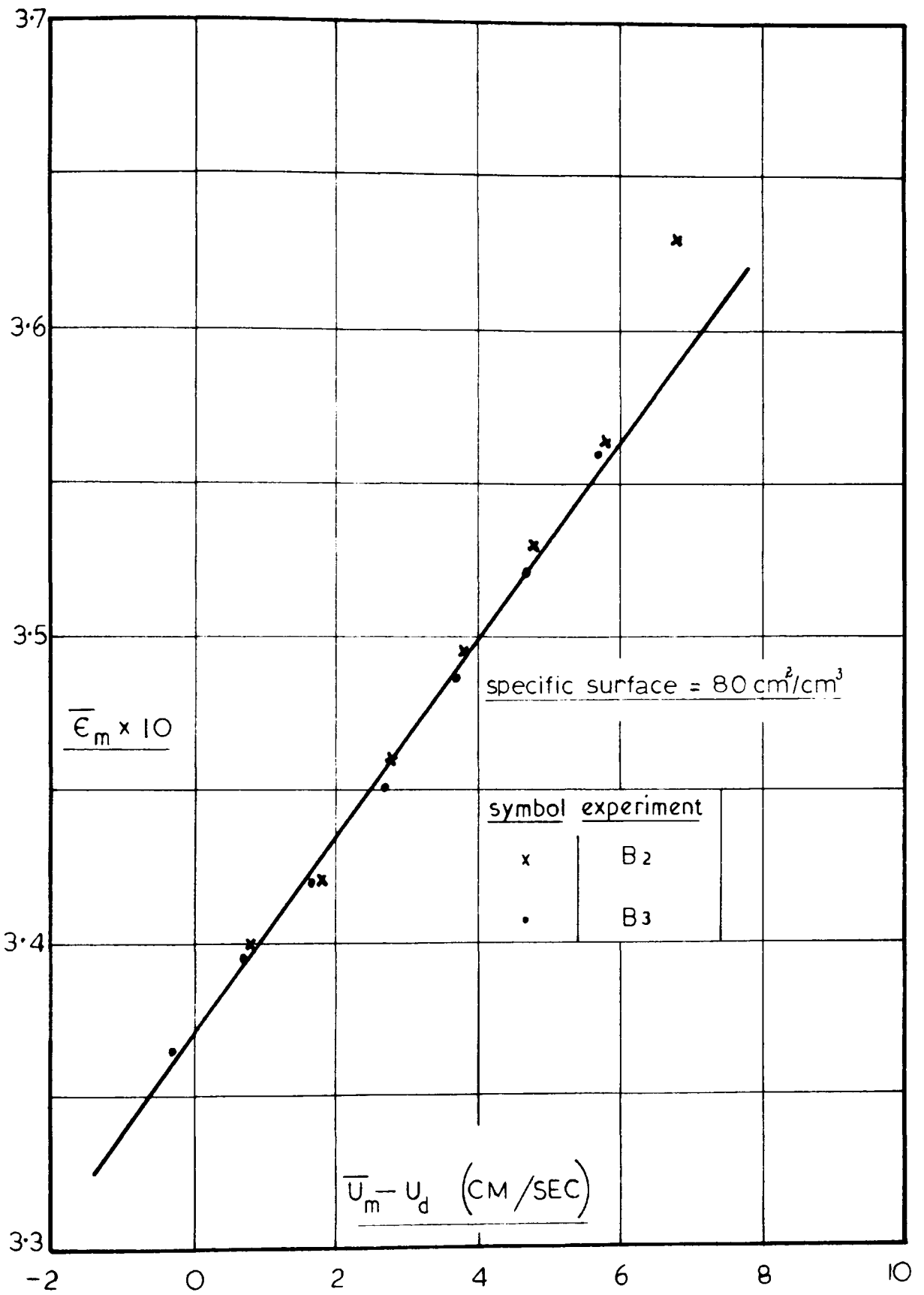


Figure 13

The overall mean void fraction ($\overline{\epsilon}_m$) in the fluidized bed versus the mean superficial velocity in excess of the deviation velocity ($\overline{U}_m - U_d$).

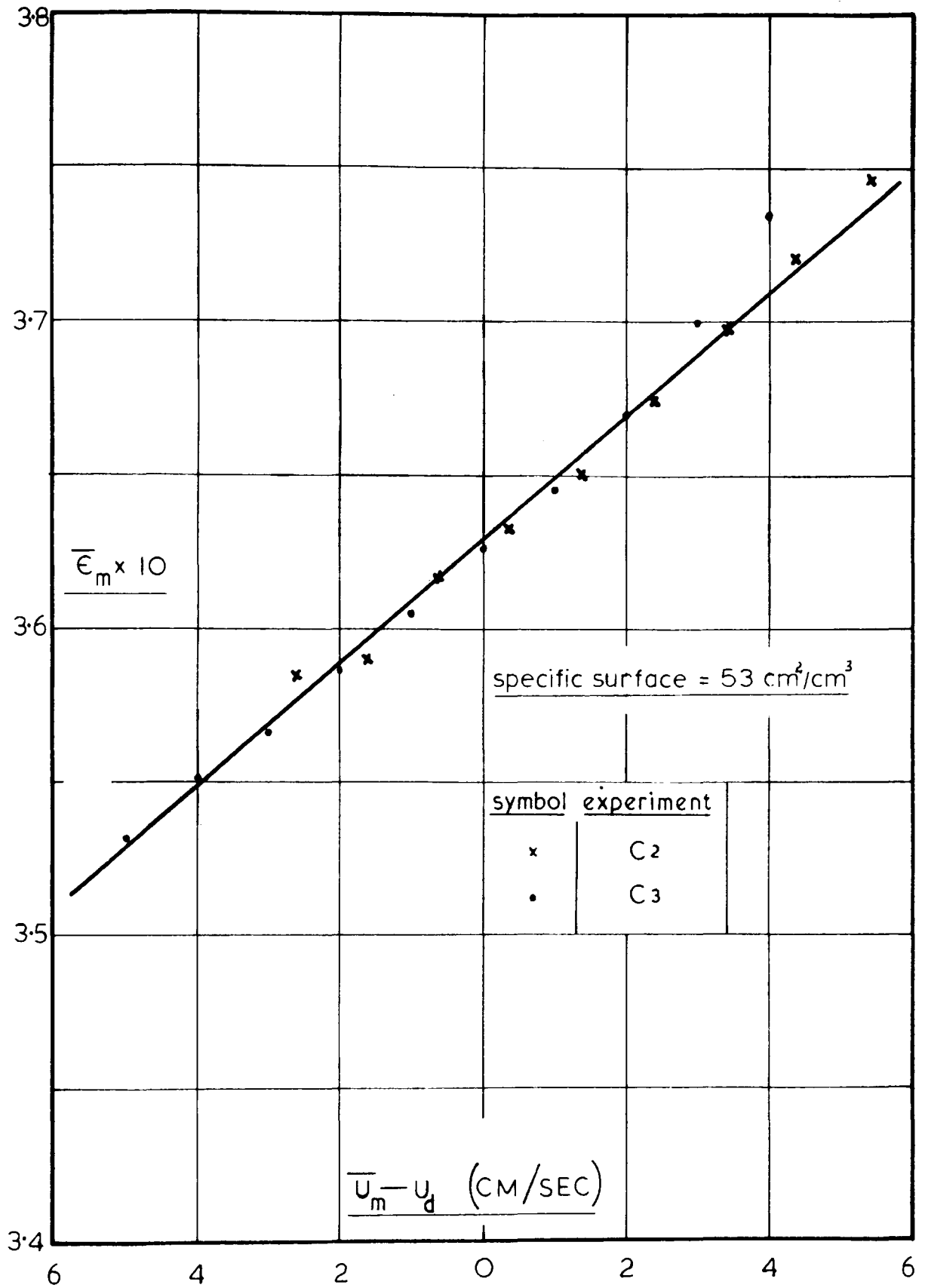


Figure 14

The overall mean void fraction ($\bar{\epsilon}_m$) in the fluidized bed versus the mean superficial velocity in excess of the deviation velocity ($\bar{U}_m - U_d$).

9.22 The effect of bed depth

The effect of bed depth on the overall mean void-fraction existing in the pulsating fluidized bed was studied by employing particles ranging from +150 mesh to 1.9 mm in diameter. Bed cross-sectional area was 6.6 cm^2 and air was used as the fluidizing medium. The maximum bed heights employed were controlled by the behaviour of the bed under pulsating conditions. The physical characteristics of the solid materials employed and the experimental conditions are summarized below:

Experiments D2 - D5

Material used: Zeolite.

Size range: 0.1 to 0.7 mm diameter.

Specific surface: $105.5 \text{ cm}^2/\text{cm}^3$

Fixed-bed depth: 15.7 cm.

Fixed-bed voidage: 0.350.

Experiment No.	Velocity Range	Pulse Frequency
	cm/sec	pulses/min
D2	7.7 - 10.3	800
D3	7.7 - 10.3	900
D4	7.7 - 10.3	1000
D5	7.7 - 11.7	1100

Experiments/...

Experiments E2 - E5

Material used: Zeolite.

Size range: 0.7 to 1.0 mm in diameter.

Specific surface: $73.3 \text{ cm}^2/\text{cm}^3$.

Fixed-bed depth: 25.0 cm.

Fixed-bed voidage: 0.368.

Experiment No.	Velocity Range	Pulse Frequency
	cm/sec	pulses/min
E2	12.7-18.0	700
E3	12.0-17.2	800
E4	13.0-18.0	900
E5	12.0-17.4	1000

Experiment F2

Material used: Rape seed.

Size range: 1.2 to 1.9 mm in diameter.

Specific surface: $51.6 \text{ cm}^2/\text{cm}^3$.

Fixed-bed depth: 58 cm.

Fixed-bed voidage: 0.365.

Experiment No.	Velocity Range	Pulse Frequency
	cm/sec	pulses/min
F2	21.2-23.8	500

The pressure-drop-velocity observations for the series of experiments D, E and F are represented graphically in figures 15, 16 and 17.

The overall mean void-fractions existing in the pulsating fluidized bed are represented graphically for the series of experiments D, E and F in figures 18, 19 and 20.

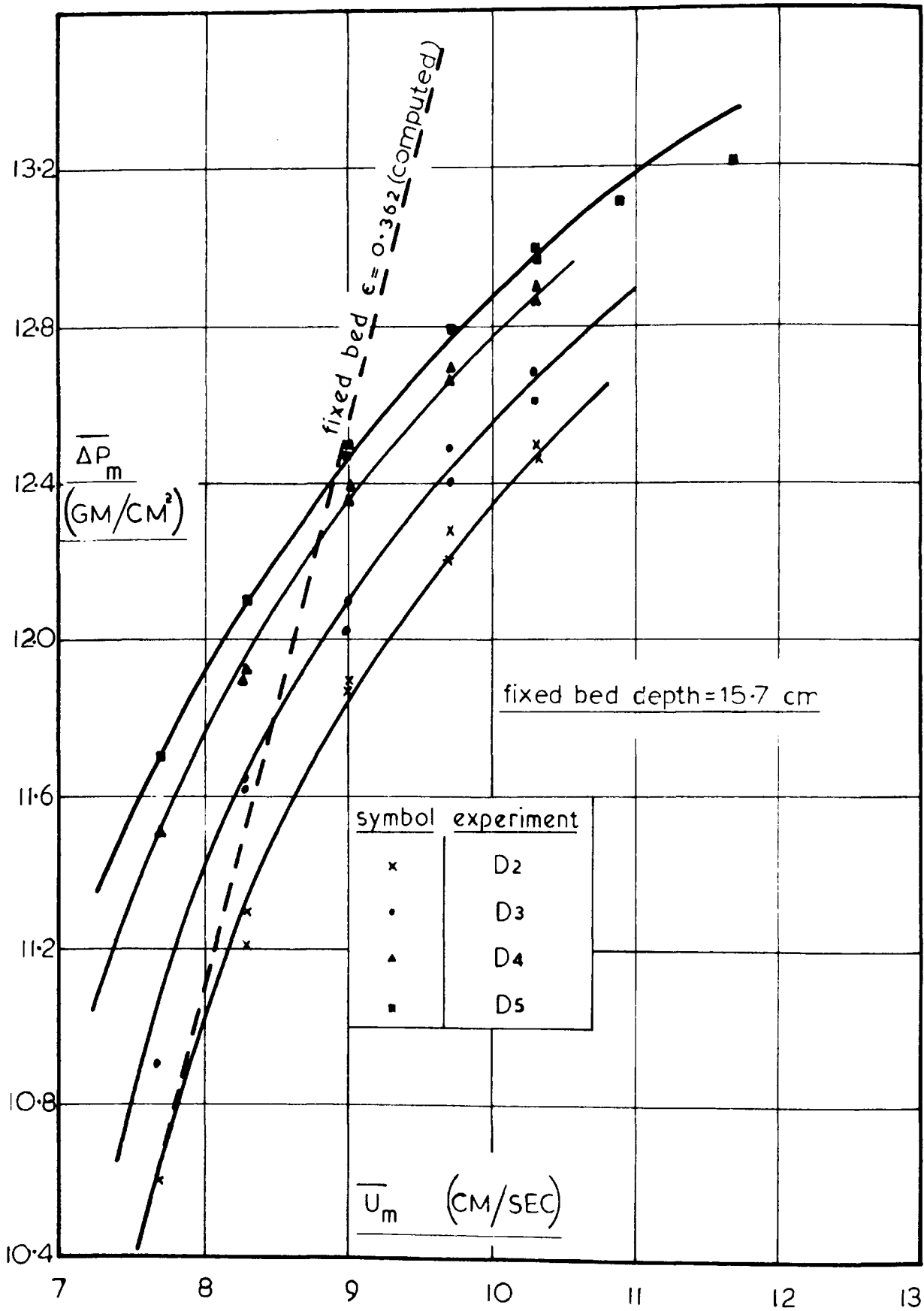


Figure 15

The mean total pressure-drop ($\overline{\Delta P_m}$) across the fluidized bed as a function of the mean superficial velocity ($\overline{U_m}$).

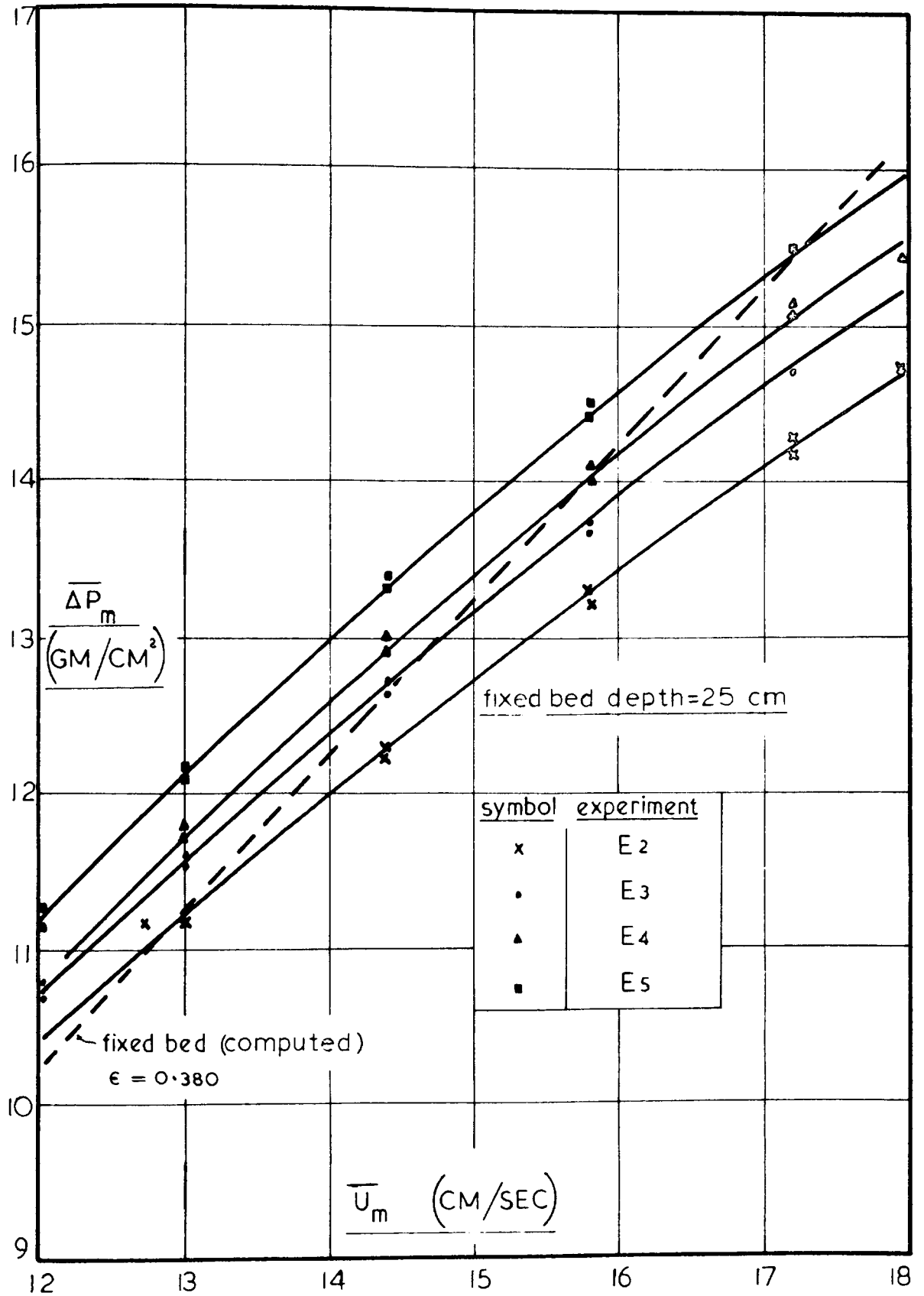


Figure 16

The mean total pressure drop ($\overline{\Delta P_m}$) across the fluidized bed as a function of the mean superficial velocity ($\overline{U_m}$).

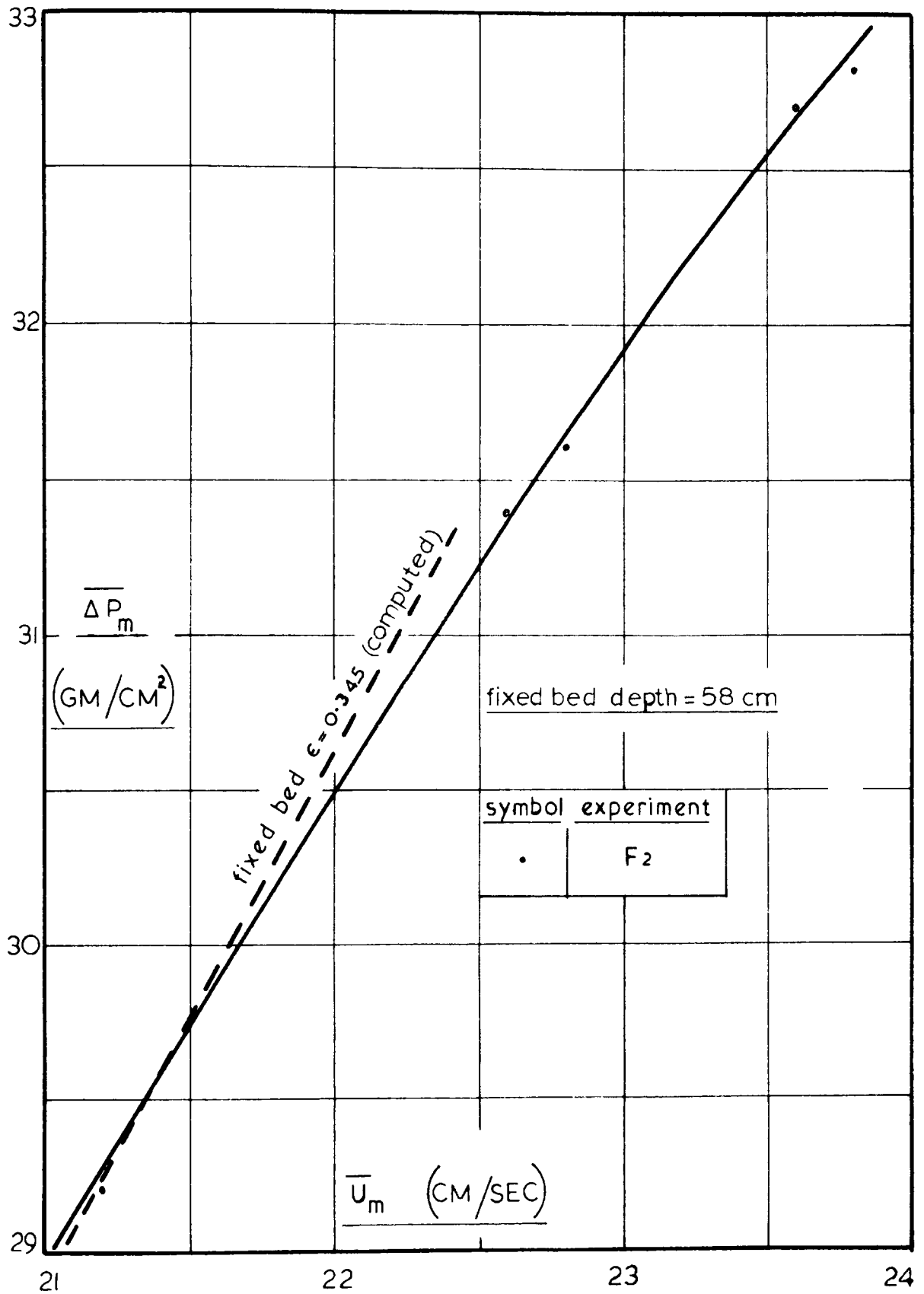


Figure 17

The mean total pressure-drop ($\overline{\Delta P_m}$) across the fluidized bed as a function of the mean superficial velocity ($\overline{U_m}$).

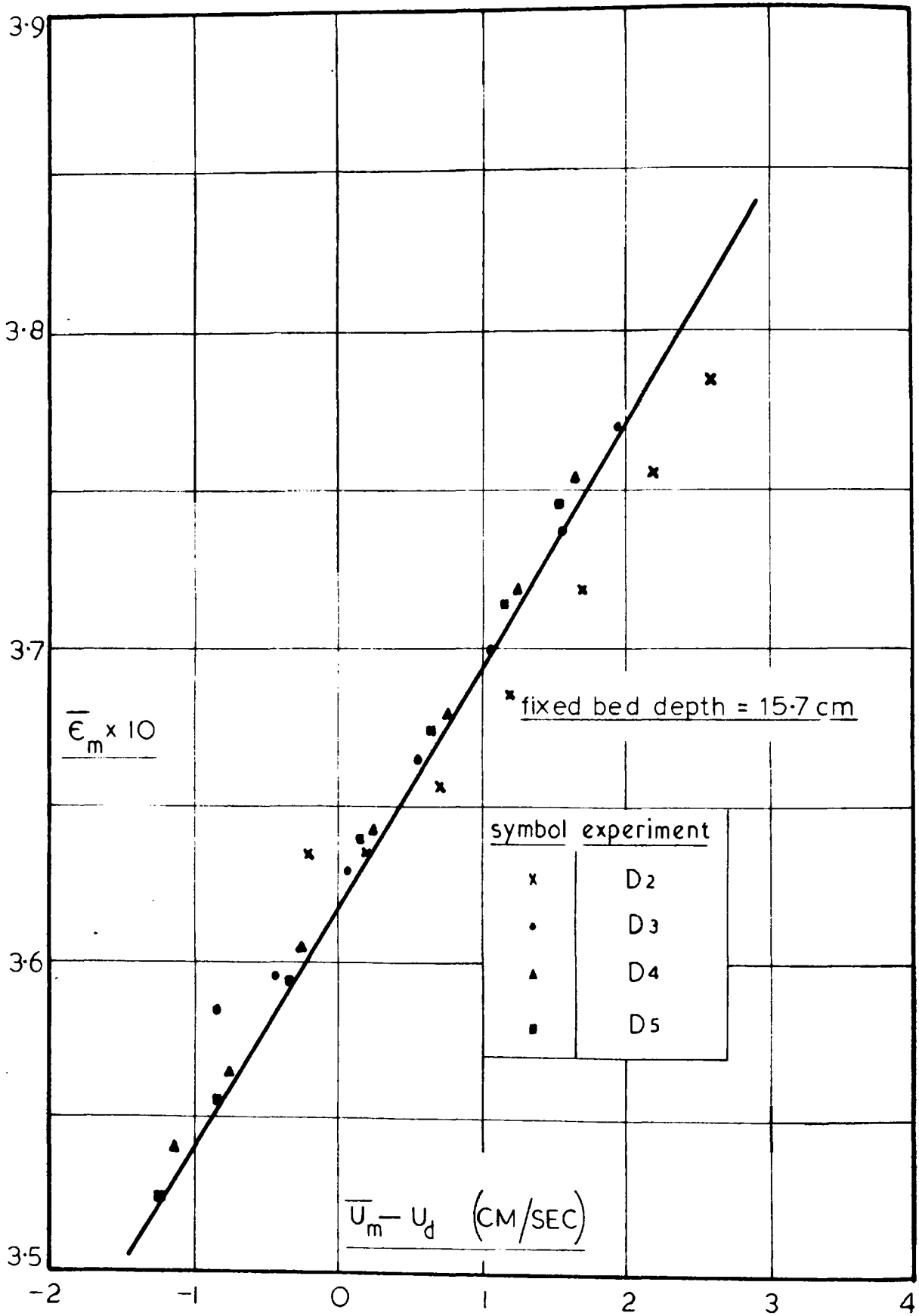


Figure 18

The overall mean void fraction ($\bar{\epsilon}_m$) in the fluidized bed versus the mean superficial velocity in excess of the deviation velocity ($\bar{U}_m - U_d$).

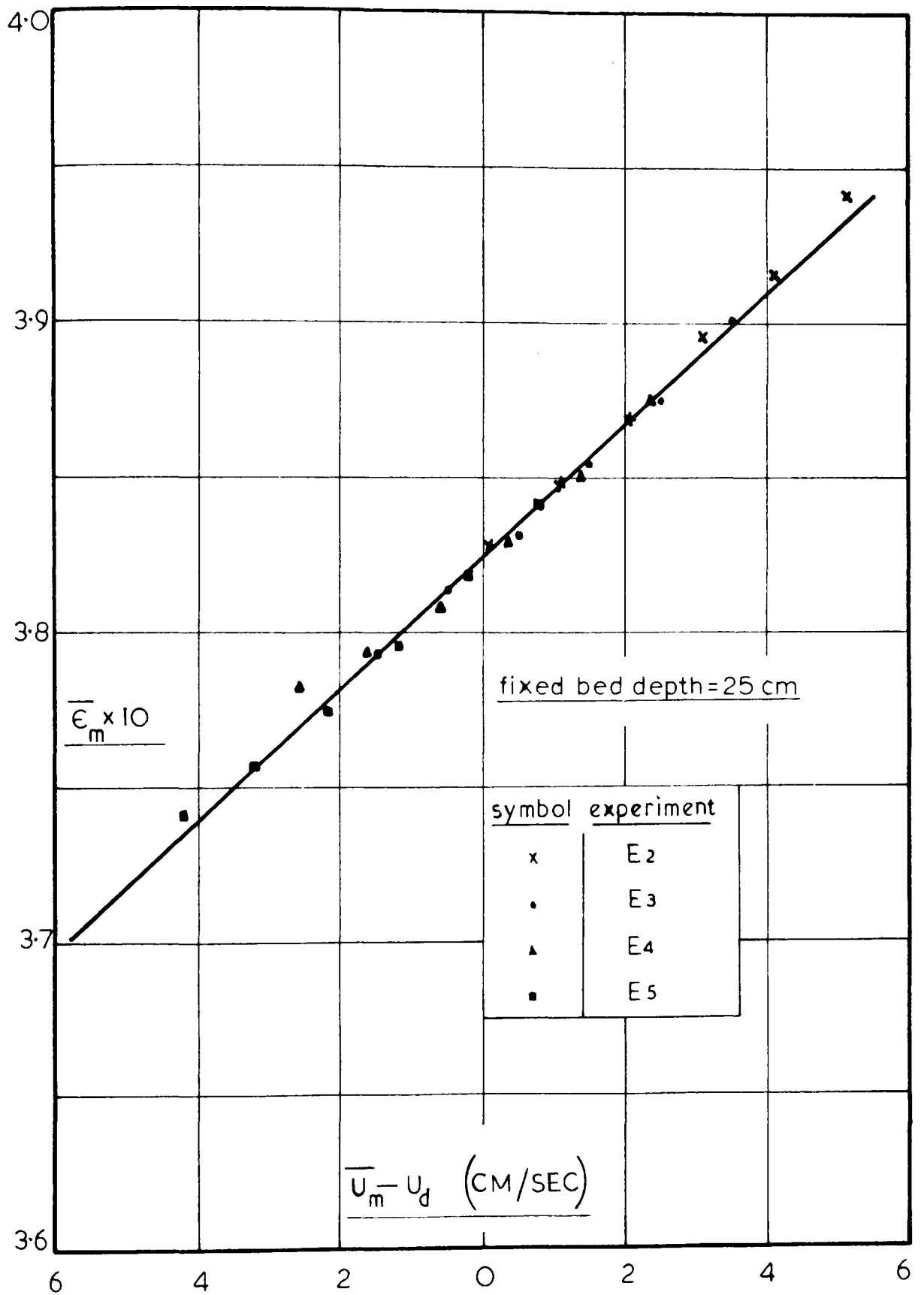


Figure 19

The overall mean void fraction ($\overline{\epsilon}_m$) in the fluidized bed versus the mean superficial velocity in excess of the deviation velocity ($\overline{U}_m - U_d$).

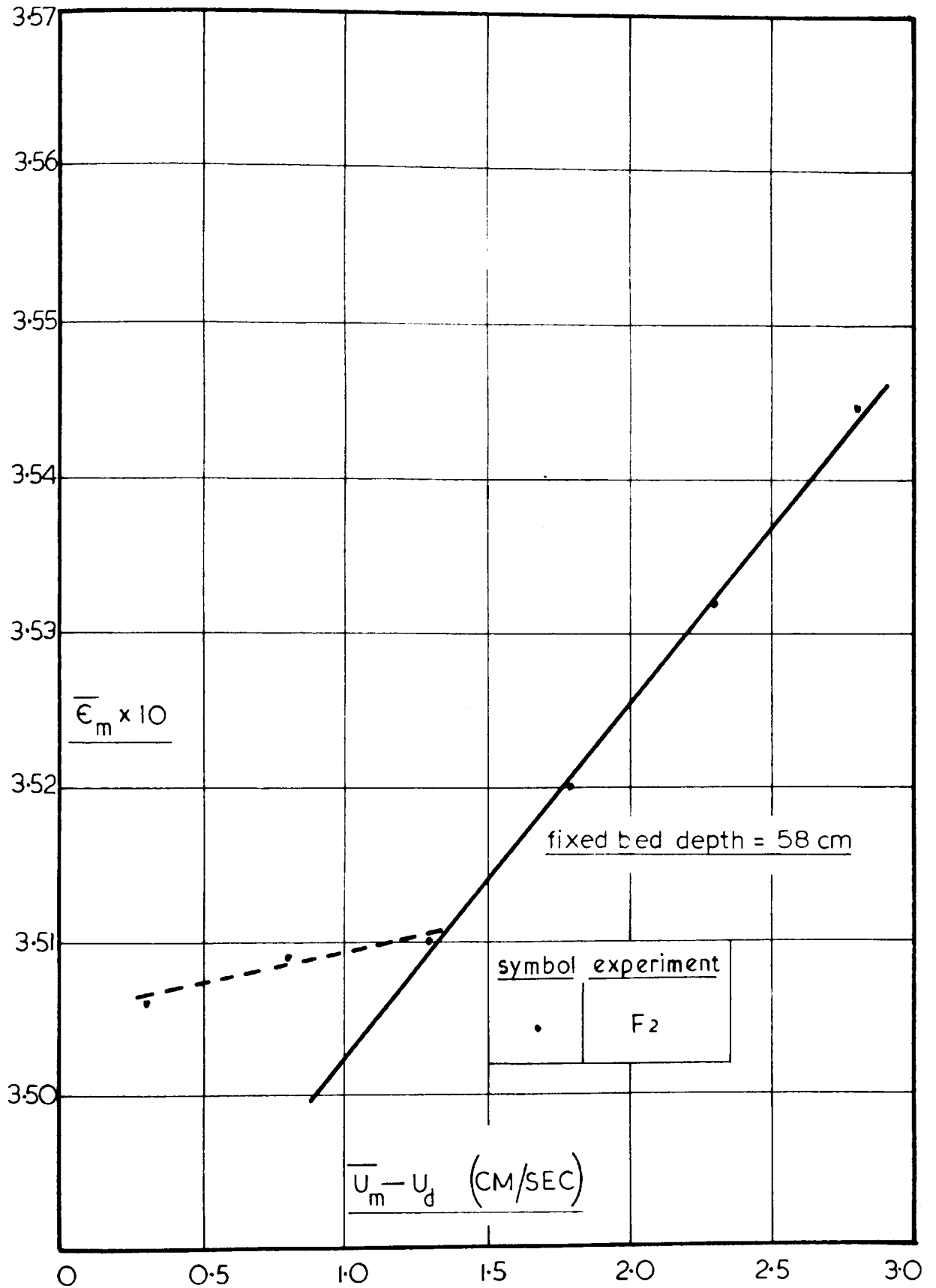


Figure 20

The overall mean void fraction ($\bar{\epsilon}_m$) in the fluidized bed versus the mean superficial velocity in excess of the deviation velocity ($\bar{U}_m - U_d$).

9.23 The effect of increased bed diameter

The effect of increased bed diameter on the overall mean void-fraction existing in the pulsating fluidized bed, was studied by employing clover seed particles. The bed cross-sectional area was increased from 6.6 cm² to 165 cm², and air was again used as the fluidizing medium. The physical characteristics of the solid material used and the experimental conditions are summarized below:

Experiments G2 - G7

Material used: clover seed.

Size range: 0.9 to 1.1 mm in diameter.

Specific surface: 80.3 cm²/cm³.

Fixed-bed depth: 11.0 cm.

Fixed-bed voidage: 0.345.

Bed area: 165 cm².

Experiment No.	Velocity Range	Pulse Frequency
	cm/sec	pulses/min
G2	8.7 - 12.8	800
G3	7.8 - 12.1	800
G4	7.8 - 12.6	900
G5	7.9 - 12.2	1000
G6	8.7 - 12.2	1100
G7	8.5 - 12.2	1200

The pressure-drop-velocity observations for experiments G are represented graphically in figure 21. The overall mean void-fractions existing in the pulsating fluidized bed are represented graphically in figure 22.

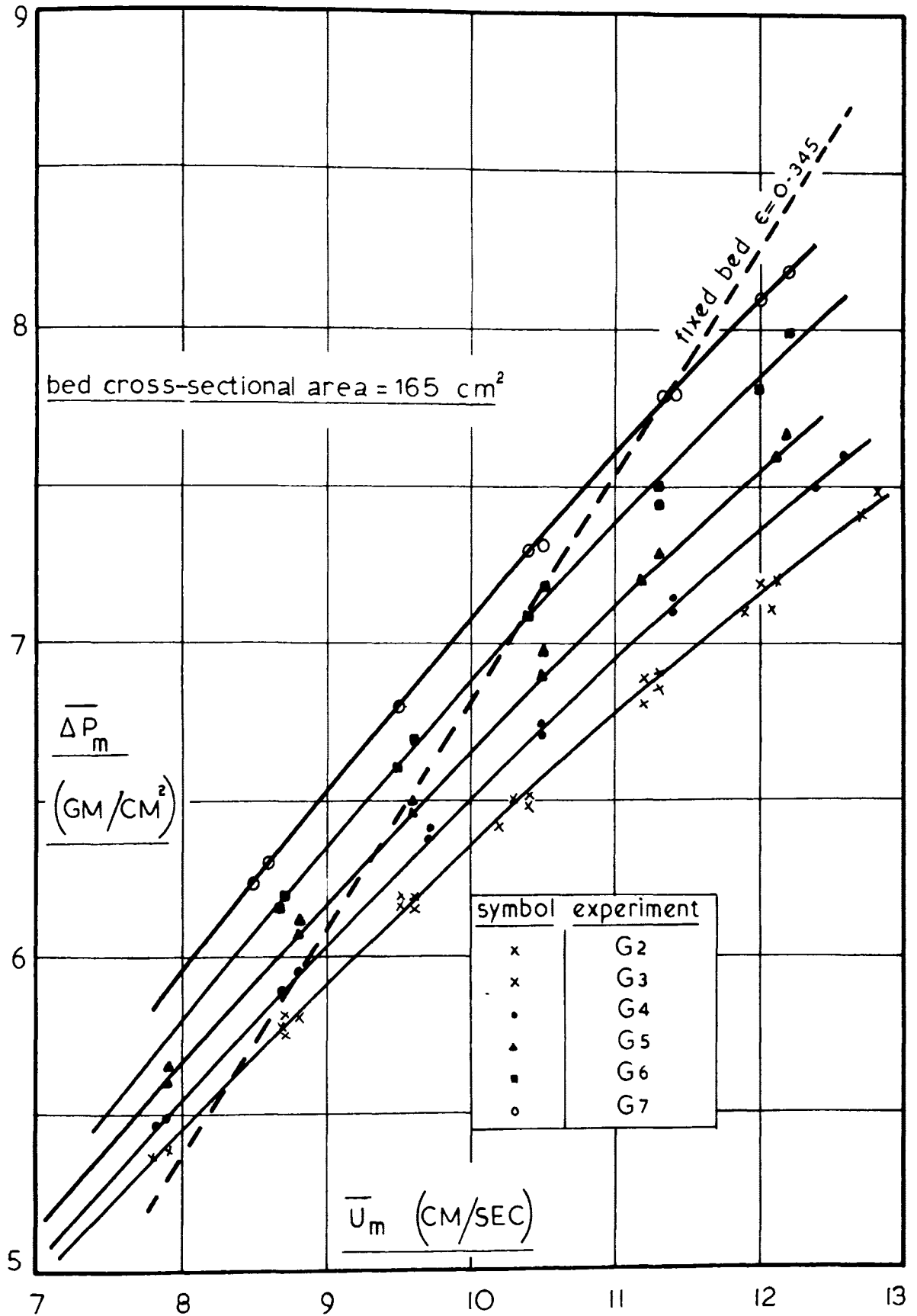


Figure 21

The mean total pressure-drop ($\overline{\Delta P_m}$) across the fluidized bed versus the mean superficial velocity ($\overline{U_m}$).

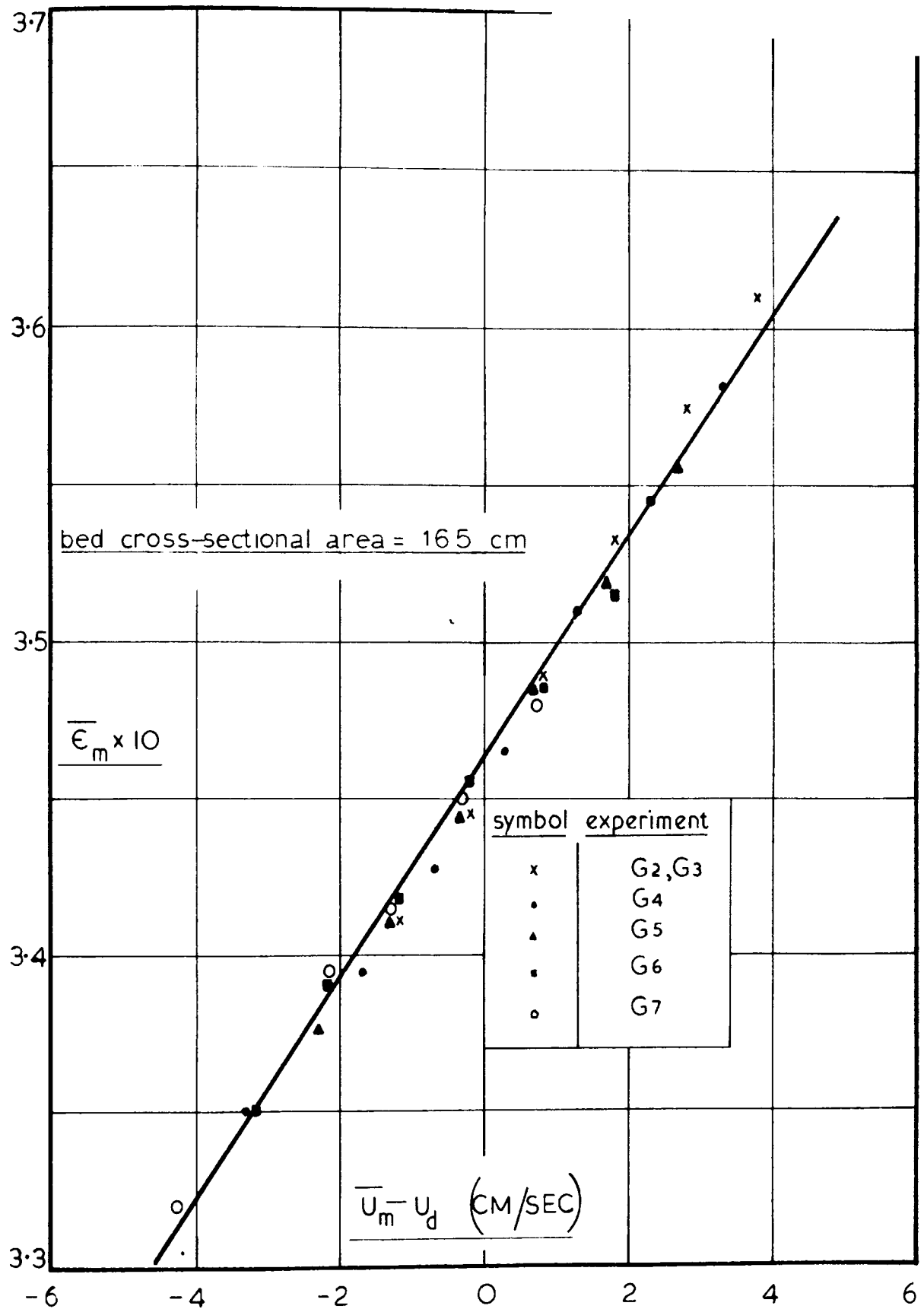


Figure 22

The overall mean void fraction ($\bar{\epsilon}_m$) in the fluidized bed versus the mean superficial velocity in excess of the deviation velocity ($\bar{U}_m - U_d$).

9.24 Reproducibility of results

The purpose of the G2 and G3 series of tests in the aforementioned table was to check the reproducibility of results obtained. The results are graphically illustrated in figure 21.

Instantaneous/...

9.25 Instantaneous functions

Experiments were performed to obtain the instantaneous pressure-drop across the pulsating fluidized bed under various conditions. From the instantaneous pressure-drop curve the instantaneous relative-velocity curve may be computed, which, in turn, yields the computed mean superficial velocity. Comparison of the computed and observed mean superficial velocities will indicate the validity of the theory.

The applied pulse-frequencies ranged from 800 to 1200 pulses/minute. In addition to the effect of the pulse frequency on the instantaneous pressure-drop, the effect of velocity variation was also studied, employing a constant pulse-frequency of 1000 pulses/minute. The physical characteristics of the solid material and the experimental conditions employed are summarized below:

Experiments/...

Experiments H1 - H7

Solid material: Clover seed.

Size range: 0.9 to 1.1 mm in diameter.

Specific surface: $80.3 \text{ cm}^2/\text{cm}^3$.

Fixed-bed depth: 11.0 cm.

Fixed-bed voidage: 0.345.

Experiment No.	Pulse Frequency pulses/min	Mean Superficial Velocity cm/sec	
		Observed	Computed
H1	1000	11.3	11.2
H2	1000	10.8	10.9
H3	1000	9.2	9.3
H4	800	10.3	10.3
H5	900	10.3	10.3
H6	1100	10.1	10.2
H7	1200	9.9	9.9

Typical instantaneous pressure-drop curves, and the corresponding computed relative superficial-velocity curves, are given in figures 23 to 26.

10./...

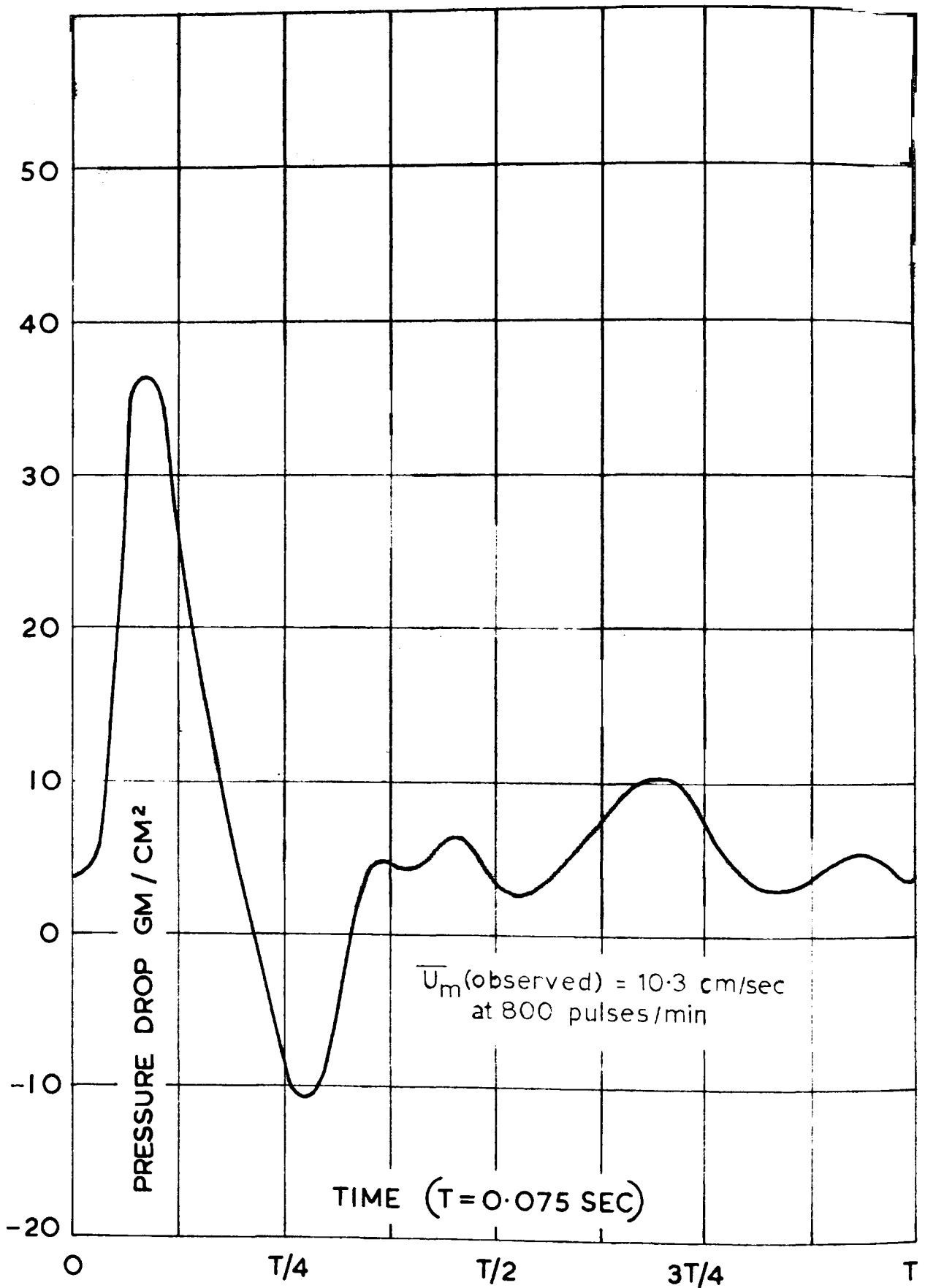


FIGURE 23 TRANSIENT PRESSURE DROP RESPONSE CURVE

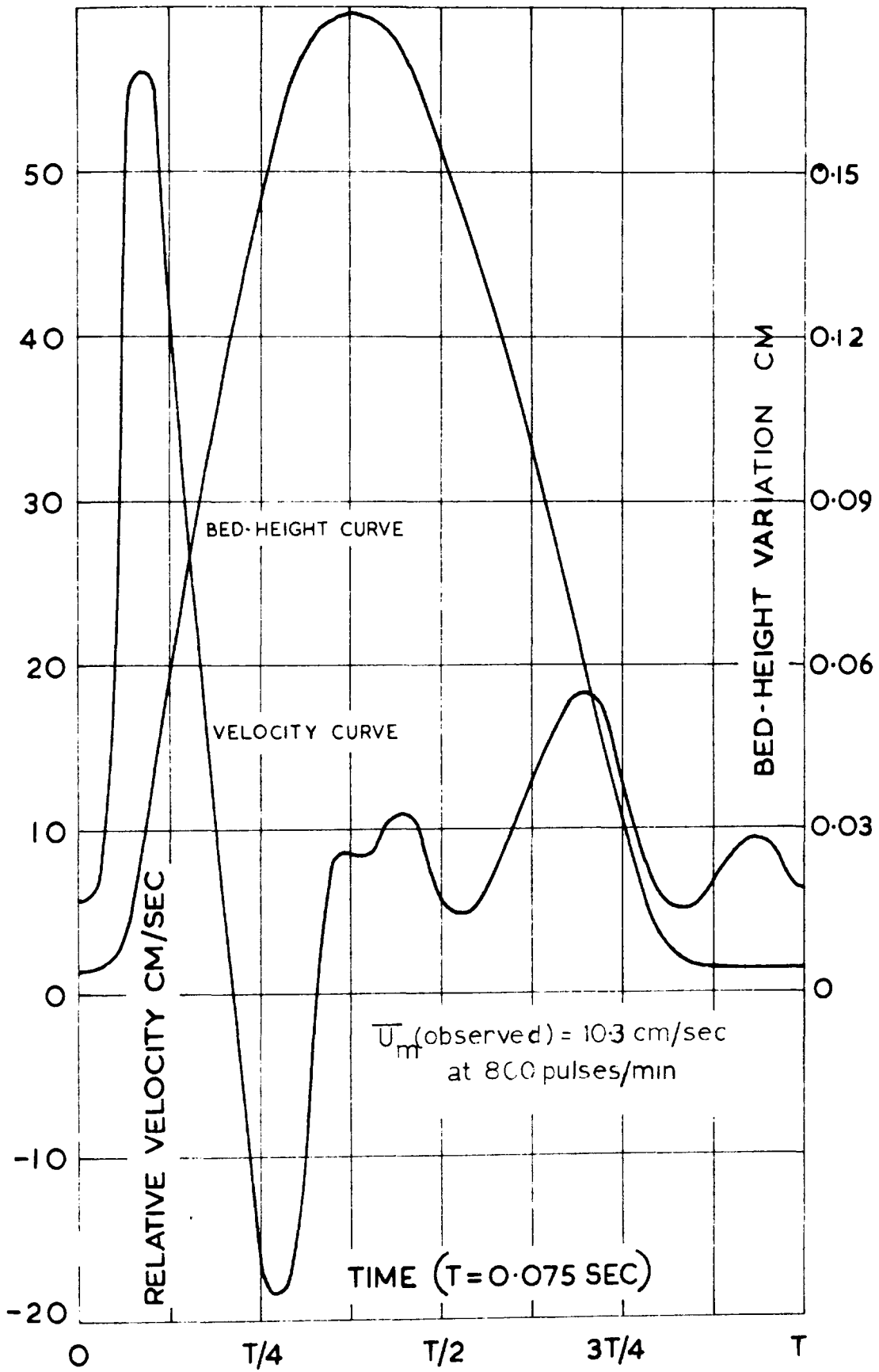


FIGURE 24 TRANSIENT RESPONSE CURVES OF VELOCITY AND BED INTERFACE

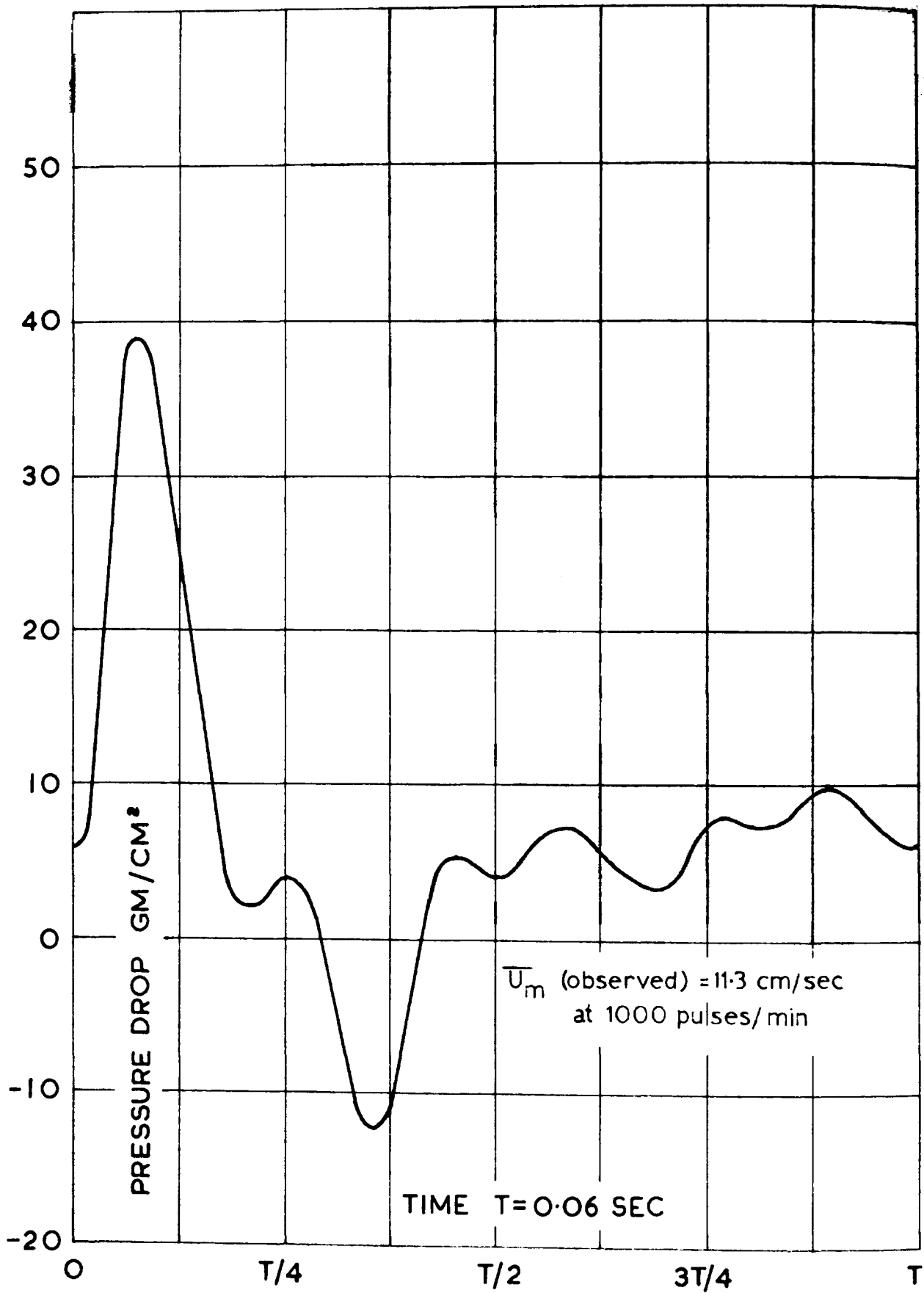


FIGURE 25 TRANSIENT PRESSURE DROP RESPONSE CURVE

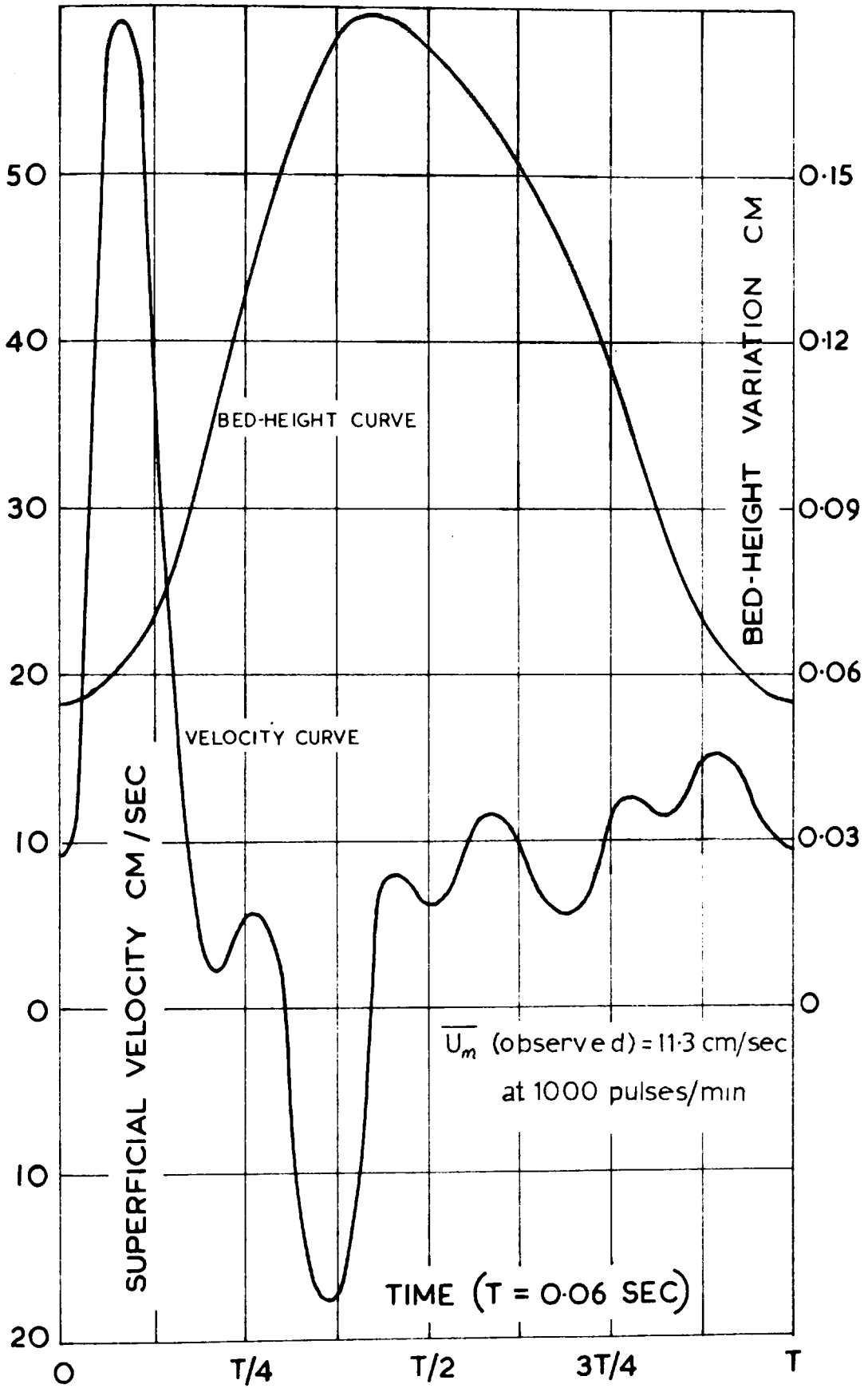


FIGURE 26 TRANSIENT RESPONSE CURVES OF VELOCITY AND BED INTERFACE

10. DISCUSSION OF RESULTS

10.1 Properties of the Pulsating Fluidized Bed.

10.11 Bubble suppression

Solids, which are otherwise difficult to fluidize, may be readily fluidized without bubble formation by a pulsating flow. A proposed mechanism for bubble suppression is given below.

Due to the inertia of the particles, a finite period is required for bubbles to form. The decay of the fluid velocity is such that the bed collapses before bubbles have developed. Thus, although the peak velocity during a pulse cycle may be sufficient for bubble formation, bubbles are still suppressed. In addition, the particle vibration will cause any small bubbles present to collapse.

10.12 Bed oscillation

At increased bed depths the bed proper attains an additional oscillation apart from particle vibration. The oscillation frequency is generally much less than the fluid pulse frequency. The following mechanism is suggested.

Due to fluid expansion, the particle displacement increases along the bed, being the greatest at the top. Due to the difference in displacement, the direction of particle motion at the top of the bed will be out of phase with that at the bottom. The particle vibration in the interior of the bed will periodically be suppressed, giving

rise/...

rise to local voidage reductions. The pressure drop across the bed will thus vary from time to time.

10.2 Fixed Bed Results

The constants a and b , employed in the evaluation of the voidage in the pulsating fluidized beds, are obtained from the fixed bed. Referring to Table A on page 39, it may be seen that the magnitude of b is roughly 1% that of a . It thus follows that the kinetic energy losses are no longer negligible. In the fixed bed the pressure drop increases parabolically with velocity.

10.3 Pulsating Fluidized Bed

10.3.1 The pressure-drop-velocity relation for the pulsating fluidized bed.

When the fluid velocity is increased, the pressure drop will initially increase parabolically, similar to uniform fluid-flow through a fixed bed. When the minimum fluidization velocity is exceeded, the pressure drop still increases but is less than the predicted parabolic value. This deviation is due to the bed-voidage increasing with fluid velocity. When the maximum fluidization velocity is exceeded, the pressure drop tends to be independent of velocity. This is due to large volumes of fluid passing through the bed as bubbles.

In the experiments, the fluid velocity was varied between the minimum and the maximum fluidization velocities. Velocities outside this region

were/...

were considered to be of lesser importance.

10.32 The effect of pulse frequency on the pressure drop.

The amplitude of particle vibration, and hence the effective bed voidage, will decrease with increase in pulse frequency. The pressure drop at constant velocity will thus increase with increase in pulse frequency. When various pulse frequencies are employed, a family of pressure-drop curves will result.

Upon increase of the pulse frequency, the particle vibration will eventually cease. This gives the upper pulse-frequency. Being a function of particle inertia, the limiting frequency will be expected to decrease with increase in particle size. As particle vibration is zero at the limit, the experimental upper frequency was taken at roughly 100 pulses/minute below the limiting value. From Experiments A and C it is seen that the upper frequency decreases from 1200 to 900 pulses/minute if the size range is increased from 0.1 - 0.7 to 1.2 - 1.9 mm in diameter.

At low pulse-frequencies pressure-drop determinations become inaccurate.

10.33 Factors limiting the bed depth.

Bed depths are limited by two factors, viz. bubble formation and bed oscillation.* If the

particle/...

* See section 10.12.

particle size range is large, segregation occurs and the smaller particles accumulate in the top of the bed. The maximum fluidization velocity thus varies along the bed, being less at the top. At increased depths, the velocity increase due to expansion may be such that bubbles form in the top of the bed. In the experimental series D, using 0.1 - 0.7 mm diameter particles, bubbles occurred at a depth of 16 cm.

For larger particles, bed oscillation limits the depth. In the experimental series E, using 0.7 - 1.0 mm diameter particles, oscillation occurred at 25 cm. In the series F, using 1.2 - 1.9 mm particles, oscillation occurred at a depth of 40 cm. The bed depth was increased to 58 cm. Oscillation became so severe that pressure-drop determinations were possible only at low pulse-frequencies.

It thus appears that the maximum bed-depth increases with increase in particle size.

10.34 Void fraction within the pulsating fluidized bed.

When the fluid velocity is increased, the voidage will initially remain constant. When the minimum fluidization velocity is exceeded, the voidage will increase with velocity. Above the maximum fluidization velocity the voidage will vary with time due to bubble formation. In Experiment F low velocities were used, due to

bed/...

bed oscillation. Here the voidage initially remains constant, as may be seen from Figure 20.

Void fraction data are represented empirically by plotting against the mean superficial velocity in excess of the deviation velocity. Referring to figures 12, 13, 14, 18, 19, 20 and 22, it will be seen that the voidage for all pulse frequencies may be correlated by a straight line. The voidage at constant velocity decreases with increase in pulse frequency.

10.35 The effect of various factors on the voidage of the pulsating fluidized bed.

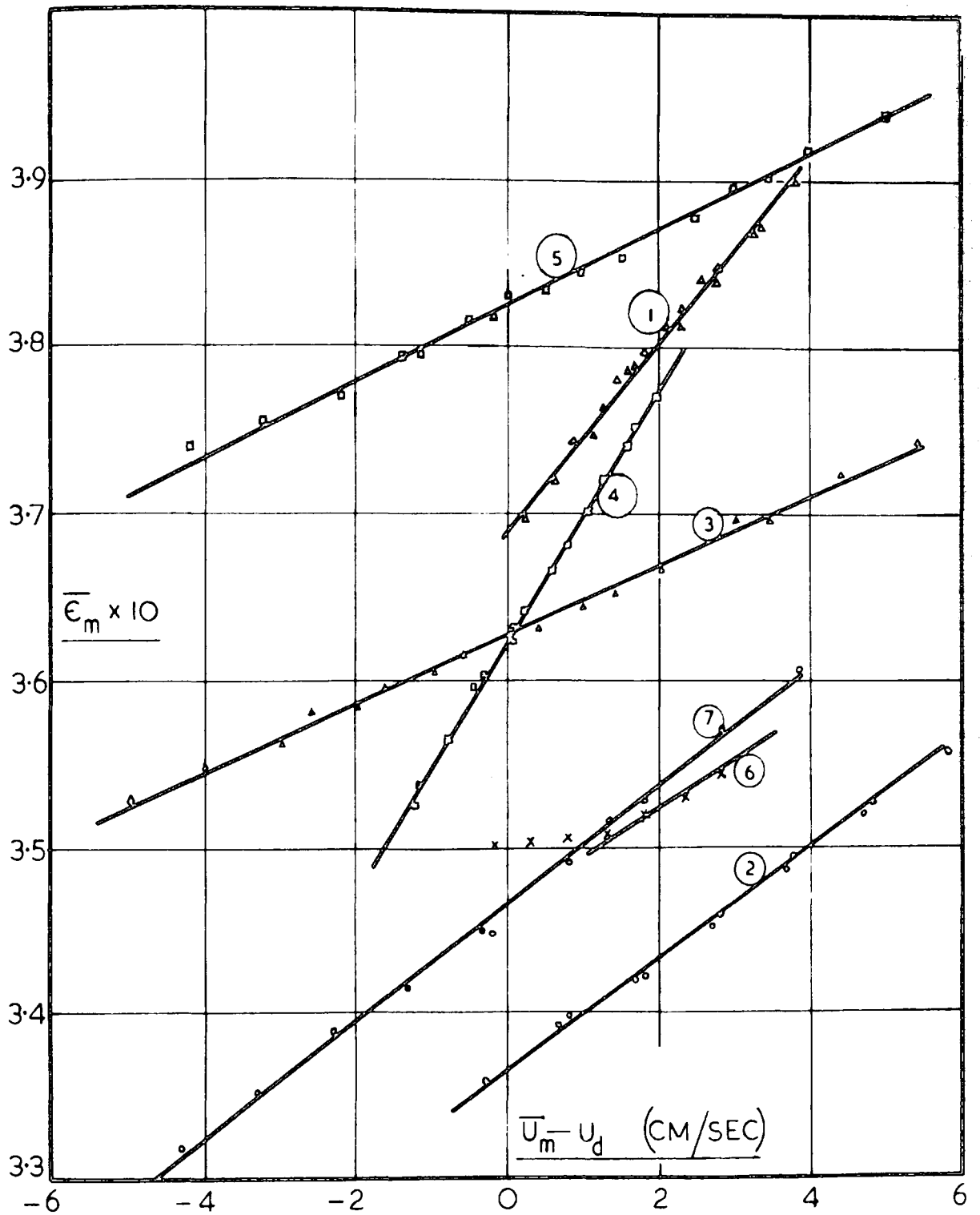
The effect of particle size, bed depth and bed diameter on the pulsating fluidized bed may be studied from the voidage correlation.

Curves 1, 2 and 3, in Figure 27, indicate that the slope of the correlation line decreases with increase in particle size. Thus, to effect a given voidage increase, the velocity required increases with increase in particle size.

Comparison of curve 1 with curve 4 and of curve 3 with curve 6 indicates an increase of slope with increase in bed depth. The effective voidage at constant velocity is, thus, a function of bed depth and decreases with increase in bed depth.

Comparison of curves 2 and 7, in Figure 27, indicates that the voidage is independent of the bed diameter.

10.36/...



curve number	material employed	fixed bed depth cm	bed area cm ²	specific surface cm ² /cm ³
1	zeolite	9.7	6.6	106.5
2	clover seed	10.1	6.6	80.3
3	rape seed	9.0	6.6	53.3
4	zeolite	15.7	6.6	105.5
5	zeolite	25.0	6.6	73.3
6	rape seed	58.0	6.6	51.6
7	clover seed	11.0	165.0	80.3

Figure 27

The overall mean void fraction ($\bar{\epsilon}_m$) as a function of the mean superficial velocity in excess of the deviation velocity ($\bar{U}_m - U_d$) for the experiments indicating the effect of particle diameter, bed depth and bed diameter on bed voidage.

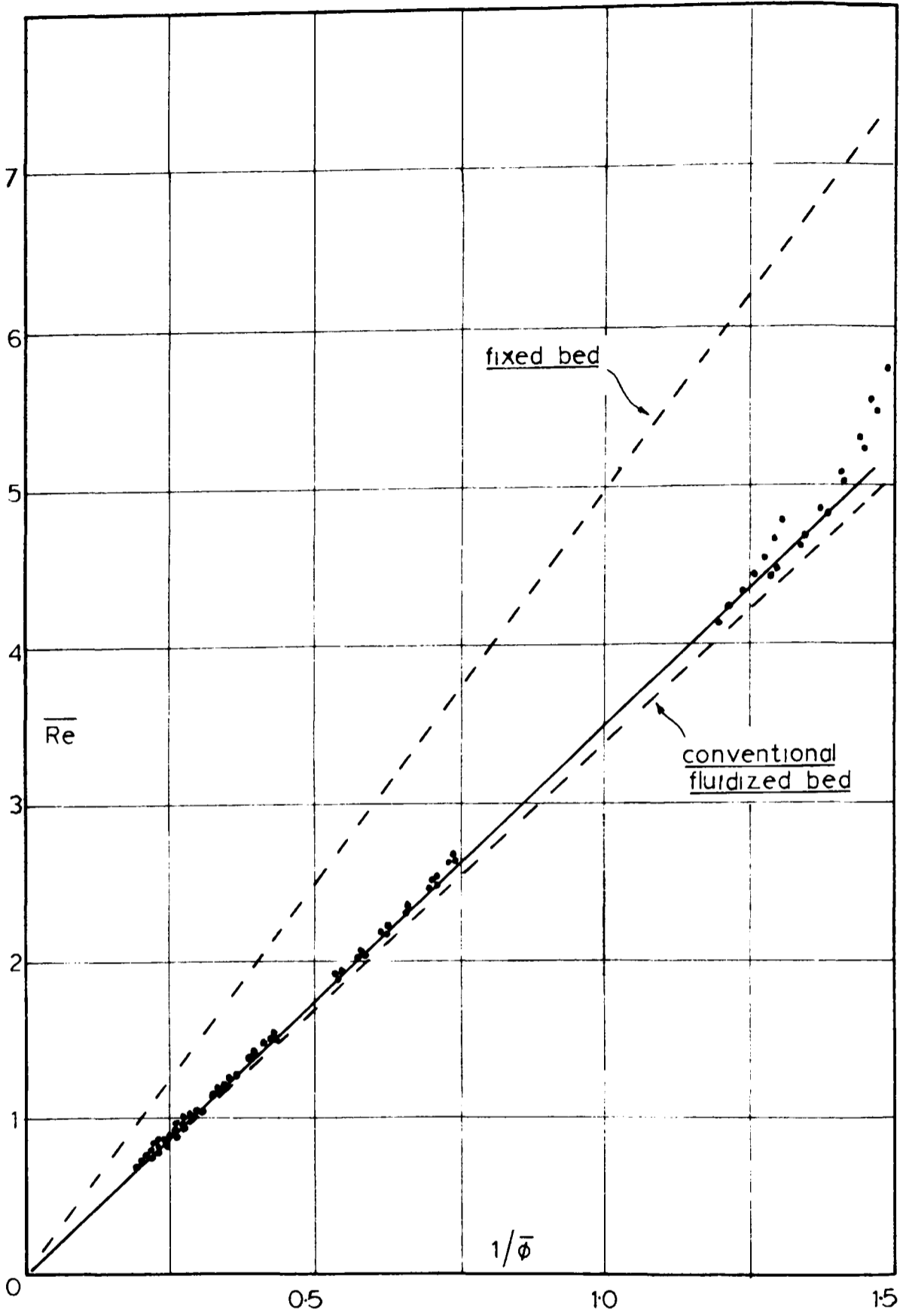


Figure 28

The modified Reynolds number (\overline{Re}) versus the inverse modified friction factor ($1/\overline{\phi}$)

10.36 Modified Reynolds number and modified friction factor.

The modified Reynolds number and the modified friction factor serve to substantiate the value of the form factor, F , obtained from theoretical considerations. The product of the dimensionless groups is given by:

$$\overline{Re} \times \overline{\phi} = \frac{5}{F^2} = 3.47$$

Correlation of the experimental data by this relation, in Figure 28, indicates that $F = 1.2$ is satisfactory.

In Figure 28 the experimental results are compared with curves for uniform fluid-flow through fixed and fluidized beds. The pulsating fluidized bed shows a curve similar to that of a conventional fluidized bed.

In Appendix 5 the product of the dimensionless groups is not constant. This may be due to the fact that in the equation for the specific surface no cognisance is taken of kinetic energy losses.

10.37 Velocity range.

The velocity range for the pulsating fluidized bed is taken as the range in which bubbles and channelling are absent. The velocity range is small and increases with particle size. In Experiment A, using particles of 0.1 to 0.7 mm in diameter, the velocity range is 6.4 - 10.4 cm/sec. In

Experiment/...

Experiment C, using 1.2 - 1.9 mm particles, the velocity range increases to 22 - 37 cm/sec. These results also indicate that the minimum fluidization velocity increases with particle size. The velocity range decreases with increase in bed depth. Comparison of Experiment C with Experiment F indicates a decrease in velocity range from 22 - 37 cm/sec to 21 - 24 cm/sec when the bed depth was increased from 9 cm to 58 cm.

10.38 Instantaneous functions

The theory facilitates the construction of the instantaneous relative-velocity curve from the instantaneous pressure-drop curve. Comparison of the computed mean superficial velocity, obtained from the instantaneous relative-velocity curve, with the observed mean superficial velocity, indicates the plausibility of the proposed theory. Observed and computed mean superficial velocities are given below.

Experiment Number	Mean Superficial Velocity cm/sec		Pulse Frequency
	Observed	Computed	Pulses/min
H1	11.3	11.2	1000
H2	10.8	10.9	1000
H3	9.2	9.3	1000
H4	10.3	10.3	800
H5	10.3	10.3	900
H6	10.1	10.2	1100
H7	9.9	9.9	1200

As may be seen, the agreement is excellent, which would seem to substantiate the proposed theory.

Figures 23 to 26 show typical instantaneous curves. The non-specific, instantaneous bed inter-

face/...

face curves are included merely to serve as an illustration of the type of motion to which the particles are subjected.

At low volumetric flow-rates the particles will be lifted due to the drag exerted on them, but the decay of the fluid velocity will be such that the particles will fall back and resettle as a fixed bed. This is illustrated in Figure 24. At increased volumetric flow-rates (refer to Figure 26), the bed expansion will be such that during the decay of the fluid velocity the particles cannot resettle into a fixed-bed configuration. The particles in their downward motion will encounter the next fluid pulse and the particle motion will be arrested and eventually reversed. Thus, at greater volumetric flow-rates the particle bed is never in a settled fixed-bed state. The phase lag between the bed interface and the fluid velocity is caused by the particle-bed inertia.

11. FINAL CONCLUSIONS

Solids, which are otherwise difficult to fluidize, are readily fluidized with pulsating fluid-flow. In pulsating beds of moderate depth, channelling and bubble formation may be effectively eliminated.

As the fluid velocity is increased, the pressure drop initially increases parabolically, similar to uniform fluid-flow through fixed beds. Above the minimum fluidization velocity the pressure drop still increases, but is less than the parabolic value. Above the maximum fluidization velocity the pressure drop becomes independent of velocity. When the bed is fluidized, the pressure drop increases with pulse frequency. Thus a family of pressure-drop curves is obtained. The pressure drop decreases as particle size increases.

The voidage of the pulsating fluidized bed, although independent of the bed diameter, was found to depend on other factors as follows:

Firstly, the voidage was found to decrease with both increasing pulse frequency and increasing bed depth (at constant velocity). Further, the voidage increased with velocity and the effect was found to depend on particle size.

The velocity range in which bubbles are suppressed is small. The velocity range at constant bed depth increases with increase in particle size. The velocity range decreases with increase in bed depth.

An/...

An upper pulse-frequency exists beyond which particles cease to vibrate. The upper pulse-frequency decreases with increase in particle size. If the bed proper oscillates, only very low pulse-frequencies are suitable.

Bed depths are limited by either bubble formation or oscillation of the bed proper. The maximum bed depths increase with particle size.

Large particles, up to 2 mm in diameter, are fluidized as readily as smaller particles.

12. APPENDICES
APPENDIX 1
FIXED-BED EXPERIMENTS

The Pressure-drop-velocity observations for the experiments performed on the various fixed beds are given in Tables 2 to 8.

The constants a and b, defined by the equation

$$\Delta P_{fm} = a U_m + b U_m^2 \dots\dots\dots (10a)$$

together with other physical characteristics of the various fixed beds, are given in Table 1.

TABLE 1

Table No.	Experiment No.	Constants		Mean Void Fraction ϵ_m	Fixed Bed Height cm	Specific Surface cm^2/cm^3
		a	$b \times 10^{-3}$			
2	A1	0.793	4.35	0.365	9.7	106.4
3	B1	0.663	4.34	0.335	10.1	80.3
4	C1	0.130	2.40	0.365	9.0	53.3
5	D1	1.520	6.10	0.350	15.7	105.5
6	E1	0.899	5.90	0.368	25.0	73.3
7	F1	0.870	13.70	0.365	58.0	51.6
8	G1	0.646	3.50	0.345	11.0	80.3

TABLE 2/...

TABLE 2

Experiment A1		
Pressure Drop Across Fixed Bed	Superficial Velocity at Mean Bed Conditions	Temperature of Fluid
ΔP_{fm}	U_{in}	
gm/cm ²	cm/sec	°C
21.7	24.4	26.5
20.7	23.1	
19.2	21.7	26.5
17.8	20.3	
16.4	18.8	26.8
15.0	17.4	
13.8	15.8	
12.5	14.6	26.5
11.1	13.2	
10.0	11.8	
8.7	10.4	26.8
7.7	9.1	
6.5	7.7	26.8
5.4	6.5	
4.4	5.3	26.8
3.4	4.0	
2.3	3.8	
1.2	1.6	26.6

TABLE 3

Experiment B1		
Pressure Drop Across Fixed Bed	Superficial Velocity at Mean Bed Conditions	Temperature of Fluid
ΔP_{fm}	U_m	
gm/cm ²	cm/sec	°C
5.1	7.4	18.9
4.7	6.7	18.9
4.6	6.0	
3.6	5.2	18.9
3.1	4.6	
2.5	3.8	19.0
1.9	2.9	
1.4	2.1	19.0
0.9	1.2	19.0

TABLE 4/...

TABLE 6

Experiment E1		
Pressure Drop Across Fixed Bed	Superficial Velocity at Mean Bed Conditions	Temperature of Fluid
ΔP_{fm}	U_m	
gm/cm ²	cm/sec	°C
24.9	23.9	18.5
23.4	22.5	
21.6	21.2	18.8
20.1	19.8	
18.4	18.4	18.9
17.0	17.0	
15.6	15.7	19.0
14.1	14.3	
12.5	12.9	19.0
11.2	11.6	
9.8	10.2	19.1
8.6	8.9	
7.2	7.6	19.2
6.0	6.3	
3.7	3.9	19.3
1.4	1.6	

TABLE 7

Experiment F1		
Pressure Drop Across Fixed Bed	Superficial Velocity at Mean Bed Conditions	Temperature of Fluid
ΔP_{fm}	U_m	
gm/cm ²	cm/sec	°C
29.4	24.3	22.3
27.3	23.0	
25.0	21.6	22.2
23.0	20.2	
20.8	18.8	22.2
19.1	17.4	
17.4	15.7	22.1
15.5	14.5	
13.7	13.1	22.2
12.2	11.8	
10.5	10.4	22.3
9.0	9.0	
7.6	7.7	22.4
6.3	6.5	
3.7	4.0	22.4
1.4	1.6	

TABLE 8/...

TABLE 8

Experiment G1		
Pressure Drop Across Fixed Bed	Superficial Velocity at Mean Bed Conditions	Temperature of Fluid
ΔP_{fm}	U_m	
gm/cm ²	cm/sec	°C
3.9	6.0	22.1
3.8	5.8	22.1
3.7	5.7	22.1
3.5	5.4	22.2
3.4	5.3	22.2
3.2	4.9	22.2
3.2	5.0	22.2
2.7	4.2	22.3
2.9	4.4	22.3
2.7	4.2	22.3
2.5	3.9	22.3
2.6	4.0	22.3
2.4	3.6	22.4
2.3	3.5	22.4
2.1	3.2	22.4
2.0	3.1	22.5
1.6	2.5	22.5
1.5	2.4	22.6
1.2	1.9	22.6
0.8	1.3	22.7

Appendix 2/...

APPENDIX 2
PULSATING FLUIDIZED BED EXPERIMENTS

The pressure-drop-velocity observations for the pulsating fluidized bed are given in Tables 10 to 32. The physical characteristics applicable to the various experiments are given in Table 9.

TABLE 9

Table No.	Experiment No.	Material	Pulse-Frequency Range pulses/min	Specific Surface cm ² /cm ³
10-13	A2 - A5	Zeolite	800 - 1100	106.4
14-15	B2 - B3	Clover Seed	800 - 900	80.3
16-17	C2 - C3	Rape Seed	800 - 900	53.3
18-21	D2 - D3	Zeolite	800 - 1100	105.5
22-25	E2 - E5	Zeolite	700 - 1000	73.3
26	F2	Rape Seed	500	51.6
27-32	G2 - G7	Clover Seed	800 - 1200	80.3

TABLE 10/...

TABLE 10

EXPERIMENT A2		
800 Pulses/min		
Mean Pressure-Drop Across Fluidized Bed	Mean Superficial Velocity	Temperature of Fluid
$\overline{\Delta P}_m$	\overline{U}_m	
gm/cm ²	cm/sec	°C
6.9	10.4	25.3
6.6	9.7	25.4
6.3	9.1	25.5
6.0	8.4	25.6
5.7	7.7	25.7
5.4	7.1	25.8
5.0	6.4	25.9
5.7	7.7	25.9
6.3	9.1	26.0
6.9	10.4	26.0

TABLE 11

EXPERIMENT A3		
900 Pulses/min		
Mean Pressure-Drop Across Fluidized Bed	Mean Superficial Velocity	Temperature of Fluid
$\overline{\Delta P}_m$	\overline{U}_m	
gm/cm ²	cm/sec	°C
7.0	10.4	26.5
6.8	9.7	26.5
6.6	9.2	26.5
6.2	8.4	26.6
5.8	7.7	26.6
5.5	7.0	26.7
5.8	7.7	26.8
6.5	9.1	26.8
7.0	10.4	26.9

TABLE 12/...

TABLE 12

EXPERIMENT A4		
1000 Pulses/min		
Mean Pressure-Drop Across Fluidized Bed	Mean Superficial Velocity	Temperature of Fluid
$\overline{\Delta P_m}$	$\overline{U_m}$	
gm/cm ²	cm/sec	°C
7.2	10.4	26.5
7.0	9.7	26.5
6.8	9.1	26.5
6.4	8.4	26.5
6.1	7.7	26.6
6.4	8.4	26.6
6.7	9.1	26.7
7.0	9.7	26.8
7.2	10.4	26.9

TABLE 13

EXPERIMENT A5		
1100 Pulses/min		
Mean Pressure-Drop Across Fluidized Bed	Mean Superficial Velocity	Temperature of Fluid
$\overline{\Delta P_m}$	$\overline{U_m}$	
gm/cm ²	cm/sec	°C
7.4	10.4	27.0
7.2	9.7	27.0
6.9	9.1	27.0
6.6	8.4	27.0
6.3	7.7	27.0
6.6	8.4	27.0
6.9	9.1	26.9
7.1	9.7	27.0
7.3	10.4	27.1

TABLE 14/...

TABLE 14

EXPERIMENT B2		
800 Pulses/min		
Mean Pressure-Drop Across Fluidized Bed	Mean Superficial Velocity	Temperature of Fluid
$\overline{\Delta P}_m$	\overline{U}_m	
gm/cm ²	cm/sec	°C
6.5	11.3	20.1
6.0	9.9	20.1
5.4	8.6	20.1
4.5	7.0	20.2
4.0	6.0	20.2
3.5	5.2	20.3
5.2	8.3	20.3
5.7	9.5	20.4
6.7	12.2	20.4

TABLE 15

EXPERIMENT B3		
900 Pulses/min		
Mean Pressure-Drop Across Fluidized Bed	Mean Superficial Velocity	Temperature of Fluid
$\overline{\Delta P}_m$	\overline{U}_m	
gm/cm ²	cm/sec	°C
6.8	12.0	20.3
6.7	11.1	20.3
6.2	9.9	20.4
5.7	8.9	20.4
5.1	7.6	20.4
4.3	6.3	20.6
5.2	7.9	20.6
6.1	9.7	20.6
6.5	10.4	20.6

TABLE 16/...

TABLE 16

EXPERIMENT C2		
800 Pulses/min		
Mean Pressure-Drop Across Fluidized Bed	Mean Superficial Velocity	Temperature of Fluid
$\overline{\Delta P_m}$	$\overline{U_m}$	
gm/cm ²	cm/sec	°C
6.7	34.1	21.6
6.3	30.8	21.6
5.7	27.6	21.6
5.3	25.6	21.7
4.8	23.0	21.7
5.3	25.6	21.7
5.8	28.1	21.8
6.3	30.8	21.8
6.6	34.0	21.8
6.8	36.7	21.8

TABLE 17

EXPERIMENT C3		
900 Pulses/min		
Mean Pressure-Drop Across Fluidized Bed	Mean Superficial Velocity	Temperature of Fluid
$\overline{\Delta P_m}$	$\overline{U_m}$	
gm/cm ²	cm/sec	°C
6.9	36.3	21.7
6.8	33.6	21.7
6.5	30.9	21.8
6.0	28.1	21.8
5.4	25.1	21.8
4.8	22.2	21.9
5.4	25.1	21.9
5.8	27.3	21.9
6.4	30.4	22.0
6.8	33.6	22.0
6.9	36.9	22.0

TABLE 18/...

TABLE 18

EXPERIMENT D2		
800 Pulses/min		
Mean Pressure-Drop Across Fluidized Bed	Mean Superficial Velocity	Temperature of Fluid
$\overline{\Delta P_m}$	$\overline{U_m}$	
gm/cm ²	cm/sec	°C
12.5	10.3	25.0
12.2	9.7	25.0
11.9	9.0	25.0
11.2	8.3	25.1
10.6	7.7	25.2
11.3	8.3	25.2
11.9	9.0	25.2
12.3	9.7	25.3
12.5	10.3	25.3

TABLE 19

EXPERIMENT D3		
900 Pulses/min		
Mean Pressure-Drop Across Fluidized Bed	Mean Superficial Velocity	Temperature of Fluid
$\overline{\Delta P_m}$	$\overline{U_m}$	
gm/cm ²	cm/sec	°C
12.7	10.3	24.9
12.5	9.7	24.8
12.1	9.0	24.6
11.6	8.3	24.7
10.9	7.7	24.8
11.6	8.3	24.9
12.0	9.0	24.9
12.4	9.7	25.0
12.6	10.3	25.0

TABLE 20/...

TABLE 20

EXPERIMENT D4		
1000 Pulses/min		
Mean Pressure-Drop Across Fluidized Bed	Mean Superficial Velocity	Temperature of Fluid
$\overline{\Delta P_m}$	$\overline{U_m}$	
gm/cm ²	cm/sec	°C
12.9	10.3	24.6
12.7	9.7	24.6
12.4	9.0	24.6
11.9	8.3	24.6
11.5	7.7	24.7
11.9	8.3	24.7
12.4	9.0	24.7
12.7	9.7	24.7
12.9	10.3	24.8

TABLE 21

EXPERIMENT D5		
1100 Pulses/min		
Mean Pressure-Drop Across Fluidized Bed	Mean Superficial Velocity	Temperature of Fluid
$\overline{\Delta P_m}$	$\overline{U_m}$	
gm/cm ²	cm/sec	°C
13.0	10.3	25.1
12.8	9.7	25.1
12.5	9.0	25.1
12.1	8.3	25.1
11.7	7.7	25.2
12.5	9.0	25.2
12.8	9.7	25.2
13.0	10.3	25.2
13.1	10.9	25.3
13.2	11.7	25.3

TABLE 22/...

TABLE 22

EXPERIMENT E2		
700 Pulses/min		
Mean Pressure-Drop Across Fluidized Bed	Mean Superficial Velocity	Temperature of Fluid
$\overline{\Delta P_m}$	$\overline{U_m}$	
gm/cm ²	cm/sec	°C
11.2	13.0	24.3
12.3	14.4	24.3
13.3	15.8	24.3
14.3	17.2	24.4
14.7	18.0	24.4
14.2	17.2	24.4
13.2	15.8	24.4
12.3	14.4	24.5
11.2	12.7	24.5

TABLE 23

EXPERIMENT E3		
800 Pulses/min		
Mean Pressure-Drop Across Fluidized Bed	Mean Superficial Velocity	Temperature of Fluid
$\overline{\Delta P_m}$	$\overline{U_m}$	
gm/cm ²	cm/sec	°C
10.8	12.0	24.4
11.6	13.0	24.4
12.7	14.4	24.5
13.7	15.8	24.5
14.7	17.2	24.5
13.7	15.8	24.5
12.6	14.4	24.6
11.5	13.0	24.6
10.7	12.0	24.6

TABLE 24/...

TABLE 24

EXPERIMENT E4		
900 Pulses/min		
Mean Pressure-Drop Across Fluidized Bed	Mean Superficial Velocity	Temperature of Fluid
$\overline{\Delta P_m}$	$\overline{U_m}$	
gm/cm ²	cm/sec	°C
11.7	13.0	24.4
12.9	14.4	24.4
14.0	15.8	24.4
15.1	17.2	24.5
15.4	18.0	24.5
15.1	17.2	24.5
14.1	15.8	24.5
13.0	14.4	24.6
11.8	13.0	24.6

TABLE 25

EXPERIMENT E5		
1000 Pulses/min		
Mean Pressure-Drop Across Fluidized Bed	Mean Superficial Velocity	Temperature of Fluid
$\overline{\Delta P_m}$	$\overline{U_m}$	
gm/cm ²	cm/sec	°C
11.2	12.0	24.4
12.1	13.0	24.5
13.3	14.4	24.5
14.4	15.8	24.5
15.5	17.2	24.6
15.6	17.4	24.6
14.5	15.8	24.6
13.4	14.4	24.7
12.1	13.0	24.7
11.2	12.0	24.7

TABLE 26/...

TABLE 26

EXPERIMENT F2		
500 Pulses/min		
Mean Pressure-Drop Across Fluidized Bed	Mean Superficial Velocity	Temperature of Fluid
$\overline{\Delta P_m}$	$\overline{U_m}$	
gm/cm ²	cm/sec	°C
32.8	23.8	20.2
31.5	22.8	20.2
29.2	21.2	20.2
31.4	22.6	20.2
32.7	23.6	20.3

TABLE 27

EXPERIMENT G2		
800 Pulses/min		
Mean Pressure-Drop Across Fluidized Bed	Mean Superficial Velocity	Temperature of Fluid
$\overline{\Delta P_m}$	$\overline{U_m}$	
gm/cm ²	cm/sec	°C
5.8	8.8	22.2
6.2	9.5	22.2
6.4	10.2	22.2
6.9	11.2	22.3
7.1	11.9	22.3
7.5	12.8	22.3
5.8	8.7	22.4
6.2	9.6	22.4
6.5	10.4	22.4
6.8	11.3	22.5
7.2	12.0	22.5
7.4	12.7	22.6

TABLE 28/...

TABLE 28

EXPERIMENT G3		
800 Pulses/min		
Mean Pressure-Drop Across Fluidized Bed	Mean Superficial Velocity	Temperature of Fluid
$\overline{\Delta P_m}$	$\overline{U_m}$	
gm/cm ²	cm/sec	°C
5.4	7.9	22.3
5.8	8.7	22.3
6.2	9.5	22.3
6.5	10.4	22.4
6.8	11.2	22.4
7.1	12.1	22.4
5.4	7.8	22.5
5.8	8.7	22.5
6.2	9.6	22.5
6.5	10.4	22.6
6.9	11.3	22.6
7.2	12.1	22.7

TABLE 29

EXPERIMENT G4		
900 Pulses/min		
Mean Pressure-Drop Across Fluidized Bed	Mean Superficial Velocity	Temperature of Fluid
$\overline{\Delta P_m}$	$\overline{U_m}$	
gm/cm ²	cm/sec	°C
5.5	7.8	22.1
5.9	8.7	22.1
6.4	9.7	22.1
6.7	10.5	22.2
7.1	11.4	22.2
7.5	12.4	22.3
5.5	7.9	22.3
6.0	8.8	22.3
6.4	9.7	22.4
6.7	10.5	22.4
7.2	11.4	22.4
7.6	12.6	22.5

TABLE 30/...

TABLE 30

EXPERIMENT G5		
1000 Pulses/min		
Mean Pressure-Drop Across Fluidized Bed	Mean Superficial Velocity	Temperature of Fluid
$\overline{\Delta P_m}$	$\overline{U_m}$	
gm/cm ²	cm/sec	°C
5.6	7.9	22.5
6.1	8.8	22.5
6.5	9.6	22.5
6.9	10.5	22.6
7.3	11.3	22.6
7.6	12.1	22.6
5.7	7.9	22.7
6.1	8.8	22.7
6.5	9.6	22.8
7.0	10.5	22.8
7.2	11.2	22.8
7.3	12.2	22.9

TABLE 31

EXPERIMENT G6		
1100 Pulses/min		
Mean Pressure-Drop Across Fluidized Bed	Mean Superficial Velocity	Temperature of Fluid
$\overline{\Delta P_m}$	$\overline{U_m}$	
gm/cm ²	cm/sec	°C
6.2	8.7	22.8
6.6	9.5	22.8
7.1	10.4	22.8
7.5	11.3	22.8
7.8	12.0	22.8
6.2	8.7	22.9
6.7	9.6	22.9
7.2	10.5	22.9
7.4	11.3	22.9
8.0	12.2	23.0

TABLE 32/...

TABLE 32

EXPÈRIMENT G7		
1200 Pulses/min		
Mean Pressure-Drop Across Fluidized Bed	Mean Superficial Velocity	Temperature of Fluid
$\overline{\Delta P}_m$	\overline{U}_m	
gm/cm ²	cm/sec	°C
6.2	8.5	22.8
6.8	9.5	22.8
7.3	10.4	22.8
7.8	11.3	22.8
8.2	12.2	22.9
6.3	8.6	22.9
6.8	9.5	22.9
7.3	10.4	22.9
7.8	11.3	23.0
8.1	12.0	23.0

Appendix 3/...

APPENDIX 3

The pressure-drop-velocity values, which are employed in the subsequent calculations, are obtained from curves drawn through the experimentally obtained values. The results are represented in Tables 34 to 40. The physical characteristics applicable to the various experiments are given in Table 33.

TABLE 33

Table No.	Experiment No.	Material	Pulse-Frequency Range pulses/min	Specific Surface cm ² /cm ³	Bed Area cm ²
34	A2-A5	Zeolite	800 - 1100	106.4	6.6
35	B2-B3	Clover Seed	800 - 900	80.3	6.6
36	C2-C3	Rape Seed	800 - 900	53.3	6.6
37	D2-D5	Zeolite	800 - 1100	105.5	6.6
38	E2-E5	Zeolite	700 - 1000	73.3	6.6
39	F2	Rape Seed	500	51.6	6.6
40	G2-G7	Clover Seed	800 - 1200	80.3	165.0

TABLE 34/...

TABLE 34

Mean Superficial Velocity	Mean Pressure-Drop Across Fluidized Bed			
	ΔP_m			
	gm/cm ²			
\bar{U}_m	Experiment A2	Experiment A3	Experiment A4	Experiment A5
cm/sec	800 Pulses/min	900 Pulses/min	1000 Pulses/min	1100 Pulses/min
7.6	5.6	5.8	6.0	6.3
8.0	5.8	6.0	6.2	6.5
8.5	6.1	6.3	6.5	6.7
9.0	6.3	6.5	6.7	6.9
9.5	6.5	6.7	6.9	7.1
10.0	6.7	6.9	7.1	7.2

TABLE 35

Mean Superficial Velocity	Mean Pressure-Drop Across Fluidized Bed	
	ΔP_m	
	gm/cm ²	
\bar{U}_m	Experiment B2	Experiment B3
cm/sec	800 Pulses/min	900 Pulses/min
6.0	4.0	4.1
7.0	4.6	4.7
8.0	5.1	5.3
9.0	5.5	5.8
10.0	6.0	6.3
11.0	6.5	6.7
12.0	6.7	6.8

TABLE 36/...

TABLE 36

Mean Superficial Velocity	Mean Pressure-Drop Across Fixed Bed	
	$\overline{\Delta P_m}$	
	gm/cm ²	
$\overline{U_m}$	Experiment C2	Experiment C3
cm/sec	800 Pulses/min	900 Pulses/min
23.0	4.8	5.0
24.0	5.0	5.2
25.0	5.2	5.4
26.0	5.4	5.6
27.0	5.6	5.8
28.0	5.8	6.0
29.0	5.9	6.2
30.0	6.2	6.4
31.0	6.3	6.5
32.0	6.5	6.7

TABLE 37

Mean Superficial Velocity	Mean Pressure-Drop Across Fluidized Bed			
	$\overline{\Delta P_m}$			
	gm/cm ²			
$\overline{U_m}$	Experiment D2	Experiment D3	Experiment D4	Experiment D5
cm/sec	800 Pulses/min	900 Pulses/min	1000 Pulses/min	1100 Pulses/min
7.6	10.5	11.0	11.4	11.6
8.0	11.0	11.4	11.8	11.9
8.5	11.5	11.8	12.1	12.2
9.0	11.9	12.1	12.4	12.5
9.5	12.1	12.4	12.6	12.7
10.0	12.4	12.6	12.8	12.9
10.4	12.5	12.7	12.9	13.0

TABLE 38/...

TABLE 38

Mean Superficial Velocity	Mean Pressure-Drop Across Fluidized Bed			
	$\overline{\Delta P_m}$			
	gm/cm ²			
$\overline{U_m}$	Experiment E2	Experiment E3	Experiment E4	Experiment E5
cm/sec	700 Pulses/min	800 Pulses/min	900 Pulses/min	1000 Pulses/min
13.0	11.3	11.6	11.7	12.1
14.0	12.0	12.4	12.6	13.0
15.0	12.7	13.1	13.4	13.8
16.0	13.4	13.9	14.2	14.6
17.0	14.1	14.6	14.9	15.3
18.0	14.7	15.3	15.6	16.0

TABLE 39

Mean Superficial Velocity	Mean Pressure-Drop Across Fluidized Bed
	$\overline{\Delta P_m}$
	gm/cm ²
$\overline{U_m}$	Experiment F2
cm/sec	500 Pulses/min
21.0	29.0
21.5	29.6
22.0	30.4
22.5	31.2
23.0	31.9
23.5	32.5
24.0	33.1

TABLE 40/...

TABLE 40

Mean Superficial Velocity	Mean Pressure-Drop Across Fluidized Bed		
	$\overline{\Delta P_m}$		
	gm/cm ²		
$\overline{U_m}$	Experiment G2, G3	Experiment G4	Experiment G5
cm/sec	800 Pulses/min	900 Pulses/min	1000 Pulses/min
7.0	4.9	5.0	5.1
8.0	5.4	5.6	5.7
9.0	5.9	6.0	6.2
10.0	6.4	6.5	6.6
11.0	6.8	6.9	7.1
12.0	7.1	7.4	7.6

TABLE 40 (continued)

Mean Superficial Velocity	Mean Pressure-Drop Across Fluidized Bed	
	$\overline{\Delta P_m}$	
	gm/cm ²	
$\overline{U_m}$	Experiment G6	Experiment G7
cm/sec	1100 Pulses/min	1200 Pulses/min
7.0	5.2	5.4
8.0	5.8	6.0
9.0	6.3	6.5
10.0	6.9	7.1
11.0	7.4	7.6
12.0	7.9	8.1

Appendix 4/...

APPENDIX 4

The overall mean void-fractions existing in the pulsating fluidized bed are represented in Tables 42 to 48. The overall mean void-fraction was evaluated from the following equation:

$$\overline{\Delta P_m} = a \left[\frac{\overline{\epsilon_m}}{\epsilon_m} \right]^3 \left[\frac{1-\overline{\epsilon_m}}{1-\epsilon_m} \right] \overline{U_m} + b F \left[\frac{\overline{\epsilon_m}}{\epsilon_m} \right]^2 \left[\frac{1-\overline{\epsilon_m}}{1-\epsilon_m} \right] \overline{U_m}^2 \dots\dots (26)$$

The physical characteristics applicable to the various experiments are given in Table 41.

TABLE 41

Table No.	Experiment No.	Material	Pulse-Frequency Range pulses/min	Specific Surface cm ² /cm ³	Bed Area cm ²
42	A2-A5	Zeolite	800 - 1100	106.4	6.6
43	B2-B3	Clover Seed	800 - 900	80.3	6.6
44	C2-C3	Rape Seed	800 - 900	53.3	6.6
45	D2-D5	Zeolite	800 - 1100	105.5	6.6
46	E2-E5	Zeolite	700 - 1000	73.3	6.6
47	F2	Rape Seed	500	51.6	6.6
48	G2-G7	Clover Seed	800 - 1200	80.3	165.0

TABLE 42/...

TABLE 42

Experiment A2		Experiment A3	
800 Pulses/min		900 Pulses/min	
Velocity in Excess of Deviation Velocity (U_d) $U_d = 6.15$ cm/sec	Overall Mean Void-Fraction in Fluidized Bed	Velocity in Excess of Deviation Velocity (U_d) $U_d = 6.70$ cm/sec	Overall Mean Void-Fraction in Fluidized Bed
$\bar{U}_m - U_d$	$\bar{\epsilon}_m$	$\bar{U}_m - U_d$	$\bar{\epsilon}_m$
cm/sec		cm/sec	
1.45	0.3772	0.9	0.3740
1.85	0.3795	1.3	0.3762
2.35	0.3820	1.8	0.3785
2.85	0.3845	2.3	0.3812
3.35	0.3871	2.8	0.3841
3.85	0.3902	3.3	0.3870

TABLE 42 (continued)

Experiment A4		Experiment A5	
1000 Pulses/min		1100 Pulses/min	
Velocity in Excess of Deviation Velocity (U_d) $U_d = 7.35$ cm/sec	Overall Mean Void-Fraction in Fluidized Bed	Velocity in Excess of Deviation Velocity (U_d) $U_d = 8.00$ cm/sec	Overall Mean Void-Fraction in Fluidized Bed
$\bar{U}_m - U_d$	$\bar{\epsilon}_m$	$\bar{U}_m - U_d$	$\bar{\epsilon}_m$
cm/sec		cm/sec	
0.25	0.3698	-0.40	0.3658
0.65	0.3720	0	0.3682
1.15	0.3746	0.50	0.3716
1.65	0.3778	1.00	0.3748
2.15	0.3810	1.50	0.3782
2.65	0.3839	2.00	0.3815

TABLE 43/...

TABLE 43

Experiment B2		Experiment B3	
800 Pulses/min		900 Pulses/min	
Velocity in Excess of Deviation Velocity (U_d) $U_d = 5.20$ cm/sec	Overall Mean Void-Fraction in Fluidized Bed	Velocity in Excess of Deviation Velocity (U_d) $U_d = 6.30$ cm/sec	Overall Mean Void-Fraction in Fluidized Bed
$\bar{U}_m - U_d$	$\bar{\epsilon}_m$	$\bar{U}_m - U_d$	$\bar{\epsilon}_m$
cm/sec		cm/sec	
0.80	0.3400	-0.30	0.3365
1.80	0.3420	0.70	0.3395
2.80	0.3460	1.70	0.3420
3.80	0.3495	2.70	0.3450
4.80	0.3530	3.70	0.3486
5.80	0.3563	4.70	0.3520
6.80	0.3630	5.70	0.3610

TABLE 44

Experiment C2		Experiment C3	
800 Pulses/min		900 Pulses/min	
Velocity in Excess of Deviation Velocity (U_d) $U_d = 25.60$ cm/sec	Overall Mean Void-Fraction in Fluidized Bed	Velocity in Excess of Deviation Velocity (U_d) $U_d = 28.00$ cm/sec	Overall Mean Void-Fraction in Fluidized Bed
$\bar{U}_m - U_d$	$\bar{\epsilon}_m$	$\bar{U}_m - U_d$	$\bar{\epsilon}_m$
cm/sec		cm/sec	
-2.60	0.3585	-5.00	0.3533
-1.60	0.3590	-4.00	0.3552
-0.60	0.3617	-3.00	0.3567
0.40	0.3632	-2.00	0.3586
1.40	0.3650	-1.00	0.3605
2.40	0.3675	0	0.3626
3.40	0.3698	1.00	0.3645
4.40	0.3721	2.00	0.3670
5.40	0.3747	3.00	0.3700
6.40	0.3780	4.00	0.3735

TABLE 45/...

TABLE 45

Experiment D2		Experiment D3	
800 Pulses/min		900 Pulses/min	
Velocity in Excess of Deviation Velocity (U_d) $U_d = 7.80$ cm/sec	Overall Mean Void-Fraction in Fluidized Bed	Velocity in Excess of Deviation Velocity (U_d) $U_d = 8.45$ cm/sec	Overall Mean Void-Fraction in Fluidized Bed
$\bar{U}_m - U_d$	$\bar{\epsilon}_m$	$\bar{U}_m - U_d$	$\bar{\epsilon}_m$
cm/sec		cm/sec	
-0.20	0.3635	-0.85	0.3587
0.20	0.3635	-0.45	0.3597
0.70	0.3656	0.05	0.3630
1.20	0.3685	0.55	0.3667
1.70	0.3719	1.05	0.3700
2.20	0.3755	1.55	0.3738
2.60	0.3785	1.95	0.3770

TABLE 45 (continued)

Experiment D4		Experiment D5	
1000 Pulses/min		1100 Pulses/min	
Velocity in Excess of Deviation Velocity (U_d) $U_d = 8.75$ cm/sec	Overall Mean Void-Fraction in Fluidized Bed	Velocity in Excess of Deviation Velocity (U_d) $U_d = 8.85$ cm/sec	Overall Mean Void-Fraction in Fluidized Bed
$\bar{U}_m - U_d$	$\bar{\epsilon}_m$	$\bar{U}_m - U_d$	$\bar{\epsilon}_m$
cm/sec		cm/sec	
-1.15	0.3540	-1.25	0.3523
-0.75	0.3565	-0.85	0.3550
-0.25	0.3605	-0.35	0.3593
0.25	0.3643	0.15	0.3635
0.75	0.3680	0.65	0.3675
1.25	0.3720	1.15	0.3715
1.65	0.3755	1.55	0.3747

TABLE 46/...

TABLE 46

Experiment E2		Experiment E3	
700 Pulses/min		800 Pulses/min	
Velocity in Excess of Deviation Velocity (U_d) $U_d = 12.9$ cm/sec	Overall Mean Void-Fraction in Fluidized Bed	Velocity in Excess of Deviation Velocity (U_d) $U_d = 14.50$ cm/sec	Overall Mean Void-Fraction in Fluidized Bed
$\bar{U}_m - U_d$	$\bar{\epsilon}_m$	$\bar{U}_m - U_d$	$\bar{\epsilon}_m$
cm/sec		cm/sec	
0.10	0.3829	-1.50	0.3793
1.10	0.3848	-0.50	0.3813
2.10	0.3869	0.50	0.3830
3.10	0.3895	1.50	0.3854
4.10	0.3915	2.50	0.3874
5.10	0.3941	3.50	0.3900

TABLE 46 (continued)

Experiment E4		Experiment E5	
900 Pulses/min		1000 Pulses/min	
Velocity in Excess of Deviation Velocity (U_d) $U_d = 15.60$ cm/sec	Overall Mean Void-Fraction in Fluidized Bed	Velocity in Excess of Deviation Velocity (U_d) $U_d = 17.20$ cm/sec	Overall Mean Void-Fraction in Fluidized Bed
$\bar{U}_m - U_d$	$\bar{\epsilon}_m$	$\bar{U}_m - U_d$	$\bar{\epsilon}_m$
cm/sec		cm/sec	
-2.60	0.3783	-4.20	0.3743
-1.60	0.3793	-3.20	0.3757
-0.60	0.3808	-2.20	0.3773
0.40	0.3830	-1.20	0.3795
1.40	0.3850	-0.20	0.3818
2.40	0.3875	0.80	0.3842

TABLE 47/...

TABLE 47

Experiment F2	
500 Pulses/min	
Velocity in Excess of Deviation Velocity (U_d) $U_d = 21.20$ cm/sec	Overall Mean Void-Fraction in Fluidized Bed
$\bar{U}_m - U_d$	$\bar{\epsilon}_m$
cm/sec	
-0.20	0.3505
0.30	0.3506
0.80	0.3509
1.30	0.3510
1.80	0.3520
2.30	0.3532
2.80	0.3545

TABLE 48

Experiment G2, G3		Experiment G4	
800 Pulses/min		900 Pulses/min	
Velocity in Excess of Deviation Velocity (U_d) $U_d = 8.20$ cm/sec	Overall Mean Void-Fraction in Fluidized Bed	Velocity in Excess of Deviation Velocity (U_d) $U_d = 8.70$ cm/sec	Overall Mean Void-Fraction in Fluidized Bed
$\bar{U}_m - U_d$	$\bar{\epsilon}_m$	$\bar{U}_m - U_d$	$\bar{\epsilon}_m$
cm/sec		cm/sec	
-1.20	0.3410	-1.70	0.3395
-0.20	0.3445	-0.70	0.3428
0.80	0.3490	0.30	0.3465
1.80	0.3533	1.30	0.3510
2.80	0.3575	2.30	0.3545
3.80	0.3610	3.30	0.3582

TABLE 48 (cont)/...

TABLE 48 (continued)

Experiment G5		Experiment G6	
1000 Pulses/min		1100 Pulses/min	
Velocity in Excess of Deviation Velocity (\bar{U}_d) $U_d = 9.30$ cm/sec	Overall Mean Void-Fraction in Fluidized Bed	Velocity in Excess of Deviation Velocity (\bar{U}_d) $U_d = 10.20$ cm/sec	Overall Mean Void-Fraction in Fluidized Bed
$\bar{U}_m - U_d$	$\bar{\epsilon}_m$	$\bar{U}_m - U_d$	$\bar{\epsilon}_m$
cm/sec		cm/sec	
-2.30	0.3375	-3.20	0.3350
-1.30	0.3411	-2.20	0.3391
-0.30	0.3445	-1.20	0.3419
0.70	0.3485	-0.20	0.3456
1.70	0.3519	0.80	0.3485
2.70	0.3555	1.80	0.3515

TABLE 48 (continued)

Experiment G7	
1200 Pulses/min	
Velocity in Excess of Deviation Velocity (\bar{U}_d) $U_d = 11.30$ cm/sec	Overall Mean Void-Fraction in Fluidized Bed
$\bar{U}_m - U_d$	$\bar{\epsilon}_m$
cm/sec	
-4.30	0.3320
-3.30	0.3350
-2.30	0.3396
-1.30	0.3415
-0.30	0.3450
0.70	0.3480

APPENDIX 5
REYNOLDS NUMBER AND FRICTION FACTORS

The modified Reynolds number and modified friction factor for the various experiments are represented in Tables 50 to 56. The Reynolds numbers and friction factors were evaluated from the equations below:

$$\overline{Re} = \frac{\rho}{\mu S} \times \frac{\overline{U_m}}{(1-\epsilon_m)} \dots\dots\dots (18)$$

$$\overline{\phi} = \frac{\epsilon_m^3 g \Delta P_m}{SF^2 K \rho \overline{U_m}^2} \dots\dots\dots (20)$$

The physical characteristics applicable to the various experiments are given in Table 49.

TABLE 49

Table No.	Ex-periment No.	Material	Pulse-Frequency Range Pulses/min	Speci-fic Surface cm ² /cm ³	Bed Area cm ²	Const-ant K cm
50	A2-A5	Zeolite	800-1100	106.4	6.6	6.16
51	B2-B3	Clover Seed	800- 900	80.3	6.6	6.71
52	C2-C3	Rape Seed	800- 900	53.3	6.6	5.71
53	D2-D5	Zeolite	800-1100	105.5	6.6	10.20
54	E2-E5	Zeolite	700-1000	73.3	6.6	15.80
55	F2	Rape Seed	500	51.6	6.6	36.83
56	G2-G7	Clover Seed	800-1200	80.3	165.0	7.20

TABLE 50/...

TABLE 50

Experiment A2			Experiment A3		
800 Pulses/min			900 Pulses/min		
Modified Reynolds Number	Modified Friction Factor	Product	Modified Reynolds Number	Modified Friction Factor	Product
\overline{Re}	$\overline{\phi}$	$\overline{Re} \times \overline{\phi}$	\overline{Re}	$\overline{\phi}$	$\overline{Re} \times \overline{\phi}$
0.763	4.52	3.45	0.759	4.56	3.50
0.806	4.31	3.47	0.802	4.32	3.46
0.860	4.06	3.49	0.855	4.07	3.48
0.914	3.83	3.50	0.909	3.85	3.50
0.969	3.64	3.52	0.964	3.64	3.51
1.026	3.46	3.56	1.02	3.47	3.54

TABLE 50 (continued)

Experiment A4			Experiment A5		
1000 Pulses/min			1100 Pulses/min		
Modified Reynolds Number	Modified Friction Factor	Product	Modified Reynolds Number	Modified Friction Factor	Product
\overline{Re}	$\overline{\phi}$	$\overline{Re} \times \overline{\phi}$	\overline{Re}	$\overline{\phi}$	$\overline{Re} \times \overline{\phi}$
0.754	4.59	3.46	0.749	4.61	3.50
0.797	4.36	3.47	0.792	4.36	3.45
0.850	4.10	3.48	0.845	4.11	3.47
0.904	3.87	3.50	0.899	3.88	3.49
0.959	3.66	3.51	0.955	3.67	3.50
1.01	3.46	3.50	1.01	3.49	3.52

TABLE 51/...

TABLE 51

Experiment B2			Experiment B3		
800 Pulses/min			900 Pulses/min		
Modified Reynolds Number	Modified Friction Factor	Product	Modified Reynolds Number	Modified Friction Factor	Product
\overline{Re}	$\overline{\phi}$	$\overline{Re} \times \overline{\phi}$	\overline{Re}	$\overline{\phi}$	$\overline{Re} \times \overline{\phi}$
0.753	4.54	3.42	0.748	4.59	3.44
0.881	3.92	3.45	0.878	3.96	3.48
1.01	3.44	3.47	1.01	3.46	3.49
1.15	3.07	3.53	1.14	3.09	3.52
1.28	2.78	3.56	1.27	2.80	3.55
1.41	2.54	3.58	1.41	2.54	3.58
1.56	2.33	3.63	1.56	2.34	3.65

TABLE 52

Experiment C2			Experiment C3		
800 Pulses/min			900 Pulses/min		
Modified Reynolds Number	Modified Friction Factor	Product	Modified Reynolds Number	Modified Friction Factor	Product
\overline{Re}	$\overline{\phi}$	$\overline{Re} \times \overline{\phi}$	\overline{Re}	$\overline{\phi}$	$\overline{Re} \times \overline{\phi}$
4.47	0.772	3.45	4.44	0.771	3.42
4.68	0.747	3.50	4.64	0.750	3.48
4.89	0.730	3.56	4.85	0.730	3.54
5.10	0.711	3.62	5.06	0.712	3.60
5.30	0.694	3.68	5.27	0.695	3.66
5.53	0.681	3.77	5.48	0.681	3.73
5.74	0.669	3.84	5.70	0.667	3.80
5.96	0.658	3.92	5.91	0.654	3.86
6.19	0.646	4.00	6.14	0.642	3.94
6.42	0.637	4.09	6.37	0.631	4.02

TABLE 53/...

TABLE 53

Experiment D2			Experiment D3		
800 Pulses/min			900 Pulses/min		
Modified Reynolds Number	Modified Friction Factor	Product	Modified Reynolds Number	Modified Friction Factor	Product
\overline{Re}	$\overline{\phi}$	$\overline{Re} \times \overline{\phi}$	\overline{Re}	$\overline{\phi}$	$\overline{Re} \times \overline{\phi}$
0.753	4.59	3.46	0.747	4.61	3.44
0.793	4.36	3.46	0.788	4.38	3.46
0.845	4.11	3.47	0.841	4.12	3.47
0.899	3.86	3.47	0.895	3.88	3.47
0.954	3.64	3.47	0.951	3.66	3.48
1.01	3.45	3.48	1.01	3.46	3.50
1.06	3.31	3.50	1.05	3.32	3.49

TABLE 53 (continued)

Experiment D4			Experiment D5		
1000 Pulses/min			1100 Pulses/min		
Modified Reynolds Number	Modified Friction Factor	Product	Modified Reynolds Number	Modified Friction Factor	Product
\overline{Re}	$\overline{\phi}$	$\overline{Re} \times \overline{\phi}$	\overline{Re}	$\overline{\phi}$	$\overline{Re} \times \overline{\phi}$
0.742	4.65	3.45	0.740	4.66	3.45
0.784	4.39	3.44	0.783	4.41	3.45
0.838	4.14	3.47	0.836	4.14	3.46
0.893	3.90	3.48	0.891	3.90	3.48
0.948	3.67	3.48	0.947	3.68	3.49
1.00	3.48	3.48	1.00	3.48	3.48
1.05	3.33	3.50	1.05	3.34	3.51

TABLE 54/...

TABLE 54

Experiment E2			Experiment E3		
700 Pulses/min			800 Pulses/min		
Modified Reynolds Number	Modified Friction Factor	Product	Modified Reynolds Number	Modified Friction Factor	Product
\overline{Re}	$\overline{\phi}$	$\overline{Re} \times \overline{\phi}$	\overline{Re}	$\overline{\phi}$	$\overline{Re} \times \overline{\phi}$
1.91	1.83	3.50	1.90	1.84	3.50
2.06	1.74	3.58	2.05	1.72	3.53
2.22	1.61	3.57	2.21	1.61	3.56
2.38	1.52	3.62	2.36	1.52	3.59
2.53	1.43	3.62	2.52	1.44	3.63
2.70	1.37	3.70	2.68	1.37	3.67

TABLE 54 (continued)

Experiment E4			Experiment E5		
900 Pulses/min			1000 Pulses/min		
Modified Reynolds Number	Modified Friction Factor	Product	Modified Reynolds Number	Modified Friction Factor	Product
\overline{Re}	$\overline{\phi}$	$\overline{Re} \times \overline{\phi}$	\overline{Re}	$\overline{\phi}$	$\overline{Re} \times \overline{\phi}$
1.90	1.84	3.49	1.89	1.84	3.48
2.04	1.72	3.51	2.04	1.73	3.53
2.20	1.61	3.54	2.19	1.62	3.55
2.35	1.52	3.58	2.34	1.53	3.58
2.51	1.44	3.62	2.50	1.44	3.60
2.67	1.38	3.68	2.65	1.37	3.63

TABLE 55/...

TABLE 55

Experiment F2		
500 Pulses/min		
Modified Reynolds Number	Modified Friction Factor	Product
\overline{Re}	$\overline{\phi}$	$\overline{Re} \times \overline{\phi}$
4.17	0.838	3.49
4.27	0.824	3.52
4.37	0.810	3.54
4.47	0.797	3.56
4.58	0.785	3.60
4.69	0.775	3.63
4.80	0.764	3.67

TABLE 56

Experiment G2, G3			Experiment G4		
800 Pulses/min			900 Pulses/min		
Modified Reynolds Number	Modified Friction Factor	Product	Modified Reynolds Number	Modified Friction Factor	Product
\overline{Re}	$\overline{\phi}$	$\overline{Re} \times \overline{\phi}$	\overline{Re}	$\overline{\phi}$	$\overline{Re} \times \overline{\phi}$
0.880	0.394	3.47	0.878	0.392	3.44
1.01	0.342	3.45	1.01	0.343	3.46
1.15	0.305	3.50	1.14	0.305	3.48
1.28	0.276	3.53	1.28	0.276	3.53
1.42	0.251	3.56	1.41	0.252	3.55
1.56	0.229	3.57	1.55	0.231	3.58

TABLE 56 (cont)/...

TABLE 56 (continued)

Experiment G5			Experiment G6		
1000 Pulses/min			1100 Pulses/min		
Modified Reynolds Number	Modified Friction Factor	Product	Modified Reynolds Number	Modified Friction Factor	Product
\overline{Re}	$\overline{\phi}$	$\overline{Re} \times \overline{\phi}$	\overline{Re}	$\overline{\phi}$	$\overline{Re} \times \overline{\phi}$
0.876	0.394	3.45	0.873	0.395	3.45
1.00	0.344	3.44	1.00	0.346	3.46
1.14	0.307	3.50	1.14	0.308	3.51
1.27	0.276	3.50	1.27	0.278	3.53
1.41	0.252	3.55	1.40	0.253	3.54
1.54	0.232	3.57	1.54	0.233	3.59

TABLE 56 (continued)

Experiment G7		
1200 Pulses/min		
Modified Reynolds Number	Modified Friction Factor	Product
\overline{Re}	$\overline{\phi}$	$\overline{Re} \times \overline{\phi}$
0.868	0.396	3.44
0.997	0.347	3.46
1.13	0.309	3.49
1.26	0.278	3.50
1.39	0.254	3.53
1.53	0.233	3.56

Appendix 6/...

APPENDIX 6
INSTANTANEOUS FUNCTIONS

The instantaneous relative-velocity curves were constructed from the instantaneous pressure-drop curves, employing equation (30). These experiments were performed on clover seeds having a specific surface of $80.3 \text{ cm}^2/\text{cm}^3$, fluidized in a bed with a cross-sectional area of 165 cm^2 .

The physical characteristics applicable to the various experiments are given in Table 57.

TABLE 57

Experiment Number	Pulse Frequency	Overall Mean Void-Fraction
	pulses/min	$\bar{\epsilon}_m$
H1	1000	0.353
H2	1000	0.351
H3	1000	0.349
H4	800	0.354
H5	900	0.352
H6	1100	0.346
H7	1200	0.341

TABLE 58/...

TABLE 58

Experiment H1		
Pulse Frequency : 1000 Pulses/min		
Observed Mean Superficial Velocity : 11.3 cm/sec		
Computed Mean Superficial Velocity : 11.2 cm/sec		
Overall Mean Void-Fraction : $\bar{\epsilon}_m = 0.353$		
Period : T = 0.06 sec		
Fraction of Period	Instantaneous Pressure Drop	Instantaneous Relative Velocity
A × T	ΔP_{im}	$U_{im} - U_{ipm}$
A	gm/cm ²	cm/sec
0	6.0	9.4
1/16	35.5	57.1
2/16	27.0	37.5
3/16	3.0	4.7
4/16	3.5	5.5
5/16	- 6.0	- 9.4
6/16	-11.2	-17.3
7/16	5.0	7.8
8/16	4.0	6.2
9/16	7.0	11.0
10/16	5.8	9.1
11/16	3.5	5.5
12/16	7.5	11.7
13/16	7.5	11.7
14/16	9.5	14.9
15/16	8.0	12.5
16/16	6.0	9.4

TABLE 59/...

TABLE 59

Experiment H2		
Pulse Frequency : 1000 Pulses/min		
Observed Mean Superficial Velocity : 10.8 cm/sec		
Computed Mean Superficial Velocity : 10.9 cm/sec		
Overall Mean Void-Fraction : $\overline{\epsilon}_m = 0.351$		
Period : T = 0.06 sec		
Fraction of Period	Instantaneous Pressure Drop	Instantaneous Relative Velocity
A × T	ΔP_{im}	$U_{im} - U_{ipm}$
A	gm/cm ²	cm/sec
0	4.8	7.2
1/16	31.5	42.5
2/16	39.0	50.3
3/16	4.6	7.0
4/16	3.8	5.8
5/16	- 4.2	- 6.3
6/16	-12.9	-19.5
7/16	6.6	10.0
8/16	5.1	7.7
9/16	7.1	10.7
10/16	8.1	12.3
11/16	3.9	5.9
12/16	7.1	10.7
13/16	6.6	10.0
14/16	8.6	13.1
15/16	7.6	11.5
16/16	4.8	7.2

TABLE 60/...

TABLE 60

Experiment H3		
Pulse Frequency : 1000 Pulses/min		
Observed Mean Superficial Velocity : 9.2 cm/sec		
Computed Mean Superficial Velocity : 9.3 cm/sec		
Overall Mean Void-Fraction : $\bar{\epsilon}_m = 0.349$		
Period : T = 0.06 sec		
Fraction of Period	Instantaneous Pressure Drop	Instantaneous Relative Velocity
A × T	ΔP_{im}	$U_{im} - U_{ipm}$
A	gm/cm ²	cm/sec
0	5.0	7.2
1/16	26.0	34.9
2/16	31.5	41.1
3/16	4.1	5.8
4/16	4.1	5.8
5/16	- 6.0	- 8.6
6/16	-10.8	-15.7
7/16	5.9	8.5
8/16	7.2	10.3
9/16	9.3	13.4
10/16	7.9	11.4
11/16	4.4	6.4
12/16	6.4	9.2
13/16	4.2	6.0
14/16	5.5	8.0
15/16	4.9	7.0
16/16	5.0	7.2

TABLE 61/...

TABLE 61

Experiment H4		
Pulse Frequency : 800 Pulses/min		
Observed Mean Superficial Velocity : 10.3 cm/sec		
Computed Mean Superficial Velocity : 10.3 cm/sec		
Overall Mean Void-Fraction : $\bar{\epsilon}_m = 0.354$		
Period : T = 0.075 sec		
Fraction of Period	Instantaneous Pressure Drop	Instantaneous Relative Velocity
A × T	ΔP_{im}	$U_{im} - U_{ipm}$
A	gm/cm ²	cm/sec
0	3.7	5.7
1/16	36.5	48.5
2/16	27.0	37.7
3/16	6.2	9.9
4/16	- 9.6	-15.5
5/16	- 5.4	- 8.7
6/16	4.7	7.6
7/16	6.0	9.5
8/16	3.2	5.2
9/16	3.7	5.7
10/16	7.5	12.0
11/16	10.2	16.3
12/16	7.2	11.5
13/16	3.1	5.0
14/16	3.8	6.1
15/16	5.2	8.3
16/16	3.7	5.7

TABLE 62/...

TABLE 62

Experiment H5		
Pulse Frequency : 900 Pulses/min		
Observed Mean Superficial Velocity : 10.3 cm/sec		
Computed Mean Superficial Velocity : 10.3 cm/sec		
Overall Mean Void-Fraction : $\overline{\epsilon}_m = 0.352$		
Period : T = 0.0666 sec		
Fraction of Period	Instantaneous Pressure Drop	Instantaneous Relative Velocity
A × T	ΔP_{im}	$U_{im} - U_{ipm}$
A	gm/cm ²	cm/sec
0	3.0	4.8
1/16	31.0	41.7
2/16	32.4	43.1
3/16	2.5	4.1
4/16	3.0	5.0
5/16	-10.5	-16.0
6/16	- 1.5	- 2.5
7/16	5.3	8.4
8/16	6.2	9.5
9/16	7.7	12.0
10/16	3.3	5.3
11/16	5.8	9.2
12/16	6.6	10.5
13/16	9.5	14.7
14/16	7.5	11.9
15/16	5.0	8.0
16/16	3.0	4.8

TABLE 63/...

TABLE 63

Experiment H6		
Pulse Frequency : 1100 Pulses/min		
Observed Mean Superficial Velocity : 10.1 cm/sec		
Computed Mean Superficial Velocity : 10.2 cm/sec		
Overall Mean Void-Fraction : $\bar{\epsilon}_m = 0.346$		
Period : T = 0.0545 sec		
Fraction of Period	Instantaneous Pressure Drop	Instantaneous Relative Velocity
A × T	ΔP_{im}	$U_{im} - U_{ipm}$
A	gm/cm ²	cm/sec
0	4.7	6.9
1/16	24.9	32.6
2/16	42.1	51.6
3/16	10.2	14.8
4/16	2.2	3.2
5/16	- 1.3	- 2.0
6/16	-14.8	-21.5
7/16	0.2	0.2
8/16	6.7	9.6
9/16	8.5	12.4
10/16	9.5	13.9
11/16	4.8	7.0
12/16	4.7	6.9
13/16	7.8	11.2
14/16	6.7	9.6
15/16	8.2	11.8
16/16	4.7	6.9

TABLE 64/...

TABLE 64

Experiment H7		
Pulse Frequency : 1200 Pulses/min		
Observed Mean Superficial Velocity : 9.9 cm/sec		
Computed Mean Superficial Velocity : 9.9 cm/sec		
Overall Mean Void-Fraction : $\bar{\epsilon}_m = 0.341$		
Period : T = 0.05 sec		
Fraction of Period	Instantaneous Pressure Drop	Instantaneous Relative Velocity
A × T	ΔP_{im}	$U_{im} - U_{ipm}$
A	gm/cm ²	cm/sec
0	7.5	10.5
1/16	27.7	34.7
2/16	35.8	43.2
3/16	7.8	11.0
4/16	2.0	3.0
5/16	- 0.3	- 0.5
6/16	-12.6	-17.7
7/16	3.1	4.5
8/16	7.2	10.2
9/16	6.7	9.5
10/16	9.2	13.0
11/16	6.7	9.5
12/16	3.7	5.4
13/16	7.2	10.2
14/16	6.0	8.5
15/16	7.7	10.7
16/16	7.5	10.5

Appendix 7/...

APPENDIX 7

Development of a mathematical theory for the pulsating bed

The energy balance¹³⁾ for unit mass of fluid in motion may be written as:

$$\frac{1}{2} \Delta U^2 + g \Delta L + \int g v dP + W + F' = 0.$$

For a fluid flowing in a horizontal duct, and if no work is done by the system, the energy balance may be reduced to the form:

$$\frac{1}{2} \Delta U^2 + g \int v dP + F' = 0$$

or

$$- g \Delta P = g \Delta P_f + \frac{1}{2} \rho \Delta U^2 \dots\dots\dots (1)$$

From equation (1) it may be observed that the total pressure loss is composed of two components, viz. the frictional component and the kinetic energy component.

Uniform fluid flow through the fixed bed

A general relationship for the pressure drop may be developed, using the Kozeny assumption that the granular bed is equivalent to a group of parallel and equal-sized channels, such that the total internal surface and the free internal volume are equal to the total packing surface and the void volume, respectively, of the randomly packed bed. The pressure drop across a channel is given by the Poiseuille equation, to which a term representing kinetic energy losses, analogous to that introduced

by/...

by equation (1), may be added:

$$gdP = \frac{32 \mu U^* dL}{d_c^2} + \frac{\rho dL U^{*2}}{L_o}$$

Since the losses occur with a frequency statistically related to the number of particles, correlating factors α and β are added to the above equation, resulting in:

$$gdP = \frac{32 \alpha \mu U^* dL}{d_c^2} + \frac{\beta \rho dL U^{*2}}{L_o} \dots\dots\dots(2)$$

The velocity of the fluid in the channels may be eliminated in favour of the superficial velocity, based on the empty container, by the mass flow balance, which on simplification yields:

$$N d_c^2 U^* = D^2 U \dots\dots\dots(3)$$

The above simplification may be introduced if the fluid velocity in the channel and the superficial velocity are evaluated at identical temperature and pressure conditions.

Equating the free volumes in the bed:

$$N \frac{\pi}{4} d_c^2 L = \frac{\pi}{4} D^2 \epsilon L$$

and therefore

$$N d_c^2 = D^2 \epsilon \dots\dots\dots(4)$$

Substitution of equation (4) in equation (3) yields:

$$U^* = \frac{U}{\epsilon} \dots\dots\dots(5)$$

The/...

The internal surface of the channels may be eliminated in favour of the surface area of the particles by the following equation:

$$N \pi d_c L = S \frac{\pi}{4} D^2 L(1 - \epsilon) \dots\dots\dots (6)$$

Substitution of equation (4) in equation (6) yields:

$$d_c = \frac{4 \epsilon}{(1 - \epsilon) S} \dots\dots\dots (7)$$

In equation (5) the fluid velocity in the channel is expressed in terms of the superficial velocity and void fraction. In equation (7) the characteristic dimension of the channel is expressed in terms of void fraction and specific surface of the particles.

Substitution of equations (5) and (7) in equation (2) yields the differential pressure-drop velocity relationship for a fixed bed as:

$$gdP = \frac{2 \alpha \mu S^2 (1 - \epsilon)^2 U dL}{\epsilon^3} + \frac{\beta \rho dL U^2}{L_o \epsilon^2}$$

The total pressure drop across the bed is given by integrating the above equation with respect to length. To integrate the above equation, it is necessary to replace the void fraction and the superficial velocity by the mean void fraction and the superficial velocity at mean bed conditions, respectively, thus:

$$g \Delta P_{fm} = \frac{2 \alpha \mu S^2 (1 - \epsilon_m)^2 U_m L}{\epsilon_m^3} + \frac{\beta \rho L U_m^2}{L_o \epsilon_m^2} \dots\dots (8)$$

Equation/...

Equation (8) is not rigorous as applied to the entire column, because it neglects the variation in fractional void volume and superficial velocity over the length of the bed. A rigorous solution would involve the substitution of the appropriate values of pressure drop and superficial velocity, at various lengths, in equation (8) and solving for the void fractions. The average void fraction and superficial velocity may then be graphically obtained. This procedure is hardly warranted for the use of mean void fraction and superficial velocity yield results well within experimental accuracy. It may be convenient at this stage to eliminate the bed length in terms of void fraction, thus:

$$1 - \epsilon_m = \frac{4M}{\rho_s \pi D^2 L} = \frac{K}{L} \dots\dots\dots (9)$$

Substitution in equation (8) yields:

$$g \Delta P_{fm} = \frac{2K \alpha \mu S^2 (1 - \epsilon_m) U_m}{\epsilon_m^3} + \frac{\beta \rho K U_m^2}{L_0 \epsilon_m^2 (1 - \epsilon_m)} \dots\dots\dots (10)$$

This is the general equation relating pressure drop and superficial velocity for fluid flow through the fixed bed.

Pulsating fluid flow through a fixed bed

In the case of pulsating fluid flow, both the velocity and pressure drop are functions of time. The instantaneous pressure-drop and instantaneous

superficial/...

superficial velocity must, therefore, be considered and are related by an equation similar to equation (10):

$$g \Delta P_{ifm} = \frac{2 \alpha K \mu S^2 (1-\epsilon_m) U_{im}}{\epsilon_m^3} + \frac{\beta K \rho U_{im}^2}{L_o \epsilon_m^2 (1-\epsilon_m)}$$

In order to obtain average figures for the cycle, the above equation must be integrated with respect to the time, and the result divided by T, the duration of a cycle, thus:

$$\frac{g}{T} \int_0^T \Delta P_{ifm} dt = 2 \alpha K \mu S^2 \frac{(1-\epsilon_m)}{\epsilon_m^3} \frac{1}{T} \int_0^T U_{im} dt + \frac{\beta K \rho}{L_o \epsilon_m^2 (1-\epsilon_m)} \frac{1}{T} \int_0^T U_{im}^2 dt \dots\dots\dots (11)$$

The integral $\frac{1}{T} \int_0^T U_{im} dt$ has a simple physical explanation which may be expressed in terms of the volume passed per cycle, Q, and the mean superficial velocity, \overline{U}_m . This relation is given by:

$$\frac{Q}{TA} = \overline{U}_m = \frac{1}{T} \int_0^T U_{im} dt \dots\dots\dots (12)$$

No simple relation which is known a priori exists between Q and $\int_0^T U_{im}^2 dt$.

It may, however, be assumed that some sort of relation does exist between this integral and Q or \overline{U}_m , i.e.

$$\frac{1}{T} / \dots$$

$$\frac{1}{T} \int_0^T U_{im}^2 dt = F \overline{U_m^2} \dots\dots\dots (12a)$$

It will be shown below that for all types of flow which are likely to occur, F, though unknown, may be expected to fall within fairly narrow limits.

F may be evaluated by the functions defined in the following equations:

$$Z = \int_0^T x dt$$

and

$$W = \int_0^T x^2 dt = \frac{F}{T} \int_0^T x dt \int_0^T x dt$$

thus:

$$F = \frac{WT}{Z^2}$$

An approximation to the modulus of the factor F may be obtained by considering a few known functions. For details, see Appendix 8.

Case I

$$x = a = \text{constant}$$

$$\therefore F = 1.$$

Case II

$$x = a\sqrt{t}$$

$$\therefore F = 1.125$$

Case/...

Case III

$$x = a \sin \omega t$$

$$\therefore F = 1.23$$

Case IV

$$x = at$$

$$\therefore F = 1.33$$

The experimental flow patterns encountered lie in a region bounded by the four curves considered above. Cases I and IV are unlikely flow patterns and in general a form factor, F , having a modulus of 1.2, seems not unlikely.

Substitution of equations (12) and (12a) in equation (11) on simplification yields:

$$g \Delta \bar{P}_{fm} = \frac{2 \alpha K \mu S^2 (1 - \epsilon_m) \bar{U}_m}{\epsilon_m^3} + \frac{\beta K \rho F \bar{U}_m^2}{L_0 \epsilon_m (1 - \epsilon_m)} \dots \dots \dots (13)$$

Pulsating fluid flow in the fluidized bed

In the pulsating fluidized bed the solid particles attain a degree of freedom and vibrate in a vertical plane. From the amplitude and frequency observations, the maximum particle velocity may be calculated, and was found to be of the order of 8 cm/sec. Thus the particle velocity may no longer be neglected in the basic equation. The instantaneous superficial velocity must, therefore, be replaced by the instantaneous relative superficial

velocity/...

velocity. The instantaneous pressure-drop-velocity relationship, in the pulsating fluidized bed, may be represented by an equation similar to equation (10), viz.:

$$g \Delta P_{im} = \frac{2 \alpha K \mu S^2 (1 - \epsilon_m) (U_{im} - U_{ipm})}{\epsilon_m^3} + \frac{\beta K \rho (U_{im} - U_{ipm})^2}{L_0 \epsilon_m^2 (1 - \epsilon_m)}$$

In order to integrate the above equation, the mean void fraction, which is a function of time, must be replaced by the overall mean void fraction, which by definition is independent of time:

$$g \Delta P_{im} = \frac{2 \alpha K \mu S^2 (1 - \bar{\epsilon}_m) (U_{im} - U_{ipm})}{\bar{\epsilon}_m^3} + \frac{\beta K \rho (U_{im} - U_{ipm})^2}{L_0 \bar{\epsilon}_m^2 (1 - \bar{\epsilon}_m)} \dots \dots \dots (14)$$

In order to obtain average figures for the cycle, the above equation is integrated with respect to time and the results divided by T, the duration of the cycle. Substitution of:

$$\bar{U}_m = \frac{1}{T} \int_0^T (U_{im} - U_{ipm}) dt$$

and $F \bar{U}_m^2 = \frac{1}{T} \int_0^T (U_{im} - U_{ipm})^2 dt$

in/...

in the integrated form of equation (14), on simplification yields:

$$g \overline{\Delta P}_m = \frac{2 \alpha K \mu S^2 (1 - \overline{\epsilon}_m) \overline{U}_m}{\overline{\epsilon}_m^3} + \frac{\beta K \rho F \overline{U}_m^2}{L_0 \overline{\epsilon}_m^2 (1 - \overline{\epsilon}_m)} \dots\dots\dots (15)$$

The above is the general equation relating the various variables in the pulsating fluidized bed.

Modified Reynolds number and friction factor

The most convenient method of representation of the experimental data, obtained from the conventional fluidized bed, was found by other investigators¹¹⁾ to be the plot of the Reynolds number versus the friction factor. To test the theoretical value assigned to the form factor, F, a modified Reynolds number and friction factor, applicable to the pulsating fluidized bed, have to be derived.

Modified Reynolds number

The Reynolds number for a fluid in motion in a duct may be written as:

$$Re = \frac{du \rho}{\mu} \dots\dots\dots (16)$$

In the pulsating fluidized bed the instantaneous Reynolds number may be defined by an equation similar to the above, viz.:

$$Re_i = \frac{d_c U^* \rho}{\mu} \dots\dots\dots (17)$$

The/...

The characteristic linear dimension in the Reynolds number may be eliminated in favour of the specific surface. Substitution of equation (7) and

$$U^* = \frac{(U_{im} - U_{ipm})}{\bar{\epsilon}_m}$$

in equation (17) yields:

$$Re_i = \frac{4 \rho (U_{im} - U_{ipm})}{\mu S (1 - \bar{\epsilon}_m)}$$

Integration of the above equation with respect to time, and dividing the result by the duration of the cycle, T, yields:

$$\int \frac{Re_i}{4} = \bar{Re} = \frac{\rho \bar{U}_m}{\mu S (1 - \bar{\epsilon}_m)} \dots\dots\dots (18)$$

Modified friction factor

For a fluid in motion in a duct, the friction factor is generally defined by an equation of the type:

$$g \Delta P = 4 \phi \frac{L}{d} \rho U^2$$

For the pulsating fluidized bed, the instantaneous friction factor may be defined by an equation similar to the above, viz.:

$$g \Delta P_{im} = \frac{4 \phi_i L \rho (U_{im} - U_{ipm})^2}{d_c \bar{\epsilon}_m^2} \dots\dots\dots (19)$$

Substitution of equations (7) and (9) in equation

(19)/...

(19), and integration of the latter with respect to time divided by the duration of the cycle (T), yields:

$$\bar{\phi} = \frac{\overline{\epsilon_m^3} g \overline{\Delta P_m}}{SF^2 K \rho \overline{U_m^2}} \dots\dots\dots (20)$$

Specific Surface (S)

The conventional relationship for the specific surface of the solid particles, as utilized in equations (18) and (20), may be modified to facilitate the evaluation of the specific surface from either the fixed or fluidized bed data.

The external surface (S_E) per gram of solids, in a bed of solid particles, is given by the equation¹⁴):

$$S_E^2 = \frac{\epsilon^3 g \Delta P}{5 U \rho^2 (1 - \epsilon)^2 L \mu}$$

The specific surface (S), on simplification of the above equation, is given by:

$$S^2 = \frac{\epsilon^3 g \Delta P}{5 U (1 - \epsilon)^2 L \mu} \dots\dots\dots (21)$$

Substitution of equation (9) in the above, yields the specific surface from uniform fluid flow data in the fixed bed, as:

$$S^2 = \frac{\epsilon_m^3 g \Delta P_{fm}}{5 U_m (1 - \epsilon_m) K \mu} \dots\dots\dots (22)$$

Substitution/...

Substitution of the instantaneous pressure drop and velocity in the specific surface equation, and integrating with respect to time and dividing by the duration of the cycle (T), yields on simplification:

$$S^2 = \frac{\overline{\epsilon_m^3} \overline{g} \overline{\Delta P_m}}{5 \overline{U_m} (1 - \overline{\epsilon_m}) K \mu} \dots\dots\dots (23)$$

Equation (23) allows the evaluation of the specific surface from the pulsating fluidized bed data.

Appendix 8 / ...

APPENDIX 8

FORM FACTOR F

An approximation of the modulus of the form factor F by consideration of a few known functions.

CASE I

$$x = a = \text{constant}$$

$$Z = \int_0^T x dt = \int_0^T a dt = aT$$

$$W = \int_0^T x^2 dt = \int_0^T a^2 dt = a^2 T$$

$$\therefore F = \frac{WT}{Z^2} = \frac{a^2 T \times T}{a^2 T^2} = 1$$

CASE II

$$x = at^{\frac{1}{2}}$$

$$Z = \int_0^T x dt = \int_0^T at^{\frac{1}{2}} dt = \frac{2}{3} aT^{\frac{3}{2}}$$

$$W = \int_0^T x^2 dt = \int_0^T a^2 t dt = \frac{1}{2} a^2 T^2$$

$$\therefore F = \frac{WT}{Z^2} = \frac{\frac{1}{2} a^2 T^2 \times T}{\frac{4}{9} a^2 T^3} = \frac{9}{8} = 1.125$$

CASE III/...

CASE III

$$x = a \sin \omega t$$

$$\begin{aligned} Z &= \int_{\omega t=0}^{\omega t=\pi} x \, dt = \int_{\omega t=0}^{\omega t=\pi} a \sin \omega t \, dt \\ &= \frac{a}{\omega} \cos \omega t \Big|_{\omega t=\pi}^{\omega t=0} = \frac{2a}{\omega} \end{aligned}$$

$$\begin{aligned} W &= \int_{\omega t=0}^{\omega t=\pi} x^2 \, dt = \int_{\omega t=0}^{\omega t=\pi} a^2 \sin^2 \omega t \, dt \\ &= \frac{a^2}{\omega} \left[\frac{\omega t}{2} - \frac{\sin 2 \omega t}{4} \right]_{\omega t=0}^{\omega t=\pi} \\ &= \frac{a^2 \pi}{2\omega} \end{aligned}$$

$$F = \frac{WT}{Z^2} = \frac{\frac{a^2 \pi}{2\omega} \times T}{\frac{4a^2}{\omega^2}} \quad \text{But } \omega T = \pi$$

$$\therefore F = \frac{a^2 \pi}{2\omega} \times \frac{\pi}{\omega} \times \frac{\omega^2}{4a^2} = \frac{\pi^2}{8} = 1.23.$$

CASE IV

$$x = at$$

$$Z = \int_0^T x \, dt = \int_0^T a t \, dt = \frac{a T^2}{2}$$

$$W = \int_0^T x^2 \, dt = \int_0^T a^2 t^2 \, dt = \frac{a^2 T^3}{3}$$

$$F = \frac{WT}{Z^2} = \frac{a^2 T^3}{3} \times T \times \frac{4}{a^2 T^4} = \frac{4}{3} = 1.33$$

APPENDIX 9

SPECIMEN CALCULATIONS

The experimental results obtained from the experimental series A1 to A5 were used, as far as possible, for the specimen calculations.

9.1 FIXED BED

Observations

The following are typical observations required for the calculation of the superficial velocity at mean bed conditions in the fixed bed:

- (1) Pressure drop across the bed: $\Delta P_{fm} = 21.7 \text{ gm/cm}^2$
- (2) Pressure above atmospheric pressure at downstream side of the bed = 12.0 gm/cm^2
- (3) Mean bed temperature = 299.5°K
- (4) Atmospheric pressure = 883.9 gm/cm^2
- (5) Superficial velocity at 883.9 gm/cm^2 and 299.5°K = 25.1 cm/sec.

Calculations

(a) Superficial velocity at mean bed conditions

Evaluation of typical superficial velocities at mean bed conditions, given in Table 2, Appendix 1, is set out below:

Mean/...

Mean absolute pressure existing in bed

$$\begin{aligned}
 &= 883.9 + 12.0 + 0.5 \times 21.7 \\
 &= 906.8 \text{ gm/cm}^2
 \end{aligned}$$

Superficial velocity at mean bed conditions

$$\begin{aligned}
 U_m &= 25.1 \times 883.9/906.8 \\
 &= 24.4 \text{ cm/sec.}
 \end{aligned}$$

(b) Evaluation of the constants a and b defined by

$$\Delta P_{fm} = a U_m + b U_m^2 \dots\dots\dots (10a)$$

Employing the data in Table 2, Appendix 1, the following calculations were made:

$$(1) \sum \Delta P_{fm}/U_m = 15.3 \text{ gm sec/cm}^3$$

$$(2) \sum \Delta P_{fm} = 197.5 \text{ gm/cm}^2$$

$$(3) \sum U_m = 228.3 \text{ cm/sec}$$

$$(4) \sum (U_m)^2 = 3788.1 \text{ cm}^2/\text{sec}^2$$

(5) Number of observations : n = 18.

Substitution of the above in equations (26) and (27) yields:

$$15.3 = 18 a + 228.3 b$$

$$197.5 = 228.3 a + 3788.1 b$$

Solving for a and b:

$$a = 0.793 \text{ gm sec/cm}^3$$

$$b = 4.35 \times 10^{-3} \text{ gm sec}^2/\text{cm}^4$$

Thus/...

Thus, the pressure-drop-velocity relationship in the fixed bed may be represented by the equation:

$$\Delta P_{fm} = 0.793 U_m + 4.35 \times 10^{-3} U_m^2$$

9.2 FLUIDIZED BED

Observations

The following are typical observations required for the calculation of the mean superficial velocity in the pulsating fluidized bed:

- (1) Pressure drop across bed: $\overline{\Delta P_m} = 5.7$
- (2) Pressure above atmospheric pressure at the upstream side of the bed = 8.7 gm/cm^2
- (3) Mean bed temperature = 298.9°K
- (4) Atmospheric pressure = 884.4 gm/cm^2
- (5) Superficial velocity at 884.4 gm/cm^2 and 298.9°K = 7.8 cm/sec .

Calculations

(a) Mean superficial velocity

Evaluation of typical mean superficial velocities, given in Table 10, Appendix 2, is set out below:

$$\begin{aligned} \text{Mean absolute pressure existing in the fluidized} \\ \text{bed} &= 884.4 + 8.7 - 0.5 \times 5.7 \\ &= 890.4 \text{ gm/cm}^2 \end{aligned}$$

Mean/...

Mean superficial velocity

$$\begin{aligned}\bar{U}_m &= 7.8 \times 884.4/890.4 \\ &= 7.7 \text{ cm/sec.}\end{aligned}$$

(b) Calculation of the overall mean void fraction

The overall mean void fraction is evaluated employing the pressure drops and velocities in Table 34, Appendix 3.

Substitution of

$$\begin{aligned}a &= 0.793 \text{ gm sec/cm}^3 \\ b &= 4.35 \times 10^{-3} \text{ gm/sec}^2/\text{cm}^4 \\ \epsilon_m &= 0.365\end{aligned} \left. \begin{array}{l} \\ \\ \end{array} \right\} \begin{array}{l} \text{From the} \\ \text{corresponding} \\ \text{fixed bed.} \end{array}$$

$$\begin{aligned}\bar{\Delta P}_m &= 5.6 \text{ gm/cm}^2 \\ \bar{U}_m &= 7.6 \text{ cm/sec}\end{aligned} \left. \begin{array}{l} \\ \end{array} \right\} \text{From Table 34, Appendix 3.}$$

$$F = 1.2$$

in

$$\bar{\Delta P}_m = a \frac{(\epsilon_m)^3}{(\bar{\epsilon}_m)^3} \frac{(1-\bar{\epsilon}_m)}{(1-\epsilon_m)} \bar{U}_m + bF \frac{(\epsilon_m)^2}{(\bar{\epsilon}_m)^2} \frac{(1-\bar{\epsilon}_m)}{(1-\epsilon_m)} \bar{U}_m^2 \dots (28)$$

yields

$$\begin{aligned}5.6 &= 0.793 \frac{(0.365)^3}{(\bar{\epsilon}_m)^3} \frac{(1-\bar{\epsilon}_m)}{(0.635)} 7.6 \\ &+ \frac{1.2 \times 4.35}{10^3} \frac{(0.365)^2}{(\bar{\epsilon}_m)^2} \frac{(0.635)}{(1-\bar{\epsilon}_m)} 7.6 \times 7.6\end{aligned}$$

Graphical solution of the above equation yields

$$\bar{\epsilon}_m = 0.3772.$$

9.3/...

9.3 SPECIFIC SURFACE

As an example the specific surface of the solid material will be evaluated at a mean superficial velocity of 8.5 cm/sec.

Substitution of the following data:

- (1) $\overline{U}_m = 8.5 \text{ cm/sec}$
- (2) $\overline{\Delta P}_m = 6.1 \text{ gm/cm}^2$ From Table 34, Appendix 3.
- (3) $\overline{\epsilon}_m = 0.382$ From Table 42, Appendix 4.
- (4) $\mu = 1.8 \times 10^{-4} \text{ gm/cm sec}^{18)}$
- (5) $L = 9.7 \text{ cm}$)
- (6) $\epsilon_m = 0.365$) From corresponding fixed bed.

in

$$S^2 = \frac{\overline{\epsilon}_m^3 g \overline{\Delta P}_m}{S \overline{U}_m (1-\overline{\epsilon}_m) K \mu} \dots\dots\dots (23)$$

where $K = L (1-\epsilon_m)$
 $= 9.7 \times 0.635$
 $= 6.16 \text{ cm}$

yields

$$S^2 = \frac{(0.382)^3 \times 981 \times 6.1}{S \times 8.5 (0.618) 6.16 \times 1.8 \times 10^{-4}}$$

$\therefore S = 107 \text{ cm}^2/\text{cm}^3$

9.4 MODIFIED REYNOLDS NUMBER

Substitution of the following typical data:

$$(1) \quad \mu = 1.8 \times 10^{-4} \text{ gm/cm sec}$$

$$(2) \quad \rho = 1.198 \times 10^{-3} \text{ gm/cm}^3$$

$$(3) \quad S = 106.4 \text{ cm}^2/\text{cm}^3 \quad (\text{Table 33, Appendix 3.})$$

$$(4) \quad \bar{U}_m = 7.6 \text{ cm/sec}$$

$$(5) \quad \bar{\epsilon}_m = 0.3772 \quad (\text{Table 42, Appendix 4.})$$

in

$$\bar{Re} = \frac{\rho}{\mu S} \times \frac{\bar{U}_m}{(1 - \bar{\epsilon}_m)}$$

yields

$$\begin{aligned} \bar{Re} &= \frac{1.198 \times 10^{-3} \times 7.6}{1.8 \times 10^{-4} \times 106.4 \times 0.6228} \\ &= 0.763. \end{aligned}$$

9.5 MODIFIED FRICTION FACTOR

Substitution of the following typical data:

$$(1) \quad \bar{U}_m = 7.6 \text{ cm/sec}$$

$$(2) \quad \bar{\Delta F}_m = 5.6 \text{ gm/cm}^2 \quad (\text{Table 34, Appendix 3})$$

$$(3) \quad S = 106.4 \text{ cm}^2/\text{cm}^3 \quad (\text{Table 33, Appendix 3})$$

$$(4) \quad \rho = 1.198 \times 10^{-3} \text{ gm/cm}^3$$

$$(5) \quad F = 1.2 \quad (\text{see text})$$

(6)/...

$$(6) \quad K = 6.16 \text{ cm}$$

$$(7) \quad \overline{\epsilon_m} = 0.3772 \quad (\text{Table 42, Appendix 4})$$

in

$$\overline{\phi} = \frac{\overline{\epsilon_m}^3 g \Delta P_m}{S F^2 K \rho \overline{U_m}^2}$$

yields

$$\begin{aligned} \overline{\phi} &= \frac{(0.3772)^3 \times 981 \times 5.6}{106.4 \times (1.2)^2 \times 6.16 \times 1.198 \times 10^{-3} \times (7.6)} \\ &= 4.54. \end{aligned}$$

9.6 INSTANTANEOUS RELATIVE VELOCITY

The instantaneous relative velocity may be calculated from equation (30):

$$\begin{aligned} (U_{im} - U_{ipm}) &= \frac{-a \left[\frac{\epsilon_m}{\overline{\epsilon_m}} \right]^3 \left[\frac{1-\epsilon_m}{1-\overline{\epsilon_m}} \right]}{2b \left[\frac{\epsilon_m}{\overline{\epsilon_m}} \right]^2 \left[\frac{1-\epsilon_m}{1-\overline{\epsilon_m}} \right]} \\ &+ \frac{\left[a^2 \left[\frac{\epsilon_m}{\overline{\epsilon_m}} \right]^6 \left[\frac{1-\epsilon_m}{1-\overline{\epsilon_m}} \right]^2 + 4b \Delta P_{im} \left[\frac{\epsilon_m}{\overline{\epsilon_m}} \right]^2 \left[\frac{1-\epsilon_m}{1-\overline{\epsilon_m}} \right] \right]^{\frac{1}{2}}}{2b \left[\frac{\epsilon_m}{\overline{\epsilon_m}} \right]^2 \left[\frac{1-\epsilon_m}{1-\overline{\epsilon_m}} \right]} \end{aligned}$$

Substitution/...

Substitution of

$$\begin{array}{l}
 a = 0.646 \text{ gm sec/cm}^3 \\
 b = 3.50 \times 10^{-3} \text{ gm sec}^2/\text{cm}^4 \\
 \epsilon_m = 0.345 \\
 \bar{\epsilon}_m = 0.353 \\
 \Delta P_{im} = 6.0 \text{ gm/cm}^2
 \end{array}
 \left. \begin{array}{l}
 \\
 \\
 \\
 \\
 \end{array} \right\} \begin{array}{l}
 \text{Table 1,} \\
 \text{Appendix 1} \\
 \\
 \text{Table 58, Appendix 6}
 \end{array}$$

yields

$$\begin{aligned}
 (U_{im} - U_{ipm}) &= \frac{-0.646 \left[\frac{0.345}{0.353} \right]^3 \left[\frac{0.647}{0.655} \right]}{2 \times 3.5 \times 10^{-3} \left[\frac{0.345}{0.353} \right]^2 \left[\frac{0.655}{0.647} \right]} \\
 &+ \frac{\left[(0.646)^2 \left[\frac{0.345}{0.353} \right]^6 \left[\frac{0.647}{0.655} \right]^2 \right]^{\frac{1}{2}}}{2 \times 3.50 \times 10^{-3} \times \left[\frac{0.345}{0.353} \right]^2 \left[\frac{0.655}{0.647} \right]} \\
 &+ \frac{\left[4 \times 3.5 \times 10^{-3} \times 6.0 \times \left[\frac{0.345}{0.353} \right]^2 \left[\frac{0.655}{0.647} \right] \right]^{\frac{1}{2}}}{2 \times 3.50 \times 10^{-3} \times \left[\frac{0.345}{0.353} \right]^2 \left[\frac{0.655}{0.647} \right]} \\
 &= 9.4 \text{ cm/sec.}
 \end{aligned}$$

13. REFERENCES

- 1) D'Arcy, H.P.G., "Les Fontaines Publiques de la Ville de Dijon", V. Belmont, Paris, (1856).
- 2) Prandtl, D., "Applied Hydro and Aero-Mechanics", McGraw-Will, New York, (1934).
- 3) Furnas, C.C., "Flow of Gases Through Beds of Broken Solids", U.S. Department of Commerce, Bureau of Mines, Bull. 307, (1929).
- 4) Dupuit, A.J.E.J., "Etudes Theoretiques et Pratiques sur le Mouvement des Eaux", (1863).
- 5) Blake, F.C., A.I.Ch.E., 14, 415, (1922).
- 6) Stanton, T.E. and Pannell, J.R., "Collected Researches", Nat'l Physical Lab., 2, (1914).
- 7) Daniels, L.S., Pet. Ref., 25, 435, (1946).
- 8) Parent, J.D., Chem. Eng. Prog., 43, 429, (1947).
- 9) Ergun, S., Chem. Eng. Prog., 48, 89, (1952).
- 10) Brillouin, M., "Lecons sur la Viscosité des Liquids et des Gas", Paris, Gauthier-Villars, (1907).
- 11) Richardson, J.F. and Meikle, R.A., Trans. Inst. Chem. Eng., 39, 348, (1961).
- 12) Rowe, P.N. and Henwood, G.A., Trans. Inst. Chem. Eng., 39, 43, (1961).

13)/...

- 13) Coulson, J.M., Richardson, J.F., "Chemical Engineering", 3rd Edition, p. 22.
- 14) Gregg, G.J., "The Surface Chemistry of Solids", Reinhold Publishing Corporation, p. 143, (1951).
- 15) Arkin, H., and Colton, R.R., "An Outline of Statistical Methods", 4th Edition, p. 53.
- 16) Ergun, S. and Orning, A., Ind. Eng. Chem., 41, 1181, (1949).
- 17) Kozeny, J., Sitzber. Akad. Wiss., Wien, Math-Naturw. Kl., (Abt. IIa), 136, 271, (1927).
- 18) Machin, K.E., Journal of Scientific Instruments, 35, 424, (1958).

=====